



Catalytic performance of advanced titanosilicate selective oxidation catalysts – a review

Jan Přečh

To cite this article: Jan Přečh (2017): Catalytic performance of advanced titanosilicate selective oxidation catalysts – a review, *Catalysis Reviews*, DOI: [10.1080/01614940.2017.1389111](https://doi.org/10.1080/01614940.2017.1389111)

To link to this article: <http://dx.doi.org/10.1080/01614940.2017.1389111>



Published online: 03 Nov 2017.



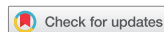
Submit your article to this journal [↗](#)



View related articles [↗](#)



View Crossmark data [↗](#)



Catalytic performance of advanced titanasilicate selective oxidation catalysts – a review

Jan Přečh

Department of Synthesis and Catalysis, J. Heyrovský Institute of Physical Chemistry of the Czech Academy of Sciences, Prague, Czech Republic

ABSTRACT

This review article aims to cover the state-of-the-art of titanasilicate catalysts for selective oxidations developed within past seven years. Many elaborated materials (e.g., layered and pillared titanosilicates, hierarchical composite materials, and others) have been prepared and thoroughly characterized; however, their catalytic properties have been usually investigated only using a single or few model substrates and compared with a benchmarking material. The main goal of this article is to summarize the novel catalysts and compare their catalytic performance with each other. The comparison is focused on epoxidation. In addition, phenol hydroxylation and sulphide oxidation are briefly covered.

ARTICLE HISTORY

Received June 20 2017
Accepted August 15 2017

KEYWORDS

Epoxidation; hydrogen peroxide; selective oxidation; titanasilicate; zeolite

1. Introduction

The modern world is mostly based on products of chemical industry. According to the current estimates, about 85% of all processes in the chemical industry are catalyzed by solid, heterogeneous catalysts [1]. In the 1960s, zeolites were first introduced as solid acid catalysts in oil refining. They have gradually replaced both toxic and corrosive acids (e.g., sulfuric acid, aluminium chloride) and solid amorphous silica-alumina catalysts. Nowadays, zeolites and related materials are widely used in large-scale industrial processes [2–4]. Zeolites are microporous crystalline materials composed of SiO_4 tetrahedra in which some of the silicon atoms are replaced by other tetravalent or trivalent cations of similar sizes such as Al^{3+} , Ti^{4+} , Ge^{4+} , B^{3+} , Fe^{3+} , Ga^{3+} , and others [5]. There exist 235 different zeolitic structures recognized to this date by the Structure Commission of the International Zeolite Association (IZA) [6] and they belong to a wider group of materials called molecular sieves. Various zeolitic structures differ in size, shape, and topology of the channel system and usually can be prepared in diverse chemical compositions. As a result, the zeolite chemistry is very rich and in industrial applications they usually represent not only technical improvement but also an environmentally friendly alternative.

CONTACT Jan Přečh  jan.prech@jh-inst.cas.cz  J. Heyrovský Institute of Physical Chemistry of the Czech Academy of Sciences, Dolejškova 2155/3, 182 23 Prague 8, Czech Republic.

Color versions of one or more of the figures in the article can be found online at www.tandfonline.com/LCTR.

© 2017 Taylor & Francis

The commercial applications of zeolites are abundant and they go hand in hand with the development of tailored zeolite-based catalysts. Most of them use acidic aluminosilicate catalysts; however, titanosilicate zeolites have also gained industrial use as selective oxidation catalysts. Titanium-silicalite-1 (TS-1) serves as a catalyst in Eni propylene oxide process, in phenol oxidation and cyclohexanone ammoxidation [7–9]. The TS-1 (Ti-MFI) was disclosed by Taramasso et al. [10] in 1983 and its discovery represents a considerable breakthrough in the field of oxidation reactions using aqueous hydrogen peroxide as the oxidant. In contrast, conventional synthetic routes toward epoxides, for instance, require the use of chlorine and a strong base, hydroperoxides, or peracids [11]. The use of such reactants produces stoichiometric amounts of organic and inorganic by-products, which need to be recycled or disposed of.

The aluminium-free TS-1 is an excellent catalyst for oxidation of small molecules (e.g., propylene, linear olefins, phenol), but the access of bulkier molecules to the active sites is limited due to relatively narrow (10-ring) pores of the material. Therefore, a number of different zeolite-based titanosilicate catalysts with more open structures were reported including large and extra-large pore titanosilicates with 12-ring and 14-ring channels, respectively, and hierarchical or lamellar titanosilicates [12–19].

In 2004, Ratnasamy, Srinivas, and Knözinger reviewed the state-of-the-art of titanosilicate catalysts discussing the nature of titanium active sites, the presence of oxo-titanium species, catalytic properties and structure-activity correlations [20]. On the occasion of Prof. Tatsumi's retirement (in 2014), Wu et al. reviewed the synthesis of Ti-MWW and related materials [21] and there exists a comprehensive e-book on Ti-MWW-based materials [22]. At the same time, Moliner and Corma briefly assessed the titanosilicate materials from the structure point of view [23]. Several highlights of the latest progress in titanosilicate research (also from material synthesis point of view) were summarized also by Xu and Wu [24].

Titanosilicates are nowadays well established selective oxidation catalysts. 4-coordinated titanium atoms, which are the active sites, act as weak Lewis acids coordinating molecules such as H_2O_2 , H_2O , NH_3 , and organic hydroperoxides. Hydrophobic character of titanosilicate zeolites suppresses concurrent adsorption of water, thus enabling use of aqueous hydrogen peroxide as oxidant. In the case of H_2O_2 the titanium atom withdraws electrons, thus reducing the electron density at the O-O bond. As a result, the coordinated H_2O_2 is more susceptible toward a nucleophilic attack, e.g., of an alkene. The titanosilicates catalyze epoxidations, hydroxylations of alkanes and arenes, oxidations of ethers to acids and cyclic ethers to lactones, oxidations of phenols to quinones, oxidations of amines to hydroxylamines, ammoxidation and sulphides to sulphoxides and sulphones with hydrogen peroxide and

organic hydroperoxides. Without the presence of peroxides, they also catalyze Beckmann rearrangement.

This review article aims to cover the state-of-the-art of titanasilicate selective oxidation catalysts developed within the past seven years. Many elaborated materials (e.g., layered and pillared titanasilicates, hierarchical composite materials, and others) have been prepared and thoroughly characterized; however, their catalytic performance is usually reported only using a single or few model substrates and compared with a benchmarking material (usually TS-1, Ti-beta, Ti-MWW, or Ti-MCM-41). In contrast, the main goal of this article is to compare the catalytic performance of various novel titanasilicate catalysts. The comparison of the catalytic performance will focus on epoxidation of linear olefins (mainly 1-hexene), cyclic olefins (mainly cyclohexene and cyclooctene), terpenes, and other reported substrates. Besides epoxidation, phenol hydroxylation, and sulphide oxidation will be briefly discussed as well.

2. Catalyst structure

In this section, synthesis and structure of the discussed catalysts is described together with brief description of their preparation methods. Further, the materials are compared in terms of their textural properties, pore sizes and shapes and titanium location and content.

The catalysts are classified into following groups (Figure 1).

- (1) Conventional titanasilicate zeolites have all 3 crystal dimensions of the same (similar) order of magnitude not possessing any cavities or other significant defects. They are divided according to their pore sizes to medium-pore titanasilicates (10-ring pores, typically having 4.5–5.5 Å in diameter), large-pore titanasilicates (12-ring pores, typically having 5.5–7 Å in diameter), and extra-large pore titanasilicates (14-ring pores or larger, typically having more than 7 Å in diameter).

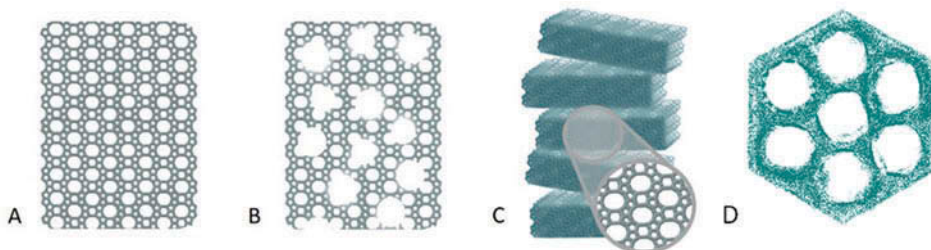


Figure 1. Schematic representation of catalyst structures: conventional titanasilicate zeolites (A), hierarchical titanasilicate zeolites (B), lamellar titanasilicate zeolites (C), and mesoporous titanasilicates (D). Adapted from Wilde et al. [25].

- (2) Hierarchical titanosilicates are materials containing more than one type of pores—typically micropores characteristic of the corresponding zeolite structure and more or less ordered system of mesopores (having 20–430 Å in diameter [26]). The mesopores are usually responsible for a better accessibility of the active centres located in the core of crystals. Composite materials consisting of more than one phase in one particle (e.g., yolk-shell structures) also belong to this group.
- (3) Lamellar titanosilicates are materials with one dimension of their crystals reduced to size close to a unit cell and mesopores exist in between the lamellae. Current state-of-the-art of lamellar (also referred to as layered, nanosheet, or two-dimensional) zeolites has been reviewed recently [14,27].
- (4) Mesoporous titanosilicates are amorphous and possess (ordered) system of mesopores having more than 20Å in diameter.

The most common titanosilicate zeolites (and usually the benchmarking catalysts) are TS-1, Ti-beta, and Ti-MWW and therefore, they are briefly introduced although discussion of their properties is not the main aim of this review.

2.1 Conventional titanosilicate zeolites

2.1.1 Medium pore titanosilicates

The titanium silicalite-1 (TS-1) [10] is the most prominent titanosilicate zeolite being used in several of industrial processes [7,9]. TS-1 is a medium pore zeolite with MFI structure and titanium isomorphously incorporated in the framework [28]. TS-1 catalyst is aluminium free and contains no alkali cations. Early findings on the TS-1 synthesis and properties were reviewed by Notari in 1993 [29] and 1996 [30]. There exist several different synthesis protocols for the TS-1 (overviewed in Perego et al. [9]) developed with particular attention to critical parameters related to the industrial use. Typically, TS-1 is prepared by direct hydrothermal synthesis using tetraethyl orthosilicate (TEOS), tetraethyl orthotitanate (or in laboratory practice tetrapropyl or tetrabutyl orthotitanate (TPOTi, TBOTi)), and tetrapropyl ammonium hydroxide (TPA-OH) as a structure directing agent (SDA). The amount of titanium isomorphously incorporated into the TS-1 framework is limited to about Si/Ti = 40 [28,31]. Vayssilov [32] presented a comprehensive review on titanium state and coordination in titanium silicalite catalysts. The synthesis is usually targeted to provide higher concentrations of titanium with the tetrahedral coordination to reach more active centres and therefore higher activity of the catalyst. Some examples of TS-1 with lower Si/Ti ratio (approx. 25–35) and no significant signals of extra-

framework titanium species were reported (e.g., Xiao et al. [33]) and this titanium content can be found in industrial samples as well [7].

Recently, research in synthesis of conventional TS-1 was focused on: (i) tuning the particle size and morphology to shorten diffusion paths inside TS-1 crystals while keeping the processability of the catalyst and (ii) templates alternative to TPA-OH. Lakiss et al. [34] prepared agglomerates of nanosized TS-1 crystals (60–80 nm) by controlled evaporation of their colloidal suspension. The resulting TS-1 possessed 3 levels of porosity, namely micropores ($0.13 \text{ cm}^3/\text{g}$), mesopores with monomodal distribution centred at about 10 nm ($0.16 \text{ cm}^3/\text{g}$) and interparticle macropores ($0.66 \text{ cm}^3/\text{g}$, observed by mercury porosimetry). TS-1 can be prepared also with tetrapropylammonium bromide (TPA-Br) as a template (TPA-Br is cheaper); however, earlier syntheses resulted in large crystals ($15 \times 8 \times 1.5 \text{ }\mu\text{m}$) what is undesirable [35,36]. Zuo et al. [37] demonstrated synthesis of the TS-1 with crystal size of 200 nm using the TPA-Br. The key factor enabling the reduction of the crystal size was seeding. The amount of seeds was more important than the crystallization time to drive the product crystal size. Varying the amount of seeds, crystal size was adjusted in range 200–1200 nm.

The titanosilicate **MWW** (Ti-MWW) is a medium pore zeolite with 2-dimensional system of 10-ring pores and $7.1 \times 18.1 \text{ \AA}$ supercages. Wu and Tatsumi effectively incorporated titanium into the framework of **MWW** in the presence of boric acid using hexamethylene imine or piperidine as SDAs [38,39]. The resulting material contains also boron atoms. The Ti-MWW is formed via lamellar precursor Ti-MWW-P (analog to aluminosilicate **MWW-P**), which condenses into fully connected zeolite upon calcination. The formation of Ti-MWW-P opens a broad area of post-synthesis modifications leading to a wide group of **MWW**-based materials with enhanced accessibility of the active sites [21]. Recently developed materials of this group are discussed below [40–43].

For the Ti-MWW-P formation, a little difference was observed between the Ti content in the synthesis gel and solid lamellar precursor and no bands characteristic for the anatase phase were observed in the UV/Vis spectrum of Ti-MWW-P. However, extra-framework Ti species are present in the material and these are transformed into anatase phase upon calcination [39]. The presence of anatase is undesirable, because anatase decomposes the oxidant while it is not active in the oxidation reaction [11]. Strong mineral acids (HNO_3 , H_2SO_4) are able to wash out the extra-framework titanium species prior to the calcination [38].

Titanium-containing **MSE** (denoted Ti-YNU-2 [17] or Ti-MCM-68 [44–46]) is another medium pore titanosilicate with multidimensional $12 \times 10 \times 10$ ring channels and 18×12 supercages, accessible via 10-ring channels. Direct crystallization of Ti-MSE is difficult [45] and it was not reported yet. The Ti-MCM-68 was prepared via dealumination of Al-MCM-68 and

subsequent Ti insertion by TiCl_4 vapors. The Ti-MCM-68 oxidizes phenol more effectively than TS-1 (see Section 3.6). The preparation of Ti-YNU-2 is very elaborate; however, it brings further improvement of catalytic properties. Making the Ti-YNU-2, a pure silica precursor YNU-2P with a lot of internal defects [47] was prepared via hydrothermal synthesis, stabilized by steaming, and Ti was inserted using TiCl_4 vapors. The Ti-YNU-2 was prepared with Si/Ti molar ratios 80–240 and it contained a significant amount of extra-framework 5- and 6-coordinated Ti species [17]. However, the authors claim that these species are also active in the oxidation catalysis and furthermore contribute to the catalyst *para*-selectivity in phenol oxidation to *para*-hydroquinone and *para*-benzoquinone (see Section 3.6). Comparison of typical textural properties and Ti contents of the discussed catalysts is provided in Table 1.

2.1.2 Large-pore titanosilicates

Ti-beta (Ti-beta) is a large-pore zeolite, which has been successfully prepared with the titanium isomorphously incorporated in the framework. First, it was reported as a titano-aluminosilicate by Cambor et al. [51] and later aluminium-free Ti-beta was prepared in the presence of tetraethylammonium hydroxide (SDA). In contrast to the TS-1, it is usually obtained in a low yield using the conventional hydrothermal synthesis [52]. To improve both yield and the catalytic properties of the Ti-beta, alternative synthetic methods, e.g., seeding of the synthesis gel with dealuminated zeolite Beta [53], use of alternative templates (e.g., di(cyclohexylmethyl)dimethylammonium cation, diquaternary ammonium SDAs based on triethylamine or 1,4-diazabicyclo[2.2.2]octane) [54,55], synthesis in fluoride media [56], and dry gel conversion method [57,58] were developed. Use of very complex polycyclic diammonium SDA enables to form pure titanosilicate beta polymorph C denoted Ti-ITQ-17 (BEC) [50]. The main reason for investigation of all these synthesis methods was to reduce or avoid using of aluminium source to prepare an aluminium-free Ti-beta. The Ti-beta was the first titanosilicate catalysts designed for selective oxidation of sterically demanding substrates [59,60].

Ti-ITQ-39 (*-ITN structure) is another large-pore titanosilicate, prepared by direct hydrothermal synthesis [61]. It is an intergrowth of 3 polymorphs with a 3-dimensional system of interconnected 12-ring and 10-ring pores. It is prepared using ethyl(ethyl-propylpiperidinium-4-yl)pyrrolidinium SDA in absence of alkali cations (what is advantageous). The titanium atoms are well incorporated in framework positions (evidenced by a clear band at 210 nm in its UV/Vis spectrum) and the catalyst provides similar results as Ti-beta (see Section 3). However, the complex SDA and long crystallization time (30 days) are significant drawbacks. Having in mind also similarity to Ti-beta (from the catalysis point of view), a practical use of Ti-ITQ-39 is hardly

Table 1. Basic comparison of structure and textural properties of the discussed conventional titanasilicate catalysts.

Titanosilicate	IZA code	Channel system	Synthesis ^a method	Typical properties ^b			References
				BET (m ² /g)	V _{mic} (cm ³ /g)	V _{tot} (cm ³ /g)	
TS-1	MFI	3D 10 × 10 ring	HTS	450	0.13	0.16	[9,10,28,31,34–37]
Ti- MWW	MWW	2D 10 × 10 ring	HTS, PS	434	0.17	0.33	[12,38,39,43,48]
Ti-ITQ-7	ISV	3D 12x12x12	HTS	n.a.	n.a.	n.a.	[49]
Ti-ITQ-17	BEC	3D 12x12x12	HTS	n.a.	n.a.	n.a.	[50]
Ti-MCM-68	MSE	3D 12x10x10 ring	PS	500	0.19	n.a.	[44–46]
Ti-YNU-2	MSE	3D 12x10x10 ring	PS	n.a.	n.a.	n.a.	[17]
Ti-beta	*BEA	3D 12x12x12 ring	HTS, F, DG	600	n.a.	n.a.	[51–60]
Ti-ITQ-39	*JTN	3D 12x10x10 ring	HTS	n.a.	n.a.	n.a.	[61]
Ti-SSZ-24	AFI	1D 12 ring	PS	329	0.14	0.16	[62]
Ti-SSZ-33	CON	3D 12x12x10 ring	PS	654	0.24	0.42	[62]
Ti-SSZ-42	IFR	1D 12 ring	PS	497	0.21	0.24	[62]
Ti-UTD-1	DON	1D 14 ring	HTS	n.a.	0.11	n.a.	[63]
Ti-CIT-5	CFI	1D 14 ring	HTS, PS	295	0.10	0.22	[62,64]
Ti- UTL	UTL	2D 14 × 12 ring	HTS	539	0.24	0.29	[19,65]
Ti-IPC-2	OKO	2D 12 × 10 ring	ADOR	383	0.15	0.22	[19,65]
Ti-IPC-4	PCR	2D 10 × 8 ring	ADOR	237	0.10	0.15	[19]

^a HTS – direct hydrothermal synthesis, PS – post-synthesis titanium introduction, F – direct synthesis in fluoride media, DG – dry gel conversion method, ADOR – synthesis via ADOR method from a parent titano-germano silicate

^b Textural properties: BET area (BET), micropore volume (V_{mic}), total pore volume (V_{tot}) determined by N₂ physisorption at –196°C and titanium content of a representative sample of the catalyst: n.a. – not available.

expectable. To complete the picture, also large-pore titano-germanosilicate Ti-ITQ-7 (**ISV**) should be mentioned. In this case, use of GeO_2 is crucial to prepare the material without seeding [49].

Post-synthesis titanium incorporation is another method to prepare large-pore titanosilicates. Wu et al. demonstrated preparation of Ti-MOR by vapor phase insertion of Ti into dealuminated mordenite. ^{18}O exchange of the samples and subsequent IR analysis confirmed that the Ti-MOR contains titanium atoms bound via 3 or 4 oxygen bridges in the aluminium vacancies [66]. The Ti-MOR proved to be able to catalyze ketone ammoxidation [67] and oxidation of aromates to fenols with hydrogen peroxide [68]. Titanium can be inserted into silanol nests formed by a selective removal of some other heteroatom from zeolite structure. In this way, large-pore titanosilicates were prepared in a two-step deboronation-titanium impregnation procedure [62]. Ti-SSZ-24 (Ti-**AFI**), Ti-SSZ-33 (Ti-**CON**), Ti-SSZ-42 (Ti-**IFR**), and Ti-CIT-5 (Ti-**CFI**) were prepared from corresponding borosilicates and impregnated by TBOTi solution, TiCl_4 solution or TiCl_4 vapors. The TiCl_4 impregnated titanosilicates contained considerable amounts of anatase phase besides the desired framework titanium species. On the other hand, the TBOTi impregnation resulted mostly in the formation of the desirable framework titanium species but with generally lower overall titanium content ($\text{Si/Ti} > 450$). Obviously, TBOTi molecule is less reactive than TiCl_4 and too bulky to diffuse easily into the core the zeolite crystals. Therefore, the local titanium content close to the crystal surface is expected to be significantly higher and there also the oxidation reactions take place. The character and connectivity of the channel system plays an important role in both titanium incorporation and subsequent catalysis. The Ti-**CON** has a three-dimensional channel system of 12- and 10-ring pores while the other zeolites have only 1-dimensional system of 12-ring pores (Ti-**CFI** 14-ring). Ti-**CON** was the only material with higher catalytic activity than conventional TS-1 (see Section 3.2). Comparison of textural properties and Ti contents of the discussed catalysts is provided in Table 1.

2.1.3 Extra-large pore titanosilicates

Among the extra-large pore zeolites, three zeolites with Ti have been prepared until now. Balkus et al. reported synthesis of Ti-**DON** (14-ring 1-dimensional channels) using a special bis(pentamethylcyclopentadienyl) cobalt(III) hydroxide SDA [63]. Our group succeeded in preparation of two novel extra-large pore titanosilicate zeolites Ti-**CFI** (1-dimensional 14-ring channels)[64] and Ti-**UTL** (2-dimensional system of intersecting 14-ring and 12-ring channels) [19]. Especially the successful synthesis of the Ti-**UTL** is important, because the Ti-**UTL** is an ADOR active titano-germanosilicate [69]. It can be transformed into a number of other titanosilicate catalysts including Ti-**OKO** (12- x 10-ring 2-dimensional channel system, denoted

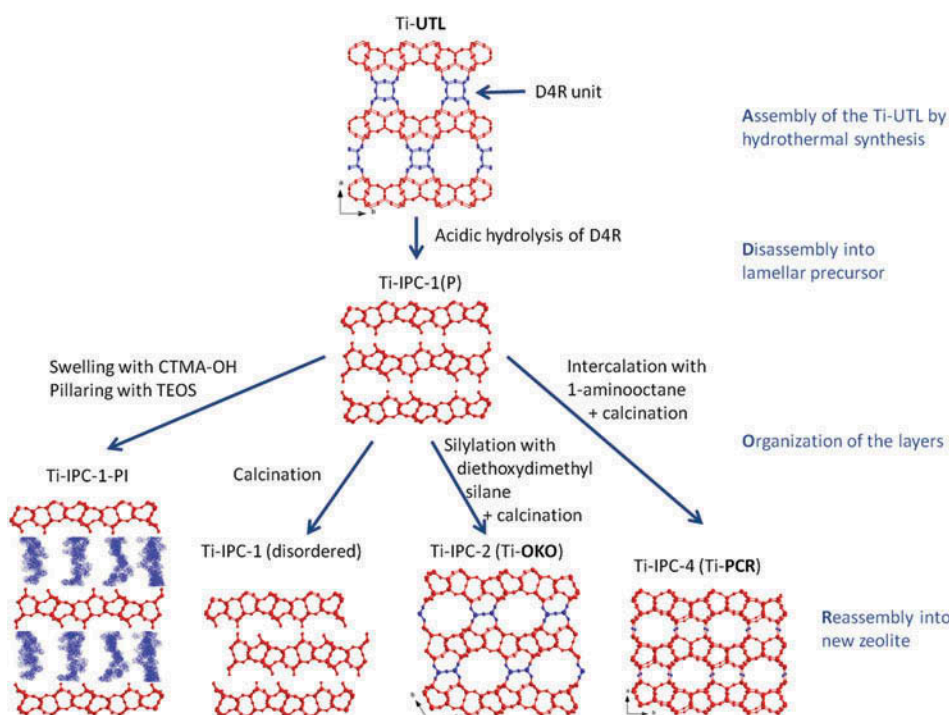


Figure 2. Ti-UTL top-down and ADOR transformation via lamellar Ti-IPC-1(P). Scheme is based on the reference [19]. CTMA-OH stands for cetyltrimethylammonium hydroxide.

also Ti-IPC-2) and Ti-PCR (10- x 8-ring 2-dimensional channel system, denoted also Ti-IPC-4) zeolites (the ADOR process) and pillared Ti-IPC-1-PI based materials (top-down transformation; see Section 2.3.1). The ADOR process itself is described in detail elsewhere [69–73]. Ti-UTL structure can be viewed as dense titanosilicate layers connected with germanium rich double 4-ring (D4R) structural units (Figure 2). Treatment of Ti-UTL with diluted hydrochloric acid (or just water) dissolves these D4R units providing lamellar material (Ti-IPC-1(P)). This lamellar material can be further treated similarly to Ti-MWW-P lamellar precursor. When the Ti-IPC-1(P) is simply calcined, a disordered material with poor textural properties denoted Ti-IPC-1 is obtained. Silylation of the Ti-IPC-1(P) with diethoxydimethylsilane in the sense of interlayer expanded zeolite synthesis (Section 2.3.2) results in formation of Ti-OKO after calcination. A fully connected zeolite is obtained thanks to a close vicinity of the silanol groups remaining after dissolution of D4R units. The Ti-IPC-1(P) layers can also be organized by intercalation with 1-amino-octane and in this case, the material condense into Ti-PCR upon calcination, similarly to formation of Ti-MWW. Comparison of the channel systems and textural properties is provided in Table 1. The Ti-UTL was prepared with Si/Ti ratio molar 100–140 and framework titanium were the dominant species. The Ti-OKO (Si/Ti = 210) and Ti-PCR (Si/Ti = 140)

are not very promising epoxidation catalysts because they are large-pore resp. medium-pore titanosilicates prepared by a multi-step procedure. Nevertheless, their successful synthesis and catalytic activity is a strong proof of concept showing that the ADOR approach is generally applicable to the zeolite synthesis.

Ti-CFI [64] was prepared using *N*-methylsparteinum hydroxide in the presence of LiOH, which is important for the CFI structure formation. The titanium content ranged from Si/Ti 106 to 23 but all samples contained also extra-framework titanium species. The ability of CFI to isomorphously incorporate titanium atoms appears to be lower than for TS-1. Treatment of the as-synthesized material with nitric acid substantially reduced the amount of extra-framework titanium species (the intensity of their characteristic UV/Vis band decreased).

2.2 Hierarchical titanosilicate catalysts

Various methods exist to introduce additional mesoporosity into zeolites. These can be divided into top-down and bottom-up approaches (Figure 3). Top-down routes comprise of post-synthesis treatment of previously grown zeolite to extract framework atoms [74–76]. For titanosilicates only base leaching (desilication) can be used because titanosilicate zeolites are resistant even to concentrated mineral acids (e.g., Ti-MWW [39]). Using bottom-up approaches, the mesopores are formed during hydrothermal synthesis of the

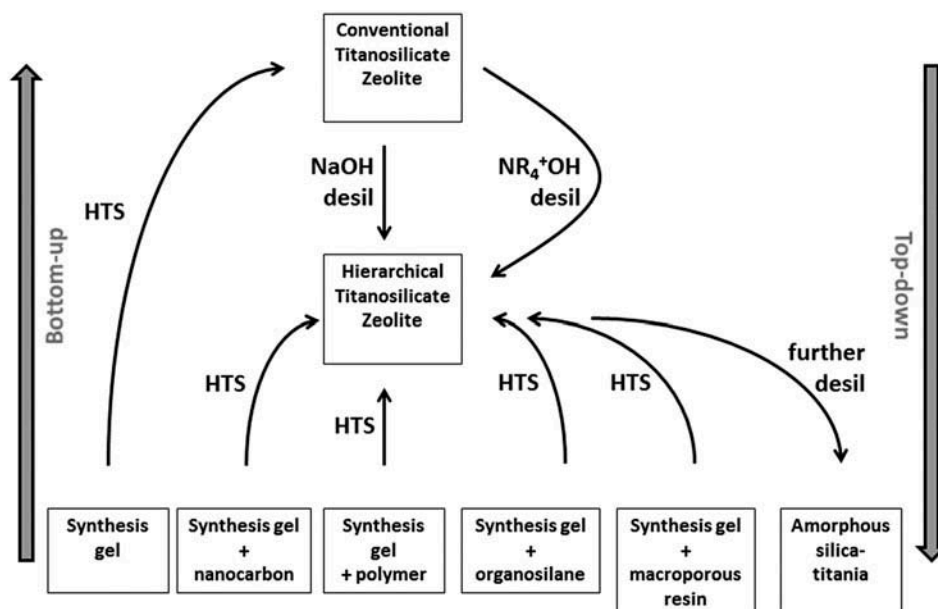


Figure 3. Different approaches to preparation of hierarchical titanosilicates. HTS stands for hydrothermal synthesis, desil stands for desilication, R stands for alkyl chain or hydrogen.

Table 2. Overview of the discussed hierarchical TS-1 materials prepared using different methods.

Titanosilicate ^a	Preparation method	Textural properties ^b					Ref.
		BET (m ² /g)	V _{mic} (cm ³ /g)	V _{meso} (cm ³ /g)	d _{meso} (nm)	Si/Ti	
TS-1	conventional synthesis	450	0.13	0.03	–	40	[82]
TS-1–0.15-SP-N-24	desilication TPA-OH/NH ₄ OH	477	0.09	0.18	16–32	41	[83]
TS/NaOH&TBAOH	desilication TBA-OH/NaOH	442	0.09	0.32	n.a.	21	[84]
C 40wt%TS-1 MW	carbon templated, microwave synthesis	382	0.06	0.14	18	100 ^c	[85]
MTS-1	RCQA-1 polymer templated	428	0.10	0.28	6–8	38.5	[79]
TS-1(O ₁)	amphiphilic organosilane assisted	716	n.a.	0.57 ^d	3.9	31	[80]
HPB-TS-1	crystallization in pores of resin	227	n.a.	0.55 ^d	30–60	30–60	[81]
TS-1(L)/MesoTS-1	polymer templated, fluoride medium	408	n.a.	0.03	3.9	3.9	[86]

^a Catalyst labels taken from original references.

^b Textural properties determined from N₂ sorption at –196°C; BET - BET area, V_{mic} micropore volume, V_{meso} mesopore volume, d_{meso} mean mesopore diameter, n.a. - not available.

^c Si/Ti ratio in the synthesis mixture

^d total pore volume

zeolite usually by incorporation of a secondary template. For hierarchical titanosilicates a wide variety of secondary templates including nanocarbon [77,78], polymers [79], long alkyl-organosilanes [80], and crystallisation in meso/macro pores of a resin [81] has been reported. Comparison of the hierarchical titanosilicate catalysts prepared using both approaches is provided in Table 2.

2.2.1 Desilication

Desilication has been studied intensively for MFI, MTW, MOR, and beta aluminosilicates and benefits of the alkaline treatment were demonstrated on a number of reactions [76]; however, reports on titanosilicate desilication are rare and the only studied parent material is TS-1.

For the TS-1 desilication with NaOH solution, low concentration of NaOH (≤0.2 mol/l) should be used, because in more concentrated solutions (0.4–0.8 mol/l) total destruction of TS-1 framework occurs readily [87]. In contrast to NaOH solutions, desilication with quarternary ammonium hydroxides is slower. Wang et al. [83] studied desilication of TS-1 using a mixture of TPA-OH and aqueous ammonia (overall concentration of OH[–] ions < 0.25 mol/l) under hydrothermal conditions (150°C). The addition of ammonia intensified the desilication process (which was slow in pure TPA-OH solution even at 150°C). Mesopore volume up to 0.18 cm³/g was achieved. Otherwise, it is hard to judge effectivity of this particular procedure since all the materials including the parent TS-1 contained a considerable amount of anatase. Desilication of TS-1 with NaOH and tetrabutylammonium hydroxide (TBA-OH) [84] for 30 min at 65°C provided a mesoporous

TS-1 with micropore volume of $0.09 \text{ cm}^3/\text{g}$, mesopore volume of $0.36 \text{ cm}^3/\text{g}$, well-preserved XRD pattern (83% crystallinity is claimed) and mostly 4-coordinated titanium. It should be noted that appropriate washing out of any alkali cation residues is very important after desilication because alkali cations strongly inhibit the catalytic activity of the resulting material [88,89].

The above data show that creation of mesoporosity by desilication in TS-1 is feasible; however, there are still issues to be investigated, i.e., influence of the used base and influence of the framework titanium on the desilication (since it is known that, e.g., the presence of aluminum influences the process a lot [76]). The authors note that for valid conclusions *inter-alia* a good quality parent material need to be used, what is not always the case in literature.

2.2.2 Secondary templating

Secondary templating is more robust than basic leaching; however, its main drawback lays in the necessity to sacrifice considerable amount of sometimes complex and costly organic material, which fills the mesopores after hydrothermal synthesis. Looking for cheap and easy to prepare secondary templates is an obvious way to follow. In what follows, we refer examples of different approaches, which were reported up-to-date.

Nanocarbon secondary templating might be considered a classical method of preparation of hierarchical zeolites in general and also titanosilicates [77,78]. From the synthesis point of view it represents simple addition of nanocarbon source into the synthesis mixture and resulting size and shape of mesopores reflect the nanocarbon morphology. Ok et al. [85] prepared mesoporous TS-1 using a combination of hard templating with 12 nm carbon nanoparticles together with microwave assisted synthesis in less than 100 min of crystallization time. The materials exhibited mesopore volume from $0.10\text{--}0.14 \text{ cm}^3/\text{g}$ (reference TS-1: $0.08 \text{ cm}^3/\text{g}$) depending on the amount of carbon used (ranging 10–40 wt. % based on silica source). Note that Koo et al. achieved mesopore volume up to $0.82 \text{ cm}^3/\text{g}$ while preparing Al-MFI under similar conditions with carbon nanoparticles (90).

Besides nanocarbon particles, polymers can be used as secondary templates. Kang et al. [79] reported synthesis of mesoporous TS-1 material denoted MTS-1 using a mesoscale random copolymer (denoted RCQA-1, average molecular weight ca. 36 kDa, synthesized by radical copolymeration of diallylamine and diallyl-dimethylammonium chloride in water) containing quarternary ammonium groups as a template. After calcination, the material exhibited a well resolved MFI XRD pattern and it contained mesopores having 6–8 nm in diameter. The mesopore volume was $0.28 \text{ cm}^3/\text{g}$. Tetrahedrally coordinated titanium was the dominant species according to the DR-UV/Vis spectroscopy, but some anatase-like phase was detected as minority. Jiang et al. [86] used a similar polymer (polydiallyldimethyl ammonium chloride) in fluoride medium synthesis. In this case a composite

material was formed having TS-1 core ($18 \times 3 \times 2 \mu\text{m}$ coffin shaped crystals) and mesoporous silica-titania shell (40–50 nm thick; composite denoted TS-1 (L)/mesoTS). No mesopores were present inside the TS-1 crystals probably because the used polymer was excluded during crystallization. Syntheses in fluoride medium are known to provide large crystals of zeolites with a decreased number of defects [91] and therefore goes against formation of hierarchical materials because the mesopores are in fact defective parts of the crystal.

Singh et al. [80] prepared mesoporous TS-1 with amphiphilic organosilane (alkyl-(3-trimethoxysilyl)ammonium chloride, where alkyl was octadecyl or tetradecyl) as pore-directing agent together with TPA-OH. The use of octadecyl organosilane led to formation of well crystalline TS-1 with increased BET area (up to $716 \text{ m}^2/\text{g}$) and total pore volume (up to $0.57 \text{ cm}^3/\text{g}$) while the samples prepared with tetradecyl organosilane were amorphous. TEM image as well as pore size analysis revealed presence of homogenous mesopores with mean diameter of about 3.5 nm. UV/Vis spectra of all the presented samples contained strong signals of extraframework and anatase titanium species because quite high titanium loadings were used in the synthesis (Si/Ti = 15, 30, and 60).

Cheng et al. [81] let the TS-1 crystallize in pores of an anion-exchange resin (Amberlite IRA-900) forming sponge-like agglomerates of the TS-1 crystals. Total pore volume of the final catalyst was $0.55 \text{ cm}^3/\text{g}$, but the BET area was rather low ($227 \text{ m}^2/\text{g}$) for crystalline TS-1 (usually $400\text{--}500 \text{ m}^2/\text{g}$ [82]) so it is questionable whether, e.g., all carbon remaining of the resin were successfully removed during calcination. The final material contained mainly 4-coordinated titanium species since the others (extraframework 5-, 6-coordinated species) were washed out with nitric acid before calcination.

2.3 Lamellar catalysts

2.3.1 Layered and pillared catalysts

Some zeolites (e.g., MWW, FER, and several others [14]) form lamellar precursors which, upon calcination, condense into fully connected zeolitic structure. These lamellar precursors can be transformed in more open structures preserving their crystallinity as well as the layered character, e.g., via swelling and pillaring, delamination, or other post-synthesis modifications [92]. The layered catalysts possess high external surface and/or wide slit-shaped mesopores in between layers. Therefore, the active sites located on the surface of the layers are well accessible even for sterically demanding molecules, which diffuse with obstacles in the micropores [93]. As a result, lamellar zeolite catalysts can offer similar or better properties in comparison

Table 3. Overview of layered and pillared titanasilicate catalysts.

Titanosilicate	IZA code	Characteristic	Textural properties ^a				Si/Ti	Ref.
			BET (m ² /g)	S _{ext} (m ² /g)	V _{mic} (cm ³ /g)	V _{tot} (cm ³ /g)		
TS-1	MFI	conventional	450	151	0.13	0.16	40	[82]
Ti-MWW	MWW	conventional	434	n.a. ^b	0.17	0.33	102	[43]
lam-TS-1	MFI	layered, C ₁₆₋₆₋₆	580	425	n.a.	0.61	57	[15]
lam-TS-1	MFI	layered, C ₁₈₋₆₋₆	511	226	0.13	0.51	33	[82]
lam-TS-1	MFI	layered, C ₂₂₋₆₋₆	510	357	0.15	0.60	58	[94]
TS-1-PiSi	MFI	silica pillared	575	337	0.11	0.46	55	[82]
TS-1-PITi	MFI	silica-titania pillared	634	402	0.10	0.37	20	[82]
Ti-MCM-36	MWW	silica pillared	786	629	0.07	0.44	57	[82]
40Si/Ti-MCM-36(E)	MWW	silica-titania pillared	1118	n.a.	0.01	0.56	15	[43,95]
Ti-IPC-1-PiSi	UTL based	silica pillared	1001	n.a.	0.00	0.67	480	[19]
Ti-IPC-1-PITi	UTL based	silica-titania pillared	910	n.a.	0.00	0.46	16	[19]
G-TiNS	MFI	Ti impregnated, layered	609	448	n.a.	0.71	98	[96]
Ti-DZ-1	MWW	Ti impregnated, delaminated	n.a.	171	0.04	0.18	67	[41]
MTS-2	MEL	self-pillared	573	333	0.11	0.76	36	[18]
HTS-1	MFI	composite	339	60	0.13	0.37	50	[97]

^a Textural properties determined from N₂ sorption at -196°C; BET - BET area, S_{ext} - external surface area, V_{mic} micropore volume, V_{tot} total pore volume, n.a. - not available.

with hierarchical zeolite catalysts [27]. Overview of the discussed catalysts is provided in Table 3.

However, creation of lamellar structures was impossible until recently for most of industrially relevant zeolites including the TS-1 material. In 2009, Ryoo group [98] disclosed the synthesis of nanosheet ZSM-5 (**MFI** aluminosilicate) and in 2011 the same group reported also the synthesis of nanosheet TS-1 (hereafter referred to as layered TS-1 or lam-TS-1) [15]. The layered TS-1 was synthesized by so-called restricted crystal growth mechanism. Specially designed diquarternary ammonium surfactant C₁₆H₃₃-N⁺(CH₃)₂-C₆H₁₂-N⁺(CH₃)₂-C₆H₁₃ (denoted C₁₆₋₆₋₆) templates the crystallization of the **MFI** structure by its hydrophilic end but long hydrophobic chain prevents the crystal growth in the crystallographic direction of *b*-axis for **MFI**. Thus, single crystals as nanosheets with a unit cell thickness are formed (Figure 4). The layered TS-1 exhibited external surface area 425 m²/g being approximately 75% of the overall BET area (580 m²/g). Reference TS-1 had BET area 393 m²/g and external surface area 65 m²/g. Titanium was present mainly with tetrahedral coordination without anatase-like phase. The Si/Ti ratio was 57. The authors showed also, that the amount of silanol groups present in the material may be adjusted by treatment of the as-synthesized layered TS-1 with diluted NH₄F aqueous solution (0.008% wt.) at 100°C. Approximately 40% of the terminal silanol groups were removed according to the IR and ²⁹Si MAS NMR forming siloxane bridges between two neighboring silanols.

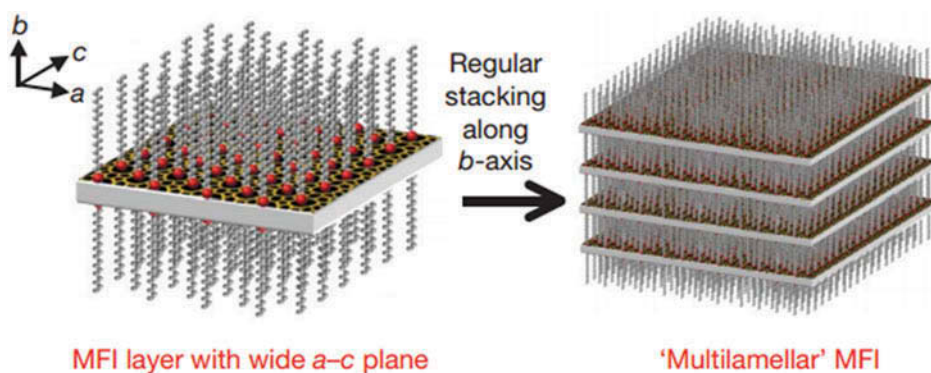


Figure 4. Surfactant templated MFI nanosheets. Adapted with permission from Choi et al. [98]. Copyright Macmillan Publishers Ltd. (2009).

Shortly after the Ryoo group, Wang et al. [94] reproduced the lam-TS-1 synthesis with C_{22-6-6} surfactant (similar to Na et al. [15], bearing a longer C_{22} hydrophobic chain). The synthesis time considerably increased with the use of a longer surfactant (from 10 days for C_{16-6-6} to 20 days). Authors also established the optimum (no article) surfactant/Si molar ratio for the crystallization, $0.04 \leq C_{22-6-6}/Si \leq 0.08$. This is close to the Ryoo group synthesis protocol (surfactant/Si = 0.07) [15]. Note that lamellar TS-1 was successfully prepared with diquarternary ammonium surfactant templates bearing C_{16} , C_{18} , and C_{22} hydrophobic chains but for pure silica MFI, the minimum chain length to obtain layered material was found C_{10} [99].

Přech et al. [82] pillared layered TS-1 with tetraethyl orthosilicate (TEOS) at 65°C to increase the interlayer distance in the final catalyst and thus the accessibility of active centres in a similar way as for Ti-MCM-36 [100] (swelling and pillaring of the Ti-MWW layers). Drawing the parallel with Ti-MCM-36, the swelling of the layers was not necessary for lam-TS-1 since it was swollen intrinsically by the surfactant template (Figure 4). The pillared TS-1 material (hereafter denoted TS-1-PiSi) exhibited increased external surface area ($384 \text{ m}^2/\text{g}$) in comparison with the layered TS-1 ($293 \text{ m}^2/\text{g}$) and the preservation of the high interlayer distance (2.5–3 nm) was characterized by a low angle X-ray diffraction line ($2\theta = 1.7^\circ$) [94]. The authors prepared also silica-titania pillars (hereafter denoted TS-1-PiT_i; in Přech et al. [82] denoted Ti-pillared TS-1), where titanium source (typically 1–10 mol% of titanium (IV) butoxide (TBOT_i)) was added into the pillaring mixture. The silica-titania pillaring significantly increased the titanium content ($\text{Si}/\text{Ti} = 14\text{--}30$ vs. $\text{Si}/\text{Ti} = 55\text{--}93$ in TS-1-PiSi) although it caused formation of extraframework titanium species (cf. DR-UV/Vis spectra in the Přech et al. [82]). Nevertheless, silica-titania pillaring strongly improved the catalytic properties of the material (see Section 3.2) especially when using $n(\text{TEOS})/n(\text{TBOT}_i) = 20/1$.

The silica-titania pillaring was successfully applied also on other lamellar zeolites. As for **MWW-P** an almost purely mesoporous titanosilicate was formed (micropore volume $0.02 \text{ cm}^3/\text{g}$, mesopore volume $0.52 \text{ cm}^3/\text{g}$) [43,95] as well as for **IPC-1P** and **Ti-IPC-1P** lamellar precursors formed by disassembly of **UTL** resp. **Ti-UTL** [19]. In all cases, the silica-titania pillared material contained extraframework Ti species (which can be removed by HNO_3 washing before calcination [43]) but in all cases the silica-titania catalysts pillared provided high conversions and yields in comparison with conventional titanosilicates in epoxidation of bulky substrates (see Section 3.2) and proved to be a robust alternative to direct hydrothermal synthesis of the titanosilicate material [19,43].

TBOTi can be used also for impregnation of **MFI** nanosheets [96] and **MWW-P** layers. Ouyang et al. [41] prepared a delaminated **MWW** titanosilicate (denoted **Ti-DZ-1**) by deboronation-delamination of **B-MWW-P** borosilicate lamellar precursor (denoted **ERB-1P**, same as in Jin et al. [43]) in aqueous $\text{Zn}(\text{NO}_3)_2$ at $\text{pH} = 1$ and subsequent insertion of titanium into the silanol nests previously occupied by boron atoms by TBOTi solution in *n*-butanol (note the same procedure as in Přech et al. [62] and Kim et al. [96]). Si/Ti ratio 67 in the final material was achieved and the UV/Vis spectrum contains a very broad band centred at approx. 230 nm; however, no absorption above 300 nm was observed evidencing no presence of anatase.

The crucial step in post-synthesis formation of lamellar titanosilicate is impregnation of the crystalline layers with titanium butoxide [96] (similar to insertion of titanium into boron vacancies [62]). The reaction of TBOTi is expected to be faster than TEOS pillaring because TBOTi is more reactive than TEOS. The TBOTi reacts preferentially with the silanol groups on the surface of the layers forming isolated Ti species, which are active in selective oxidation catalysis. During the silica-titania pillaring, the TEOS plays role of an inert solvent in the initial phase similarly to 1-butanol in case of impregnation.

Chen et al. synthesized a multilamellar **MEL** type titanosilicate catalyst (denoted **MTS-2**) [18]. Its morphology might be considered similar to Ryoo nanosheet **MFI** [15]; however, the material is closer to Tsapatsis self-pillared pentasil material [101] (intergrowth of **MEL** and **MFI** with a house of cards morphology). Also the synthesis procedure is similar to self-pillared pentasil (tetrabutylammonium and cetyltrimethylammonium hydroxides (**CTMA-OH**) as SDAs). From the structural point of view, it represents an ultimate goal of the layered titanosilicate synthesis: a fully crystalline material with very open structure. A sample of **MTS-2** exhibited external surface area $333 \text{ m}^2/\text{g}$, and total pore volume $0.76 \text{ cm}^3/\text{g}$ while BET area was $573 \text{ m}^2/\text{g}$ and micropore volume $0.11 \text{ cm}^3/\text{g}$ being composed of crystalline phase only.

Si/Ti ratio ranged between 35 and 40 with 4-coordinated titanium as dominant species.

Li et al. [97] prepared a conventional/layered composite catalyst denoted HTS-1. It was a core/shell structure where the core was conventional TS-1 while the shell comprised of crystalline lamellar nanosheets with a unit-cell thickness. The shell was formed by desilication/recrystallization process with diquarternary ammonium surfactant denoted C_{18-6-3} (*vide supra*) in hydroxide form together with NaOH to boost the alkalinity. This surfactant normally templates the crystallization of lamellar TS-1 according to the Ryoo procedure [15]. In this process the hydroxide was responsible for the desilication and the dissolved framework species of TS-1 core served as a silica and titanium source for crystallization of the lamellar shell around the parent crystal. The desilication-recrystallization occurred at hydrothermal conditions. The resulting composite exhibited increased mesopore volume ($0.24 \text{ cm}^3/\text{g}$ vs. TS-1: $0.02 \text{ cm}^3/\text{g}$, lam TS-1: $0.18 \text{ cm}^3/\text{g}$). The composite contained 4-coordinated as well as extraframework and anatase-like titanium species (cf. UV/Vis spectra). The overall titanium content did not change dramatically (ICP-AES: Si/Ti = 46 (parent) vs. Si/Ti = 50 (HTS-1)) while the XPS analysis revealed Si/Ti = 193 in the catalyst shell.

A special group of layered zeolite-based materials are the so-called delaminated zeolites. These are prepared from layered zeolite precursors by an ultrasound treatment in a basic medium or by other techniques allowing to partially break the interlamellar hydrogen bonds and orientate the layers randomly one to another. Ideally, the resulting material has a house of cards morphology and wide slit-shaped mesopores in between the layers. Pioneering work in this area has been done by the Corma group [102,103]. Shortly after, delaminated zeolites containing titanium were introduced as well. Of these, Ti-ITQ-2 [104], del-Ti-MWW [105], Ti-MCM-56 [106], Ti-ITQ-6 [107], and Ti-ECNU-8 [108] materials should be mentioned for the complete picture. The first three materials are composed of MWW crystalline layers while Ti-ECNU-8 and Ti-ITQ-6 have FER structure.

2.3.2 Interlayer expanded titanosilicates

Interlayer expanded titanosilicates (IEZ) are well-ordered materials, where a silicon (or titanium) atom is inserted in between two silanol groups located on the surface of layers of a lamellar precursor (Figure 5). Among the (titanosilicate) zeolites, which can undergo the interlayer expansion, the Ti-MWW is the most prominent and the most studied material. IEZ titanosilicates are listed in Table 4.

Fan et al. (2004) reported a material denoted Ti-YNU-1 [110], in which the Ti atoms are in bridging positions between the expanded MWW layers [111]. To some extent, the Ti-YNU-1 can be compared with silica-titania pillared catalysts (see Section 2.3.1). Ti-YNU-1 possesses 12-ring channels

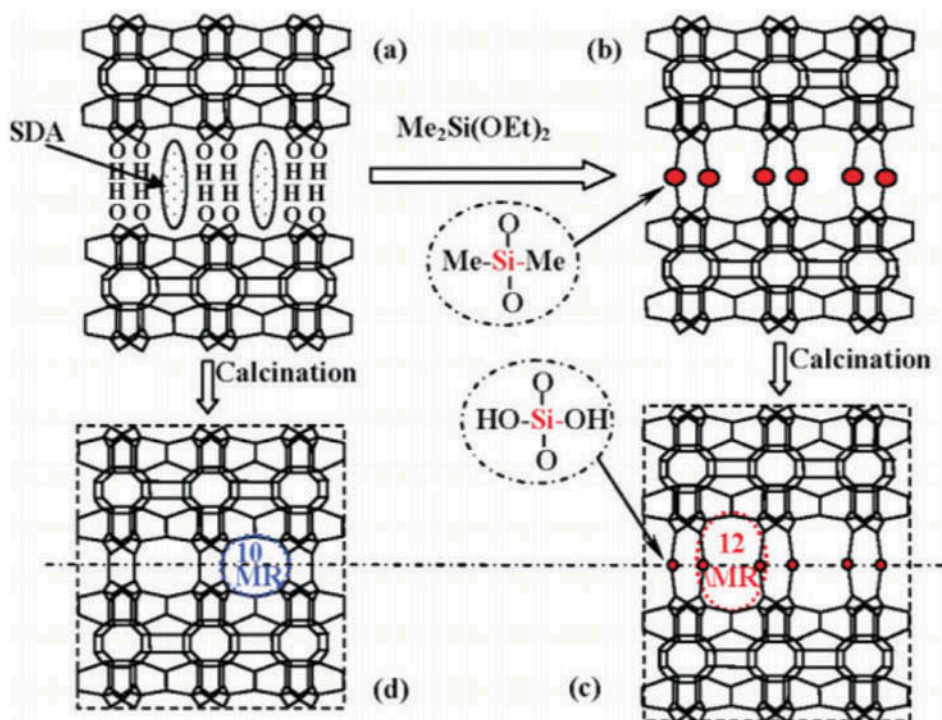


Figure 5. Synthesis route to obtain MWW (d) and IEZ-MWW (c) from MWW-P (a). Reprinted with permission from Wu et al. [109]. Copyright American Chemical Society (2008).

Table 4. Overview of IEZ titanasilicate catalysts.

Titanosilicate	IZA code	Pore size (Å) ^a	Characteristic	Typical properties ^b			Ref.
				BET (m ² /g)	V _{tot} (cm ³ /g)	Si/Ti	
Ti-MWW	MWW	5.3	Zeolite	434	0.33	102	[43]
Ti-YNU-1	MWW	6.6 ^c	IEZ	676	0.2	227	[110–114]
Ti-MWW-exp	MWW	5.3, 7.3	IEZ	n.a.	n.a.	58	[115]
Ti-IEZ-MWW(Si)	MWW	n.a.	IEZ	563	n.a.	119	[40,116,117]
Ti-IEZ-MWW(SiSi)	MWW	n.a.	IEZ	574	n.a.	49	[40]
Ti-COE-3	CDO	5.4	IEZ	189	0.09	149	[33]
Ti-COE-4	CDO	5.5	IEZ	294	0.14	150	[33]

^a Pore size determined from low pressure Ar adsorption at -196°C

^b Textural properties determined from N_2 sorption at -196°C ; BET - BET area, V_{tot} total pore volume, n.a. - not available.

^c Pore size from the crystal structure

(6.6 x 5.5 Å) in the positions where the Ti-MWW has only 10-ring channels (4.0 x 5.5 Å) and YNU-1 interlayer distance is expanded by 2.59 Å in comparison with MWW. Ti-YNU-1 possesses more uniform distribution of Ti sites characterized by a narrow band centred at 210 nm (like the TS-1) [112] although the bridging titanium atom in Ti-YNU-1 should be a $\text{Ti}(\text{OSi})_2(\text{OH})_2$ species. The spectrum of Ti-MWW usually contains a broad band at 220–230 nm [11] which points to tripodal coordination of Ti atoms [20]. The

titanium content in Ti-YNU-1 is relatively low ($\text{Si/Ti} > 150$ [112]), but this is the case of a number of otherwise very active epoxidation catalysts (e.g., Přeč and Čejka [19], Přeč et al. [62]). Attempting to increase the titanium content using the conventional method, the formation of Ti-YNU-1 is accompanied by Ti-MWW phase [113]. Si/Ti ratio 83 was achieved using deironated deFe-YNU-1 as precursor [114]. Molliner and Corma prepared a material denoted Ti-MWW-exp [115] by recrystallization of pure silica MWW (ITQ-1) with a titanium source, water and piperidine. The obtained material was characterized by Si/Ti ratio 58 and a single band at 210 nm in the UV/Vis spectrum. Argon adsorption suggested two distinct types of pores: pores with 5.3 Å in diameter (consistent with the intralamellar pores in MWW structure) and 7.3 Å pores which are expected to originate from the structure expansion similarly to Ti-YNU-1.

Xu et al. [40] applied so-called stabilization [14] with dichlorodimethylsilane (final material denoted Ti-IEZ-MWW(Si)) and dimeric $\text{Cl}(\text{CH}_3)_2\text{-Si-Si}(\text{CH}_3)_2\text{Cl}$ (final material denoted Ti-IEZ-MWW(SiSi)) in HNO_3 medium on the MWW-P lamellar precursor. Note that also diethoxydimethylsilane may be used for the stabilization [116,117]. The insertion of dimeric silanes required pre-swelling of the MWW-P with cetyltrimethylammonium bromide (CTMA-Br). The titanium was introduced by impregnation with H_2TiF_6 aqueous solution. As a result of the stabilization, the *c*-parameter of the unit cell (the interlayer distance) increased by 2.5 Å (consistent with the similar Ti-YNU-1 [111]) for $\text{SiCl}_2(\text{CH}_3)_2$ use and 5.8 Å with the use of $\text{Cl}(\text{CH}_3)_2\text{-Si-Si}(\text{CH}_3)_2\text{Cl}$, in comparison with conventional MWW. The UV/Vis spectra of the materials after titanium insertion contained a strong absorption band at 220 nm and a shoulder between 230–260 nm. The 220 nm band is typical for the Ti sites in the MWW structure [11] and the spectrum generally points to isolated titanol active sites $\text{Ti}(\text{OH})(\text{OSi})_3$ [20] whose presence is expectable with respect to the preparation procedure.

In addition to Ti-MWW-based catalysts, Xiao et al. [33] reported two interlayer expanded titanosilicates (denoted Ti-COE-3 and Ti-COE-4) composed of Ti-RUB-36 layers (CDO structure). The Ti-COE-3 was prepared from Ti-RUB-36 [118] by stabilization with dichlorodimethylsilane in acidic media (similarly to Ti-IEZ-MWW [40]). The Ti-COE-3 was template free and contained dimethylsilane bridging groups between the layers. Calcination of Ti-COE-3 led to transformation of the dimethylsilane bridges to dihydroxysilane bridges forming Ti-COE-4. The prepared materials possessed 10-ring pores of 5.4–5.5 Å in diameter (while CDO zeolite has 2-dimensional 8-ring channel system) and therefore the pore size was close to TS-1. The Ti-COE-3 and Ti-COE-4 were characterized by Si/Ti ratio 150 and framework 4-coordinated titanium species were predominant in both materials; however, formation of some anatase (UV/Vis band at 330 nm) and even

rutile TiO₂ (UV/Vis band at 380 nm) occurred during the interlayer expansion procedure.

2.4 Mesoporous titanosilicate catalysts

In 1992, ordered mesoporous molecular sieves were disclosed by Mobil researchers [119]. These siliceous materials show uniform mesopores with sizes up to 43 nm; however, their walls are built of amorphous silica. Corma et al. first reported Ti-containing MCM-41 [120]. Similar molecular sieve called Ti-HMS (hexagonal mesoporous silica) was prepared by Tanev et al. [121]. Tatsumi et al. prepared Ti-MCM-48 which possesses a 3-dimensional channel system with a cubic symmetry [122] and Ti-SBA-15, which is similar to Ti-MCM-41, but the main channels are connected with micropores [123]. In addition, the SBA-15 synthesis generally enables formation of wider pores than MCM-41. Recently, also hexagonal Ti-SBA-12 [16] and cubic Ti-SBA-16 [16] and Ti-KIT-5 [124] were prepared. The Ti-SBA-16 and Ti-KIT-5 are very similar (e.g., shape of the isotherms, BET area 800 m²/g vs. 700–800 m²/g) and their synthesis procedures differ only in details (the same SDA (Pluronic F127), similar composition of the synthesis mixture, synthesis temperature and time 80°C, 48 h vs. 100°C, 24 h) so it is possible that both Ti-SBA-16 and Ti-KIT-5 are in fact the same material, although slightly different symmetry group is ascribed to each of them (*Im3m* vs. *Fm3m*).

From the synthesis point of view, there are generally two approaches, universal for all the above mesoporous catalysts: (i) direct hydrothermal synthesis, usually with tetrapropyl orthotitanate as a Ti source and (ii) post-synthesis atom planting with titanocene dichloride (originally disclosed by Maschmeyer et al. [125]).

In the case of direct synthesis, original procedures developed for pure silica molecular sieves are optimized for presence of titanium source [16,121]. A drawback of direct synthesis is that part of titanium atoms is trapped inside the walls and therefore it is inaccessible but on the other hand, it is a single step procedure. The atom planting is a robust and universal method. The titanocene dichloride is usually introduced from a solution in CHCl₃ [125–127]. All the above materials are active in epoxidation of bulky substrates (e.g., norbornene) with bulky oxidants such as tert-butyl hydroperoxide (TBHP), clearly showing the expected benefits of mesoporous structure. However, in particular directly synthesized Ti mesoporous catalysts differ through references in distribution of titanium species and especially presence or absence of anatase (e.g., Kumar and Srinivas [16] vs. Anand et al. [124]) and there is no clear correlation between synthesis conditions and the anatase formation. Nevertheless, the undesirable influence of anatase phase usually does not manifest itself in epoxidation with organic

Table 5. Overview of mesoporous titanasilicate catalysts.

Titanosilicate	Symmetry	Synthesis ^a	Typical properties ^b				Ref.
			BET (m ² /g)	V _{tot} (cm ³ /g)	Mean pore size (Å)	Si/Ti	
Ti-MCM-41	Hexagonal	HTS,PS	936	0.49	20	56	[120,125–128]
Ti-HMS	hexagonal	HTS,PS	1031	1.11	26–30	100 ^c	[121,127]
Ti-MCM-48	cubic	HTS,PS	1296	n.a.	26	n.a.	[122,129]
Ti-SBA-15	hexagonal	PS	561	0.84	58	25–270	[123,127,129,130]
Ti-SBA-12	hexagonal	HTS	1015	1.49	59	39	[16]
Ti-SBA-16	cubic	HTS	765	0.67	35	54	[16]
Ti-KIT-5	cubic	HTS	849	0.58	55	5–19	[124]
Ti-MMS	–	HTS, PMMA	1053	n.a.	30+ macro	250	[131]
TiSil-HPB-60	–	HTS, anion resin	618	n.a.	450	36	[132]
BMB-TiSil	–	HTS, anion resin	792	1.03	35 + 310	33	[133]

^a HTS – direct hydrothermal synthesis, PS – post-synthesis titanium introduction, PMMA – polymethyl-methacrylate colloidal crystals as secondary template, anion-exchange resin as secondary template

^b Textural properties: BET area (BET), total pore volume (V_{tot}) and mean pore size determined by N₂ physisorption at –196°C and titanium content of a representative sample of the catalyst; n.a. – not available.

^c Si/Ti of the synthesis mixture

hydroperoxides. Table 5 compares basic features and characterisation of the above catalysts.

In addition to titanium incorporation, hydrophobicity is another issue receiving attention in development of the mesoporous titanosilicates. General drawback of mesoporous titanosilicates is high concentration of silanol groups on the surface of their walls resulting from their amorphous character. The surface silanols negatively influence the activity and selectivity of the catalyst especially in epoxidation reactions [128]. The hydrophobicity of the catalyst may be increased by silylation with trimethylsilyl chloride [134] or hexamethyldisilazane [126] but the thermal stability of such silylated catalyst is limited. A novel approach is introduction of fluorosilane species, which can withstand even calcination at 500°C in air [130]. Triethoxyfluorosilane is the usual fluorosilylation agent and it can be used for postsynthesis silylation [130] as well as a component of the synthesis mixture [135]. The effect of fluorosilylation was proved by analysis of water adsorption/desorption isotherms at 25°C where the water adsorption capacity at $p/p_0 = 0.6$ decreased by 85% in comparison with non-silylated catalyst and capillary condensation of water shifted to higher water relative pressure (ca. $p/p_0 = 0.65$ (conventional) vs. 0.85 (fluorosilylated)) [130].

Last but not least, all the secondary templates (mainly particles of polymers and resins), which are used in syntheses of hierarchical titanosilicate zeolites (see Section 2.2), can be used also in preparation of amorphous mesoporous titanosilicates [131–133].

2.5 Metal-titanosilicate composites

Titanosilicate catalysts are able to activate hydrogen peroxide but not oxygen [20]. Utilization of a catalyst, which would be able to generate H_2O_2 *in-situ* would simplify the overall selective oxidation process and overcome safety and environmental issues connected to H_2O_2 production, purification, and storage. Catalysts containing palladium or gold nanoparticles possess this ability [136,137]. Gold-containing catalysts are intensively studied for gas phase oxidation of propylene [138–143] while palladium containing catalysts found their use also in liquid phase oxidation [144–146]. Hayashi et al. [138] were the first who demonstrated epoxidation of propylene to propylene oxide with hydrogen and oxygen co-reactants using a gold-titanium oxide based catalyst. It is questionable if the titanium was the hydrogen peroxide-activating species in this particular case (bulk TiO_2 oxide does not activate H_2O_2 for selective oxidation [11]); nevertheless, this report brought attention to noble metal/titanosilicate bifunctional catalyst.

Discussing the liquid phase oxidation with Pd/titanosilicate catalysts, it was found that location of metal nanoparticles on the surface of titanosilicate catalysts such as TS-1 or Ti-MCM-41 does not provide sufficient effectivity of the H_2 and O_2 use. Considerable amount of produced H_2O_2 diffuse to the external solvent phase or is further decomposed [144]. Pd nanoparticles in core of the catalyst particles enhance the probability of the produced H_2O_2 contact with Ti site and subsequent selective oxidation reaction (Figure 6). Okada et al. [145,146] designed a core-shell structured catalyst (denoted Pd/SiO₂@Ti-MS), which consists of a silica core (average diameter 280 nm) supporting Pd nanoparticles (average size 3.5 nm). This Pd/SiO₂ catalyst is covered by mesoporous titanosilicate shell (about 30-nm thick, formed from TEOS and tetrapropyl orthotitanate using cetyltrimethylammonium bromide as SDA). This setup brought effective utilisation of the formed H_2O_2 . Similar catalyst where Pd was randomly distributed in the mesoporous phase was less active in subsequent catalytic tests. The final material contained 1 wt. % of Pd and 0.6 wt. % of Ti mostly in the form of 4-coordinated

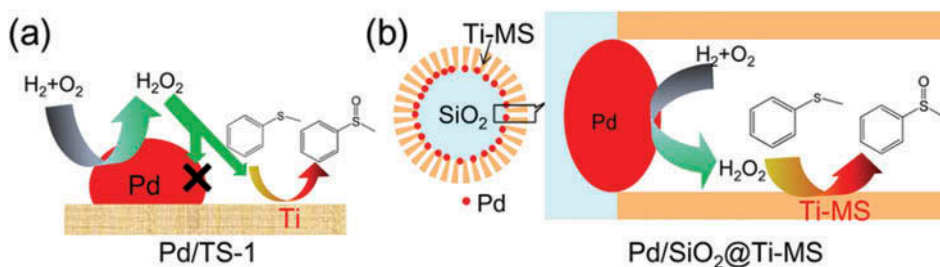


Figure 6. Schematic illustration of the conventional (Pd/TS-1) and core-shell (Pd/SiO₂@Ti-MS) catalyst. Reprinted with permission from Okada et al. [146]. Copyright American Chemical Society (2012).

species. Hydrophobicity of the mesoporous titanosilicate phase may be increased by addition of triethoxyfluorosilane (15 mol % optimum) during its synthesis [135]. Presence of triethoxyfluorosilane decreases the pore volume ($V_{\text{tot}} = 0.24$ vs. $V_{\text{tot}} = 0.30$ without its use) but on the other hand it brings positive effect on both conversion and selectivity of the sulfoxidation test reaction (see Section 3.5).

Omitting the dense SiO_2 core leads to egg-shell structured nanoreactors [147,148], where the Pd nanoparticles are encapsulated in mesoporous titanosilicate hollow spheres (denoted Pd@Ti-HHS, Figure 7). The titanosilicate spheres had 60–200 nm in diameter with about 15-nm thick wall and several Pd nanoparticles (diameter of about 4 nm) were located in each sphere. The Pd@Ti-HHS was prepared using oil-in-water microemulsion. Stearic acid (used as oil-phase) played also role of a surfactant and counter anion to Pd^{2+} ions (precursor of Pd nanoparticles). The mesoporous spheres precipitated from TEOS, tetrapropyl orthotitanate (TPOTi), and aminopropyl triethoxy silane (APTES). Interaction of the amino-group of APTES with stearic acid directed the precipitation around the oil droplets. The titanosilicate phase contained

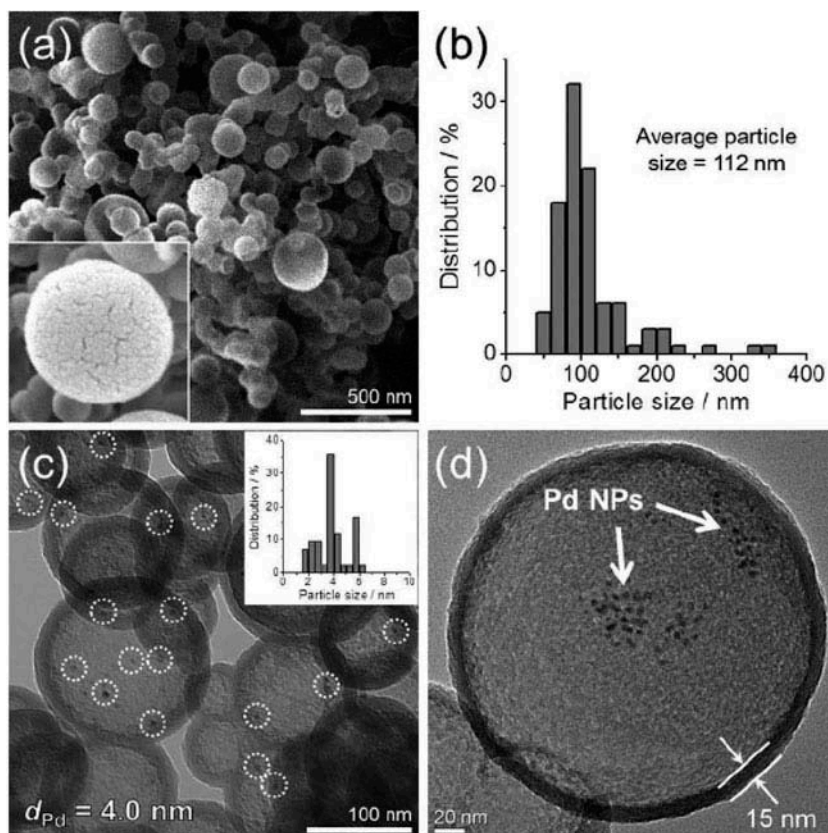


Figure 7. (a) FE-SEM image; (b) particle size distribution diagram; (c,d) TEM images of Pd@Ti-HHS. The inset in (c) shows a size distribution of encapsulated Pd nanoparticles. Reprinted with permission from Kuwahara et al. [148]. Copyright John Wiley and Sons (2017).

1.36 wt. % of Ti mainly in form of 4-coordinated species with titanol group [20] (exhibiting UV absorption at 220 nm). Comparison of Pd@Ti-HHS catalytic performance with other Pd/titanosilicate composites is provided in Section 3.5.

3. Catalytic performance

It was mentioned above that the TS-1 disclosure is a milestone in oxidation catalysis. Formerly known catalysts such as Ti(IV)/SiO₂ [149,150] were able to selectively oxidize propylene with organic hydroperoxides; however, their use with hydrogen peroxide was impossible for strong competitive adsorption of water as well as low activity in H₂O₂ activation. In contrast, the TS-1 was the first heterogeneous oxidation catalyst being able to activate aqueous hydrogen peroxide to selectively oxidize organic compounds [10,151]. The zeolite-based titanosilicate catalysts in general possess this ability thank to isolated titanium atoms in their structure (not connected to any other titanium atom via oxygen bridge). Besides oxygen, the use of H₂O₂ as the oxidant is highly convenient from both the economic and environmental point of view. The H₂O₂ possesses high content of the active oxygen and the only by-product is water [9]. It has been mentioned in the introduction, that titanosilicate zeolites catalyze effectively a number of different selective oxidation reactions. Among these, epoxidation of C = C double bond is the most frequently studied and it is usually the test reaction when reporting a novel titanosilicate catalyst. For epoxidation of sterically undemanding molecules such as propylene, linear olefins in general and to some extent phenol, the medium pore TS-1 is suitable and a well-established catalyst. Therefore, main research attention is nowadays focused on catalysts for epoxidation of sterically demanding molecules and for these cyclohexene and cyclooctene are the most abundant model substrates.

The variety of titanosilicate catalysts with enhanced accessibility of the active centres is very rich (*vide supra*) and when reported, novel catalysts are usually compared with a benchmarking material which is mostly the TS-1, Ti-beta, Ti-MWW, or Ti-MCM-41 (analogs of industrially relevant aluminosilicate zeolites). However, there might be strong differences even among different samples of these benchmarking materials (particularly in crystal size, titanium content and titanium species distribution). Fortunately, most of the authors use just about four different sets of experimental conditions for basic comparison of the reported catalyst and benchmarking catalyst (Table 6). Therefore, comparison of different titanosilicate catalysts is simple and straightforward. If a group of similar catalysts is reported (e.g., differing in certain synthesis condition), the best performing sample (providing the highest conversion or yield) has been selected.

A typical catalytic experiment (through all the discussed references unless otherwise specified) is performed in a 10–50 ml stirred glass reactor equipped

Table 6. General experimental conditions for batch catalytic experiments.

Method	Substrate (mmol)	Oxidant (mmol)	Solvent (ml)	Catalyst (mg)
I	10	10	10	50
II	4 or 4.5	2.25	4.5	60
III	12	3.3	10	35
IV	4	1	3	50

with a reflux condenser, which is heated by an oil bath or aluminium heating block to a temperature of 60°C. The reaction mixture is composed of a substrate, catalyst in form of powder, aqueous hydrogen peroxide (30–50 wt. %), solvent (acetonitrile or methanol) and in some cases an internal standard. The evaluated key parameters are conversion of the substrate, selectivity to the epoxide or epoxide yield. In some cases H₂O₂ efficiency is calculated showing the share of H₂O₂ effectively spent in selective oxidation and not decomposed. Note that conversion in this review is defined as $X = [\text{substrate consumed}]/[\text{substrate initially present in the reaction mixture}]$; in some references (e.g., Na et al. [15] and Kim et al. [96]), conversion is defined in a slightly different way and therefore it has been recalculated. Unfortunately, the selectivity is not always compared at the same or similar conversion level and therefore such comparison is not always straightforward. In this article, the substrate conversion level for a selectivity value is always marked (column X(S) in Tables 7–14. If a conversion and selectivity profile is presented in the original paper, selectivity at 10%, 20%, or 25% conversion (depending on substrate and other available data) is presented although this conversion was achieved later than in time at which the conversion is compared. In some cases either only selectivity or only epoxide yield is reported. In such a case, the other parameter was calculated from conversion and the reported one. Where appropriate, also turn-over-numbers ($\text{TON} = [\text{substrate conversion in mmol}]/[\text{titanium in mmol}]$ after certain reaction time) are compared. These are either taken from references or calculated from conversion, Si/Ti ratio of the catalyst and experimental details.

3.1 Epoxidation of linear alkenes

Linear alkenes (most abundant 1-hexene and 1-octene) are the most simple and sterically undemanding substrates. In the alkene epoxidation, first 1,2-epoxide is formed, which can undergo hydrolysis to 1,2-diol or solvolysis forming hydroxyether. Alternatively, an allylic carbon atom can be oxidized [33], but this is rare for linear alkenes.

Tatsumi et al. were the first to study systematically the epoxidation of linear olefins over TS-1 catalyst. They found that the rate of epoxidation decreases with increasing length of the hydrocarbon chain [153]. TS-1 (and

Table 7. Epoxidation of 1-hexene with hydrogen peroxide over different titanosilicate catalysts; data are sorted by catalytic experiment method and epoxide yield.

Catalyst	Catalyst ^a classification	Si/Ti	Temp. (°C)	Solvent ^a	Time (h)	X ^b (%)	y (%)	S (%)	X(S) (%)	Exp. ^c conditions	Notes ^d	Ref
Ti-MCM-41-G	MMS	97	60	ACN	2	0.3	0.1	50	0.1	III	H ₂ O ₂	[96]
Ti-MCM-41-D	MMS	51	60	ACN	2	0.3	0.2	55	0.1	III	H ₂ O ₂	[96]
Ti-MCM-41	MMS	61	60	ACN	2	0.4	0.3	71	0.1	III	H ₂ O ₂	[15]
lam MFI - G	layered	98	60	ACN	2	1.0	0.7	75	4	III	H ₂ O ₂	[96]
lam-TS-1	layered	54	60	ACN	2	3.3	3.1	95	12	III	H ₂ O ₂	[96]
F-lam-TS-1	layered	54	60	ACN	2	3.5	3.3	95	13	III	H ₂ O ₂	[15]
lam TS-1	layered	57	60	ACN	2	3.8	3.6	95	14	III	H ₂ O ₂	[15]
TS-1	medium pore	55	60	ACN	2	5.4	5.4	99	20	III	H ₂ O ₂	[15]
TS-1	medium pore	49	60	ACN	2	5.5	5.2	95	20	III	H ₂ O ₂	[96]
Ti-MCM-41	MMS	41	60	ACN	2	0.2	0.2	99.1	0.1	I	H ₂ O ₂	[94]
Ti-MCM-41	MMS	41	60	MeOH	2	0.4	0.4	90.3	0.1	I	H ₂ O ₂	[94]
Ti-COE-4	IEZ	150	60	MeOH	4	14.2	1.0	7	14	I	H ₂ O ₂	[33]
Ti-COE-3	IEZ	149	60	MeOH	4	8	1.6	20	8	I	H ₂ O ₂	[33]
lam-TS-1	layered	58	60	ACN	2	4.1	4.1	99.4	4	I	H ₂ O ₂	[94]
lam-TS-1	layered	25	60	MeOH	2	5.4	5.4	99	5	I	H ₂ O ₂	[97]
lam-TS-1	layered	58	60	MeOH	2	6.5	6.0	92.1	7	I	H ₂ O ₂	[94]
Ti-IEZ-MWW(Si)	IEZ	119	60	ACN	2	8.6	8.4	98	9	I	H ₂ O ₂	[40]
TS-1	medium pore	46	60	MeOH	2	9.1	9.1	99	9	I	H ₂ O ₂	[97]
TS-1	medium pore	44	60	ACN	2	10.1	10.0	99	10	I	H ₂ O ₂	[45]
IEZ-Ti-MWW	IEZ	94	60	ACN	2	12.1	11.5	95	10	I	H ₂ O ₂	[116]
TS-1	medium pore	41	60	ACN	2	12.1	12.1	99.6	12	I	H ₂ O ₂	[94]
Ti-MWW	medium pore	68	60	ACN	2	13.1	12.1	92.7	10	I	H ₂ O ₂	[95]
nano TS-1	nanosized medium pore	52	60	MeOH	2	17	17	99	17	I	H ₂ O ₂	[97]
Ti-beta	large pore	46	60	ACN	2	18.6	18.4	99	20	I	H ₂ O ₂	[45]
TS-1	medium pore	31	60	MeOH	4	21.2	20.6	97	20	I	H ₂ O ₂	[33]
TS-1	medium pore	41	60	MeOH	2	25.2	24.0	95.2	25	I	H ₂ O ₂	[94]
HTS-1	composite	50	60	MeOH	2	26.1	26.1	99	26	I	H ₂ O ₂	[97]
Ti-IEZ-MWW(SiSi)	IEZ	49	60	ACN	2	29.5	29.2	99	30	I	H ₂ O ₂	[40]
Ti-MWW	medium pore	n.a.	60	ACN	2	41.6	41.0	98.6	40	I	H ₂ O ₂	[152]
Ti-MWW	medium pore	44	60	ACN	2	54.2	52.0	96	50	I	H ₂ O ₂	[40]
Ti-MSE-cal	large pore	69	60	ACN	2	55.7	55.1	99	50	I	H ₂ O ₂	[45]

(Continued)

Table 7. (Continued).

Catalyst	Catalyst ^a classification	Si/Ti	Temp. (°C)	Solvent ^a	Time (h)	X ^b (%)	y (%)	S (%)	X(S) (%)	Exp. ^c conditions	Notes ^d	Ref
F-Ti- MWW	medium pore	30	60	ACN	2	58.5	57.9	98.9	60	I	H ₂ O ₂	[152]
Ti-MCM-41	MMS	59	60	MeOH	5	4.9	0.4	8.2	5	II	H ₂ O ₂ , 27 mg cat., 7 ml solv.	[132]
TiSii-HPB-60	MMS	36	60	MeOH	5	12.6	1.1	8.7	10	II	H ₂ O ₂ , 27 mg cat., 7 ml solv.	[132]
TS-1	medium pore	35	60	MeOH	5	29.4	18.8	64	30	II	H ₂ O ₂ , 27 mg cat., 7 ml solv.	[132]
Ti-beta	large pore	83	60	MeOH	2	19.6	8.6	44	20	IV	H ₂ O ₂	[61]
Ti-ITQ-39	large pore	163	60	MeOH	3.5	19.2	10.8	56	20	IV	H ₂ O ₂	[61]
Ti-ITQ-39	large pore	163	60	ACN	3.5	14.2	13.9	98	15	IV	H ₂ O ₂	[61]
TS-1	medium pore	33	60	ACN	5	18	17.6	98	20	IV	H ₂ O ₂	[61]
TS-1	medium pore	33	60	MeOH	7	18.9	18.5	98	20	IV	H ₂ O ₂	[61]
Ti-beta	large pore	83	60	ACN	1	19.6	19.2	98	20	IV	H ₂ O ₂	[61]

^a MMS – mesoporous molecular sieve, IEZ – interlayer expanded zeolite, ACN – acetonitrile, MeOH – methanol

^b X – alkene conversion, y – epoxide yield, S – selectivity to epoxide, X(S) – conversion level at which the selectivity is given

^c Catalytic experiment method according to Table 6.

^d Oxidant and deviations from the experimental conditions described in Table 6, if any.

Table 8. Epoxidation of 1-octene over different titanosilicate catalysts; data are sorted by oxidant and epoxide yield.

Catalyst	Catalyst classification	Si/Ti	Temp. (°C)	Solvent	Time (h)	X ^a (%)	y (%)	S (%)	X(S) (%)	Exp. ^b conditions	Notes ^c	Ref
Ti-CFI	extra-large pore	36	50	ACN	3	26	0.5	2	25	II	H ₂ O ₂ 83 mg cat., 10 ml solv.	[64]
TS-1	medium pore	46	60	MeOH	2	2	2	99	2	I	H ₂ O ₂	[97]
lam-TS-1	Layered	25	60	MeOH	2	2.5	2.5	99	2	I	H ₂ O ₂	[97]
nano TS-1	nanosized medium pore	52	60	MeOH	2	6	6	99	6	I	H ₂ O ₂	[97]
HTS-1	Composite	50	60	MeOH	2	8	8	99	8	I	H ₂ O ₂	[97]
TS-1	medium pore	38	50	ACN	3	56	14.6	26	50	II	H ₂ O ₂ 83 mg cat., 10 ml solv.	[64]
F-Ti-MWW	medium pore	30	60	ACN	2	18.1	16.5	91.2	20	I	H ₂ O ₂	[152]
Ti-MWW	medium pore	n.a.	60	ACN	2	20.2	18.7	92.4	20	I	H ₂ O ₂	[152]
TS-1	medium pore	41	100	decane	4	9.6	9.5	99	10	I	68 mg cat., only solv. from TBHP	[83]
TS-1-0.15P-N-24	hierarchical	41	100	decane	4	13.4	13.3	99	10	I	68 mg cat., only solv. from TBHP	[83]

^a X – alkene conversion, y – epoxide yield, S – selectivity to epoxide, X(S) – conversion level at which the selectivity is given

^b Catalytic experiment method according to Table 6.

^c Oxidant and deviations from the experimental conditions described in Table 6, if any.

Table 9. Epoxidation of 2-hexene; adapted from Kubota and Inagaki [45].

Catalyst	Catalyst classification	Si/Ti	Time (h)	X ^a (%)	y (%)	S (%)	X(S) (%)	Exp. ^b conditions	Epox ^c cis/trans
Ti-beta	large pore	46	2	26.1	25.8	99	25	I	68/32
Ti-MSE-cal	large pore	69	2	36.7	36.3	99	40	I	72/28
TS-1	medium pore	44	2	60.1	59.5	99	60	I	67/33

^aX – alkene conversion, y – epoxide yield, S – selectivity to epoxide, X(S) – conversion level at which the selectivity is given

^bCatalytic experiment method according to Table 6; oxidant: H₂O₂, temperature 60°C, solvent: acetonitrile, cis/trans ratio of the alkene 32/68

^ccis/trans ratio of the epoxide

titanosilicates in general) acts as an electrophile and therefore relative reactivity of different alkenes is dependent on nucleophilicity of the double bond; however, both restricted transition state shape selectivity and diffusion of reactants and products also contribute to the ordering of the reactivity. Thus, the electronic effect might be (and in many cases is) masked [154].

Another important parameter influencing the epoxidation is solvent. Van der Waal and van Bekkum [155] studied solvent effect in epoxidation of 1-octene using aluminium free Ti-beta. In methanol at 40°C, the reaction did not occur at all (while the TS-1 provided 4.1% conversion after 1 h) and at 60°C, the main product is the hydroxy-methoxyoctane. The zero activity of Ti-beta at 40°C was explained by the hydrophilic character of the material. When water and methanol were strongly adsorbed on the surface, the access of the 1-octene to the active sites was limited. When less polar solvents were used (ethanol, 2-propanol, *tert*-butanol) at 40°C, conversions 0.7%, 1.9%, and 0.3%, respectively, were observed after 1 h. Use of slightly basic acetonitrile (ACN) as solvent resulted in suppression of acid catalyzed the ring opening reactions, which were observed in the above alcohols at 60°C. The acidity comes out of the catalyst itself because the titanium sites exhibit slight Lewis acidity.

Wu et al. [12] reported increased activity of Ti-MWW in comparison with TS-1 in 1-hexene epoxidation in acetonitrile at 60°C. The Ti-MWW catalyst with the highest Ti content (Si/Ti = 38) provided conversion 44.8% with 99% selectivity while the conversion over the TS-1 was only 5.8%. This was the first example of a catalyst, which was more active than the TS-1 in epoxidation of 1-hexene. Later on, it was pointed out that for different catalysts (Ti-MWW, TS-1, Ti-beta) different solvents are the optimal to provide the highest conversion and selectivity [100,156]. Ti-beta and Ti-MWW exhibit much higher activity when acetonitrile is used as a solvent instead of methanol. For the TS-1 it is vice versa. The same effect for TS-1 vs. Ti-beta (different solvent being optimal for different catalysts) was observed also in Moliner and Corma [61] (Table 7). Ti-ITQ-39 was found to stand in between the Ti-beta and TS-1 giving higher

Table 10. Epoxidation of cyclohexene with hydrogen peroxide over different titanasilicate catalysts; data are sorted by catalytic experiment method and epoxide yield.

Catalyst	Catalyst classification ^a	Si/Ti	Temp. (°C)	Solvent ^a	Time (h)	X ^b (%)	Y (%)	S (%)	X(S) (%)	Exp. ^c conditions	Notes ^d	Ref
TS-1	medium pore	46	60	ACN	2	0.2	n.a.	n.a.	–	I		[97]
lam-TS-1	layered	25	60	ACN	2	1.6	n.a.	n.a.	–	I		[91]
nano TS-1	nanosized	52	60	ACN	2	2.4	n.a.	n.a.	–	I		[97]
HTS-1	composite	50	60	ACN	2	3.5	n.a.	n.a.	–	I		[97]
Ti-COE-3	IEZ	149	60	MeOH	4	4.2	0.2	5	4	I	mostly allylic oxidation	[33]
Ti-MCM-41	MMS	41	60	ACN	2	5.2	0.3	5.6	5	I	mostly allylic oxidation	[94]
Ti-MWW	medium pore	159	60	ACN	2	2.3	0.5	22	2	I		[42]
Ti-COE-4	IEZ	150	60	MeOH	4	14	0.6	4	14	I	mostly allylic oxidation	[33]
TS-1	medium pore	41	60	ACN	2	2.8	0.6	22	3	I	mostly allylic oxidation	[94]
lam-TS-1	layered	58	60	ACN	2	4	0.8	19	4	I	mostly allylic oxidation	[94]
TS-1	medium pore	44	60	ACN	2	4.2	1.3	31	5	I	mostly allylic oxidation	[45]
Ti-MWW	medium pore	68	60	ACN	2	4.1	1.7	41	4	I	mostly ring opening	[116]
TS-1	medium pore	31	60	MeOH	4	2.3	2.0	89	2	I		[33]
Ti-IEZ-MWW	IEZ	132	60	ACN	2	7.9	4.6	58	8	I		[42]
Ti-MWW	medium pore	68	60	ACN	5	5	4.7	93	5	I		[115]
Ti-IEZ-MWW(Si)	IEZ	119	60	ACN	2	7.9	5.1	65	8	I		[40]
Ti-MWW	medium pore	44	60	ACN	2	12.7	7.9	62	12	I		[40]
Ti-YNU-1	IEZ	90	60	ACN	2	14.6	10.2	70	15	I		[42]
IEZ-Ti-MWW	IEZ	94	60	ACN	2	20.7	11.8	57	20	I		[116]
Ti-MSE-cal	large pore	69	60	ACN	2	14.4	12.6	87	12	I		[45]
Ti-IEZ-MWW(Si)	IEZ	49	60	ACN	2	20.3	14.4	71	20	I		[40]
Ti-IEZ-MWW-RSC	IEZ	167	60	ACN	2	17.9	15.4	86	20	I		[42]
Ti-beta	large pore	46	60	ACN	2	28.5	16.7	59	30	I	mostly ring opening	[45]
Ti-MWW exp(2)	IEZ	159	60	ACN	5	18	16.9	94	18	I		[115]
Ti-MWW exp(1)	IEZ	58	60	ACN	5	35	33.3	95	35	I		[115]
TS-1 (L)	layered	n.a.	60	ACN	5	8.5	0.7	8.5	8	II	100 mg cat., mostly ring opening to diol (S = 69%)	[86]
TS-1(L)/mesoTS	composite	n.a.	60	ACN	5	14.4	0.8	6.1	15	II	100 mg cat., mostly ring opening to diol (S = 73%)	[86]
Ti-MCM-41	MMS	50	60	ACN	5	19.6	0.9	4.6	20	II	50 mg cat., mostly ring opening	[133]

(Continued)

Table 10. (Continued).

Catalyst	Catalyst classification ^a	Si/Ti	Temp. (°C)	Solvent ^b	Time (h)	X ^b (%)	Y (%)	S (%)	X(S) (%)	Exp. ^c conditions	Notes ^d	Ref
TS-1	medium pore	35	60	ACN	5	4.5	1.7	38	5	II	mostly ring opening	[81]
Ti-MCM-41	MMS	59	60	ACN	5	28.8	2.6	9	3	II		[132]
TS-1	medium pore	100	70	ACN	5	11.1	3.2	29	10	I	25 mg cat., 5 mmol H ₂ O ₂ , allylic oxidation (S = 44%)	[85]
TS-1	medium pore	35	60	ACN	5	8.2	3.7	45	4	II		[132]
TS-1	medium pore	21	60	ACN	6	5.2	3.9	75	5	II	50 mg cat.	[84]
HPB-TS-1	hierarchichal	41	60	ACN	5	15.9	4.7	29	15	II	mostly ring opening	[81]
C 40wt.% TS-1 MW	hierarchichal	100	70	ACN	5	21.1	5.1	24	20	I	25 mg cat., 5 mmol H ₂ O ₂	[85]
BMB-TiSiI	MMS	33	60	ACN	5	33.7	7.2	21	30	II	50 mg cat., mostly ring opening	[133]
TiSiI-HPB-60	MMS	36	60	ACN	5	20.2	8.2	41	20	II	mostly ring opening	[132]
TS-1/NaOH&TBAOH	hierarchichal	33	60	ACN	6	20	16.0	80	20	II	50 mg cat.	[84]
TS-1	medium pore	55	60	ACN	2	0.4	0.4	99	1	III		[15]
Ti-MCM-41	MMS	61	60	ACN	2	2.9	0.4	14	10	III		[15]
lam-TS-1	layered	57	60	ACN	2	3.1	1.3	43	10	III		[15]
F-lam-TS-1	layered	54	60	ACN	2	6.9	4.8	69	25	III		[15]
TS-1	medium pore	33	60	ACN	3.5	26.3	6.0	23	25	IV	mostly allylic oxidation (S = 77%)	[61]
Ti-HTQ-39	large pore	163	60	ACN	1	23.9	10.5	44	25	IV	allylic oxidation (S = 48%)	[61]
Ti-beta	large pore	83	60	ACN	2	25.6	15.4	60	25	IV	allylic oxidation (S = 33%)	[61]

^a MMS – mesoporous molecular sieve, IEZ – interlayer expanded zeolite, ACN – acetonitrile, MeOH – methanol

^b X – alkene conversion, Y – epoxide yield, S – selectivity to epoxide, X(S) – conversion level at which the selectivity is given

^c Catalytic experiment method according to Table 6

^d Deviations from the experimental conditions described in Table 6, if any major oxidation product other than epoxide.

Table 11. Epoxidation of cyclohexene with *tert*-butyl hydroperoxide over different titanasilicate catalysts; data are sorted by epoxide yield.

Catalyst	Catalyst ^a classification	Si/Ti	Temp. (°C)	Solvent ^a	Time (h)	X ^b (%)	y (%)	S (%)	X(S) (%)	Exp. ^c conditions	Notes ^d	Ref
TS-1	medium pore	41	60	ACN	2	0.1	0.1	95	0.1	—	—	[94]
TS-1	medium pore	47	60	ACN	2	1.2	1.2	99	1	—	—	[18]
Ti-MWW	medium pore	38	60	ACN	2	4.2	4.2	99	4	—	—	[94]
Ti-beta	large pore	40	60	ACN	2	5.3	5.2	99	5	—	—	[94]
Ti-DZ-1	layered	67	60	octane	2	8.1	6.6	82	8	—	56 mg cat.	[41]
50TS-1	medium pore	197	80	decane	2	11	11	99	10	—	5 mmol TBHP, 3 ml solv.	[48]
MTS-1	hierarchical	36	60	ACN	2	14	14	99	15	—	—	[18]
lam TS-1	layered	58	60	ACN	2	17	17	99	17	—	3.6 mmol TBHP, 100 mg cat.	[94]
Ti-MCM-41	MMS	41	60	ACN	2	18	18	99	18	—	—	[94]
50Ti(B)-MCM-22 ^e	medium pore	240	80	decane	2	26	26	99	25	—	5 mmol TBHP, 3 ml solv.	[48]
Ti-KIT-5 (-15)	MMS	14.2	60	ACN	6	44	28	63	40	—	200 mg cat.	[124]
50Ti(P)-MCM-22 ^e	medium pore	340	80	decane	2	29	29	99	30	—	5 mmol TBHP, 3 ml solv.	[48]
50Ti(E)-MCM-22 ^e	medium pore	98	80	decane	2	42	41	99	40	—	5 mmol TBHP, 3 ml solv.	[48]
Ti-MCM-41	MMS	33	40	CH ₂ Cl ₂	12	44	42	95	45	—	5 mmol TBHP, 100 mg cat.	[16]
Ti-SBA-12	MMS	39.1	40	CH ₂ Cl ₂	12	45	45	100	45	—	5 mmol TBHP, 100 mg cat.	[16]
40Si/TiMCM-36E	Si-Ti-pillared	15.3	80	decane	2.5	50	46	91	50	—	7 mmol TBHP	[43]
Ti-SBA-16	MMS	53.8	40	CH ₂ Cl ₂	12	46	46	100	45	—	5 mmol TBHP, 100 mg cat.	[16]
A Si/Ti MCM-36E	Si-Ti-pillared	173	80	decane	2.5	60	57	95	60	—	7 mmol TBHP	[43]

^a MMS – mesoporous molecular sieve, IEZ – interlayer expanded zeolite, ACN – acetonitrile

^b X – alkene conversion, y – epoxide yield, S – selectivity to epoxide, X(S) – conversion level at which the selectivity is given

^c Catalytic experiment method according to Table 6

^d Deviations from the experimental conditions described in Table 6, if any

^e Ti-MWW structure; original reference labels were kept for clarity.

Table 12. Epoxidation of *cis*-cyclooctene over different titanasilicate catalysts; data are sorted by epoxide yield.

Catalyst	Catalyst classification ^a	Si/Ti	Temp. (°C)	Solvent ^a	Time (h)	X ^b (%)	y (%)	S (%)	X(S) (%)	Exp. ^c conditions	Notes ^d	Ref
TS-1	medium pore	49	60	ACN	2	0.2	0.2	n.d.		III	H ₂ O ₂	[96]
TS-1	medium pore	55	60	ACN	2	0.2	0.2	99	1	III	H ₂ O ₂	[87]
Ti-IPC-2	large pore	210	60	ACN	4	11.2	0.4	n.d.		II	H ₂ O ₂ , 50 mg cat.	[19]
Ti-CIT-5 (TiCl ₄) (Ti-CFI) ^e	extra-large pore	109	60	ACN	4	3.5	0.9	n.d.		II	H ₂ O ₂ , 50 mg cat.	[62]
Ti-MCM-41-G	MMS	97	60	ACN	2	1.2	1.0	83	4	III	H ₂ O ₂	[96]
Ti-SSZ-42 (TiCl ₄ , g) (Ti-IFR) ^e	large pore	72	60	ACN	4	3.9	1.1	35	5	II	H ₂ O ₂ , 50 mg cat.	[62]
Ti-MCM-41	MMS	61	60	ACN	2	1.8	1.3	74	6	III	H ₂ O ₂	[87]
Ti-MCM-41-D	MMS	51	60	ACN	2	1.7	1.4	81	5	III	H ₂ O ₂	[96]
Ti-CFI	extra-large pore	36	60	MeOH	3	3.2	2.1	66	3	II	H ₂ O ₂ , 30 mg cat.	[64]
TS-1	medium pore	100	70	ACN	5	4.5	2.3	51	5	I	5 mmol H ₂ O ₂ , 25 mg cat.	[85]
lam-TS-1	Layered	57	60	ACN	2	2.6	2.4	91	10	III	H ₂ O ₂	[87]
lam MFI - G	Layered	98	60	ACN	2	2.7	2.5	95	10	III	H ₂ O ₂	[96]
Ti-CFI(40)	extra-large pore	36	60	ACN	3	4.8	2.6	54	5	II	H ₂ O ₂ , 30 mg cat.	[64]
lam-TS-1	Layered	54	60	ACN	2	2.8	2.7	97	10	III	H ₂ O ₂	[96]
TS-1	medium pore	44	60	ACN	4	5.9	2.9	55	10	II	H ₂ O ₂ , 50 mg cat.	[19]
TS-1	medium pore	44	60	ACN	4	8	3	42	20	II	H ₂ O ₂ , 50 mg cat.	[82]
TS-1-PISt-b	Pillared	55	60	ACN	4	6.5	3.5	58	20	II	H ₂ O ₂ , 50 mg cat.	[82]
F-lam TS-1	Layered	54	60	ACN	2	4.2	4.0	95	15	III	H ₂ O ₂	[87]
Ti-UTL	extra-large pore	139	60	ACN	4	14	4.7	30	20	II	H ₂ O ₂ , 50 mg cat.	[19]
Ti-beta	large pore	116	60	ACN	4	14	4.7	32	20	II	H ₂ O ₂ , 50 mg cat.	[19]
C 40wt.% TS-1 MW	Hierarchichal	100	70	ACN	5	9.3	7.6	82	10	I	5 mmol H ₂ O ₂ , 25 mg cat.	[85]
Ti-IPC-1PI	Pillared	480	60	ACN	4	21	8	38	20	II	H ₂ O ₂ , 50 mg cat.	[19]
Ti-MCM-36	Pillared	57	60	ACN	4	18	8	54	20	II	H ₂ O ₂ , 50 mg cat.	[82]
Ti-MCM-41	MMS	50	60	ACN	5	8.9	8.3	93	10	II	H ₂ O ₂ , 50 mg cat.	[133]
50TS-1	medium pore	197	80	decane	2	9	8.9	99	10	I	5 mmol TBHP, 3 ml solv.	[48]
HPB-TS-1	Hierarchichal	41	60	ACN	5	15	14	91	15	II	H ₂ O ₂	[81]
TS-1-PITi (60)b	Si-Ti-pillared	30	60	ACN	4	19	14	76	20	II	H ₂ O ₂ , 50 mg cat.	[82]
TS-1-PITi (10)b	Si-Ti-pillared	14	60	ACN	4	19	15	80	20	II	H ₂ O ₂ , 50 mg cat.	[82]
TS-1-PITi (20)b	Si-Ti-pillared	20	60	ACN	4	21	17	76	20	II	H ₂ O ₂ , 50 mg cat.	[82]
Ti-SSZ-33 (TiCl ₄) (Ti-CON) ^e	large pore	81	60	ACN	4	26	22	90	20	II	H ₂ O ₂ , 50 mg cat.	[62]
Ti-IPC-1-PITi (100)	Si-Ti-pillared	69	60	ACN	4	35	25	80	20	II	H ₂ O ₂ , 50 mg cat.	[19]
BMB-TiSil	MMS	33	60	ACN	5	29	26	90	30	II	H ₂ O ₂ , 50 mg cat.	[133]

(Continued)

Table 12. (Continued).

Catalyst	Catalyst classification ^a	Si/Ti	Temp. (°C)	Solvent ^a	Time (h)	X ^b (%)	y (%)	S (%)	X(S) (%)	Exp. ^c conditions	Notes ^d	Ref
Iam-TS-1	Layered	58	60	ACN	2	26.5	26.4	99.7	25	I	TBHP	[94]
Ti-SSZ-33 (TBOTi)	(Ti- CON) ^e large pore	450	60	ACN	4	37	28.3	77	20	II	H ₂ O ₂ , 50 mg cat.	[62]
50Ti(B)-MCM-22 (Ti- MWW) ^e	medium pore	240	80	decane	2	44.1	43.9	99.6	45	I	5 mmol TBHP, 3 ml solv.	[48]
50Ti(P)-MCM-22 (Ti- MWW) ^e	medium pore	340	80	decane	2	44.4	44.1	99.3	45	I	5 mmol TBHP, 3 ml solv.	[48]
50Ti(E)-MCM-22 (Ti- MWW) ^e	medium pore	98	80	decane	2	46.6	46.3	99.4	45	I	5 mmol TBHP, 3 ml solv.	[48]

^a MMS – mesoporous molecular sieve, Si-Ti-pillared – silica-titania pillared, ACN – acetonitrile, MeOH – methanol

^b X – alkene conversion, y – epoxide yield, S – selectivity to epoxide, X(S) – conversion level at which the selectivity is given

^c Catalytic experiment method according to Table 6

^d Oxidant and deviations from the experimental conditions described in Table 6, if any

^e Original marking from references is kept for clarity, marking used in this review is provided in brackets

Table 13. Epoxidation of cyclohexene with hydrogen peroxide over different titanasilicate catalysts; data are sorted by epoxide yield.

Catalyst	Catalyst classification	Si/ Ti	Temp. (°C)	Solvent	Time (h)	X ^a (%)	y (%)	S (%)	X(S) (%)	Exp. ^b conditions	Notes ^c	Ref
TS-1	medium pore	49	60	ACN	2	0.2	n.d.	n.d.	–	III		[96]
TS-1	medium pore	100	70	ACN	5	1.3	0.7	54	1	I	5 mmol H ₂ O ₂ , 25 mg cat.	[85]
Ti-beta	large pore	116	60	2-propanol/ACN 2:1	2	0.7	0.7	99	6	II	50 mg cat.	[158]
Ti-UTL	extra-large pore	139	60	2-propanol/ACN 2:1	2	1.3	1.2	95	6	II	50 mg cat.	[158]
Ti-MCM-41-G	MMS	97	60	ACN	2	2.6	2.2	83	3	III		[96]
C 40wt.% TS-1 MW	hierarchical	100	70	ACN	5	5.7	2.3	40	5	I	5 mmol H ₂ O ₂ , 25 mg cat.	[85]
Ti-MCM-41-D	MMS	51	60	ACN	2	3.1	2.5	81	3	III		[96]
lam MFI – G	layered	98	60	ACN	2	5.2	4.9	95	5	III		[96]
lam-TS-1	layered	54	60	ACN	2	5.1	4.9	97	5	III		[96]
TS-1-TiPI	Si-Ti-pillared	20	60	2-propanol/ACN 2:1	2	11.5	10.9	95	10	II	50 mg cat.	[158]
Ti-IPC-1-TiPI	Si-Ti-pillared	16	60	2-propanol/ACN 2:1	2	19.1	18.6	97	10	II	50 mg cat.	[158]

^a MMS – mesoporous molecular sieve, Si-Ti-pillared – silica-titania pillared, ACN – acetonitrile

^b X – alkene conversion, y – epoxide yield, S – selectivity to epoxide, X(S) – conversion level at which the selectivity is given

^c Catalytic experiment method according to Table 6

^d Deviations from the experimental conditions described in Table 6, if any

Table 14. Epoxidation of norbornene with hydrogen peroxide in ACN over different catalysts; data are sorted by reaction time and epoxide yield.

Catalyst	Catalyst ^a classification	Si/ Ti	Temp. (°C)	Time (h)	X ^b (%)	y (%)	S (%)	X(S) (%)	Exp. conditions ^c	Ref
TS-1	medium pore	49	60	2	0.7	n.d.	n.d.		III	[96]
Ti-MCM-41-G	MMS	97	60	2	3.3	2.5	75	3	III	[96]
Ti-MCM-41-D	MMS	51	60	2	4.1	3.0	74	4	III	[96]
lam MFI – G	layered	98	60	2	5.0	4.3	85	5	III	[96]
lam-TS-1	layered	54	60	2	6.1	5.0	83	6	III	[96]
TS-1	medium pore	44	60	4.5	2.8	1.8	65	3	V	[82]
Ti- UTL	extra-large pore	139	60	4	3.0	3.0	n.d.		V	[19]
Ti- CFI (TiCl ₄)	extra-large pore	109	60	4	4.9	3.3	50	8	V	[62]
Ti-beta	large pore	116	60	4	53	3.8	8	20	V	[19]
TS-1-PISi	pillared	55	60	4.5	11	5.5	52	10	V	[82]
Ti- CFI (60)	extra-large pore	63	60	4	29	5.8	20	30	VI	[64]
lam TS-1	layered	33	60	4.5	12	6.1	42	10	V	[82]
Ti-IPC-1PISi	pillared	480	60	4	49	6.5	19	20	V	[19]
Ti-MCM-36	pillared	57	60	4.5	24	8.5	26	10	V	[82]
Ti-IPC-1-TiPI (30)	Si-Ti-pillared	16	60	4	57	12.6	30	20	V	[19]
TS-1-PITi	Si-Ti-pillared	20	60	4.5	23	14.8	56	10	V	[82]
Ti- CON (TiCl ₄)	large pore	81	60	4	19	15.4	75	12	V	[62]

^a MMS – mesoporous molecular sieve, Si-Ti-pillared – silica-titania pillared,

^b X – alkene conversion, y – epoxide yield, S – selectivity to epoxide, X(S) – conversion level at which the selectivity is given

^c III – 12 mmol S, 3.3mmol H₂O₂, 10ml solv., 35 mg cat, V - 5.3 mmol S, 2.65 mmol H₂O₂, 8 ml solv., 50 mg. cat, VI-3.2 mmol S, 1.6 mmol H₂O₂, 6 ml solv., 50 mg cat.

conversion in methanol (19.2% vs. 14.2% after 3.5 h) but higher selectivity in ACN (98% vs. 56%) [61]. Regarding also the reaction time when about 20% conversion was achieved [61] and titanium content, two conclusions are evident (for microporous catalysts): (i) wider pores bring lower diffusion limitations and therefore higher reaction rate and (ii) the more active sites, the higher reaction rate while the size and dimensionality of the pore system is similar.

Comparing the catalytic results in term of catalyst structure, we observe that mesoporous molecular sieves (MMS) are not suitable for epoxidation of 1-hexene (Table 7) and linear alkenes in general. Negligible conversions are observed because of their hydrophilic character which results in strong competitive adsorption of water [15,94,96,132]. In contrast, conventional titanosilicate zeolites bring the highest conversions and yields of 1,2-epoxyhexane among all the reported catalysts. The most active catalysts (providing the highest conversions and TON numbers) were F-Ti-MWW (TON = 211 after 2 h) [152], Ti-MSE-cal (TON = 462 after 2 h) [45] and Ti-MWW (TON = 287 after 2 h) [40]. Note these TON in contrast to those provided by TS-1 in acetonitrile (ranging from TON = 29 [61] to TON = 61 [15] after 2 h) but also in methanol (from TON = 30 [61] to TON = 124 [94] after 2 h). Treatment of the the F-Ti-MWW with KCl solution led to further

increase in 1-hexene conversion as the K^+ ions help to wash out free F^- remaining in the catalyst structure.

The Ti-IEZ-MWW type catalysts provide conversions and epoxide yields comparable with conventional TS-1. Eventhough their titanium content is usually lower (e.g., Si/Ti = 119 [40] vs. TS-1 Si/Ti = 44 [45]) and therefore TON are higher (123 vs. 53), the Ti-IEZ-MWW catalysts are not more effective catalysts than conventional Ti-MWW (neither in term of conversion nor the TON). Reason is obvious: during the interlayer expansion, bridging – Si(OH)₂- groups are formed in between the zeolite layers. Presence of these groups causes an increase in hydrophilicity of the material, which is not compensated by considerably better accessibility of the active sites. 1-hexene diffuses easily in the 10-ring channels and the expansion of the channels to 12-ring is not a big difference. Therefore the reaction rate driving property remains the hydrophilicity of the catalyst.

Surfactant templated lam-TS-1 catalysts provided significantly lower conversions in comparison with conventional TS-1 [15,94,96]. However, in this case the explanation remains unclear. One could expect that the lam-TS-1 contains more terminal silanol groups in comparison with conventional TS-1 and therefore will be more hydrophilic, but decreasing of the amount of silanols by 40% had negligible effect on 1-hexene conversion [15]. On the other hand, a HTS-1 (composite of conventional and layered TS-1) provided the highest conversion (26.1% after 2 h) and TON (157 after 2 h) of all the TS-1 based catalysts. The HTS-1 was prepared by desilication-recrystallization process. During this process mesopores were created in the core TS-1 crystal and thus this desilicated TS-1 phase (and not the lamellar shell phase) appears to be responsible for the increased activity [97].

In epoxidation of 1-octene (Table 8), similar features as for 1-hexene can be observed but the advantage of conventional titanosilicate catalysts does not seem to be as strong as for 1-hexene. Conventional and lamellar TS-1 catalysts provided similar conversion (2 resp. 2.5% after 2 h) [97]. One more time Ti-MWW catalysts provided the highest yield of cyclooctene oxide [152]. A conversion of 26% after 3 h at 50°C is reported for extra-large pore titanosilicate Ti-CFI but the epoxide yield was only 0.5% at this time [64]. The results obtained with HTS-1 catalyst suggest that desilication may be the way how to improve catalytic properties of TS-1 based catalysts but only data with TBHP as oxidant are available for comparison of conventional and desilicated TS-1 [83].

The seek for new catalysts focuses on materials for epoxidation of sterically demanding molecules and therefore linear alkenes other than the above model substrates (with exception of industrially relevant C₃ alkenes; Section 3.4) are not subject of interest. Data for 2-hexene were reported by Kubota et al. [45] (Table 9) testing the properties of Ti-MSE. The Ti-MSE-cal catalyst provided higher conversion than Ti-beta (36.7% vs. 26.1% after 2 h)

but it did not gain the TS-1 performance (conversion 60.1%). In the case of 2-hexene, i.e., *cis/trans* selectivity is an issue. Ti-MSE-cal exhibited quite high *cis* selectivity (*cis*-2-hexene is oxidized about 3 times faster than *trans*-2-hexene) but this is the case of most titanosilicate catalysts (e.g., TS-1, TS-2, Ti-beta). The only exception, exhibiting strong *trans*-selectivity is the Ti-MWW [157]. Note that the epoxidation itself is stereospecific [30,45].

3.2 Epoxidation of cyclic olefins

Cyclohexene has molecular dimension of about 5.0 Å [40], which is comparable with the size of medium pore zeolites such as TS-1 and Ti-MWW. Thus, in contrast to 1-hexene, cyclohexene suffers from strong diffusion constraints when diffusing in the 10-ring pores. Furthermore, the epoxide ring in 1,2-epoxycyclohexane is highly strained [15] and therefore prone to ring opening reactions. Thanks to these properties, cyclohexene is a very sensitive model substrate to test catalytic properties of catalysts designed for epoxidation of sterically demanding molecules. Its homologues cycloheptene, cyclooctene, cyclodecene, and cyclododecene are used to investigate catalytic properties of catalysts with highly open structures such as hierarchical and lamellar titanosilicates and mesoporous titanosilicates. The C₇–C₁₂ cycloalkenes are less prone to oxidation of allylic carbon atom than cyclohexene and corresponding epoxides are significantly more stable than 1,2-epoxycyclohexane (compare selectivity data in Tables 10, 12, and 13).

Cyclohexene in reaction system with aqueous hydrogen peroxide and a titanosilicate catalyst undergoes basically two oxidation routes. The desired is epoxidation of the C = C double bond, which can be followed by undesired acid catalyzed ring opening reaction with water or alcohol (if the alcohol is used as solvent) forming 1,2 cyclohexane diol or alkoxy-cyclohexanol (or sometimes rearrangement of the epoxide to form cyclohexanone). In addition, cyclohexene can undergo allylic oxidation forming cyclohex-2-en-1-ol and subsequently cyclohex-2-en-1-on. The epoxidation route is connected with heterolytic breaking of O-O bond in titanium-peroxide species while the allylic oxidation occurs via oxidation mechanism involving ·OH radicals [132,133]; but there is no straightforward connection between catalyst structure and tendency to the allylic oxidation (Table 10).

Table 10 lists data for epoxidation of cyclohexene with hydrogen peroxide over different titanosilicate catalysts. It is evident that conversions and epoxide yields obtained using medium-pore zeolites are significantly lower than these obtained with large-pore titanosilicates and IEZ titanosilicates. Contrary to linear alkenes, molecular diffusion is the rate-determining parameter for the first oxidation reaction. Observing the TS-1 catalyst results using the most common experimental conditions I (Table 6), the conversion spans from 0.2% after 2 h [97] to 4.2% [45]. The range of conversions of Ti-

MWW catalysts lays higher (2.3–12.7 % after 2 h [40,42]), probably thank to Ti-**MWW** side pockets which increase the (well accessible) external surface. Cyclohexene conversions up to 35% were achieved using the IEZ-**MWW**-based catalysts [115].

Calculating the TON after 2 h, the difference resulting from increased accessibility of the titanium sites in Ti-IEZ-**MWW** catalysts is even higher because the Ti-IEZ-**MWW** catalysts have Si/Ti ratios usually higher than 100: TS-1 TON = 1–22 < Ti-**MWW** TON = 34–67 < Ti-IEZ-**MWW** TON = 113–359. The activity of lam-TS-1 catalysts in this case fall into the medium pore group of catalysts [15,94] (TON = 5–77). Simple explanation of their low performance by their more hydrophilic character is not sufficient here, because free hydroxyl groups are present also on the bridging groups in IEZ catalysts. Nevertheless, decrease of the amount of surface silanol groups brought a significant increase of cyclohexene conversion and epoxide selectivity in this case (conversion lam-TS-1 3.1% vs. F-lam-TS-1 6.9% after 2 h, method III) [15]. Also, the low activity is not caused by presence of extra-framework or anatase-like titanium species. Hierarchical TS-1 catalysts (and also amorphous titanosilicates) provided high conversions (e.g., TiSil-BMB conversion 33.7% after 5 h [133]) although they suffered strongly from epoxide ring opening reactions [84,85,132,133]. The only exception was hierarchical TS-1/NaOH&TBAOH providing 20% conversion with 16% epoxide yield after 5 h (method II).

Regarding the selectivity, rationalization of the data is even less straightforward than in the case of conversions and TONs. Thus making a catalyst providing high selectivity of cyclohexene epoxidation remains still more art than engineering. It was mentioned above that cyclohexene oxide undergoes easily ring opening reactions and cyclohexene is prone to allylic oxidation. Note also that the reaction conditions are not optimized to maximize the epoxide yield, but kept always the same to provide a sort of catalyst characterisation. As a result, epoxide selectivity over 80% was achieved over only with few of catalysts: TS-1 at 2% conversion [33], Ti-**MWW** at 5% conversion [115], and Ti-IEZ-**MWW**-RSC and Ti-**MWW**-exp at 20% conversion [42,115].

When *tert*-butyl hydroperoxide (TBHP) is used as oxidant instead of H₂O₂ under water free conditions, the only driving parameter remains diffusion. Therefore, more open structures bring both higher conversion and yield (Table 11). The selectivity ranges between 90 and 100% even at 50% conversion [16,43]. Note that the highest conversions were achieved over mesoporous titanosilicates Ti-MCM-41, Ti-SBA-12, and Ti-SBA-16 [16] and also with silica-titania-pillared MCM-36 catalysts [43] and titanium(IV) alkoxide-grafted **MWW** catalysts [48]. Alkoxide grafting (and silica-titania pillaring) results in formation of titanium sites on the external surface because, e.g., titanium(IV) isopropoxide is too bulky to diffuse into

MWW micropores and these sites are then responsible for high catalyst activity. On the other hand, TS-1 is practically inactive (even after 80 h the conversion is below 1% [94]) because both cyclohexene and TBHP cannot easily diffuse in micropores. This can be slightly overcome by increasing the reaction temperature to 80°C [48].

Temperature plays a crucial role in any chemical reaction. Shen et al. conducted a rare study on the influence of temperature on epoxidation with hydrogen peroxide over a titanasilicate catalyst [112]. Cycloheptene was used a test substrate and large pore Ti-beta (denoted Ti-beta-44 in the reference) and interlayer expanded Ti-YNU-1 were examined as the catalysts (Figure 8). The conversion after 1 h increased almost linearly from about 7% at 0°C to almost 60% at 75°C while an opposite trend was observed in term of selectivity. Note that in addition to increasing temperature also increasing

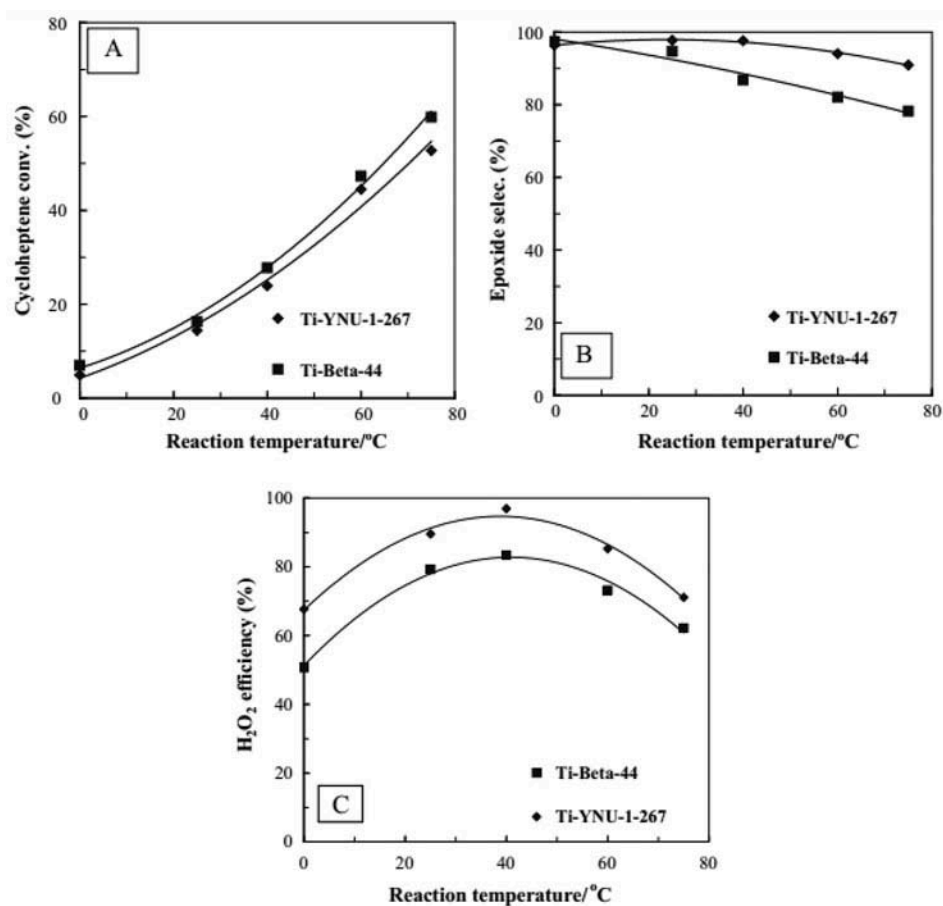


Figure 8. Dependence of cycloheptene conversion (A), epoxide selectivity (B), and hydrogen peroxide efficiency (C) on reaction temperature; reaction conditions: 5 mmol cycloheptene, 7.5 mmol H₂O₂, 5 ml ACN, 100 mg catalyst, 1 h. Reprinted with permission from Shen et al. [112]. Copyright Elsevier (2011).

conversion has a negative influence on selectivity. Epoxide selectivity decreased, e.g., for Ti-beta from 95% at 40% conversion to about 80% at 65% conversion (at 60°C). Interestingly a maximum in hydrogen peroxide efficiency was found at 40°C. The authors explain the observation by thermal decomposition of H₂O₂ at higher temperature but explanation of the low efficiency at low temperature is unclear. A reason could be that at low temperature ineffective decomposition of the Ti-peroxo complexes is favored over epoxidation probably for slow diffusion of substrate molecules to the active sites.

Cyclooctene is another widely used model substrate for evaluation of the performance of catalysts designed for epoxidation of sterically demanding molecules. *Cis*- isomer is used exclusively; highly strained *trans*- isomer is not available from major R&D chemical suppliers. Data for cyclooctene epoxidation are listed in Table 12. Unfortunately, data for most of MWW based titanosilicates are not available but trends in structure-activity relations are similar to these observed for cyclohexene. Not surprisingly, the conventional TS-1 catalysts provide the lowest conversions as cyclooctene is unable to enter their micropores and therefore any catalytic activity is restricted to the external surface of the crystals. In this sense, the advantages of layered TS-1 begins to be noticeable. Cyclooctene conversions up to 4.2% after 2 h (conditions III, Table 6) were observed while conventional TS-1 provided only 0.2% conversion [15]. This is an order of magnitude improvement, which outperforms carbon-templated hierarchical TS-1 (providing 9.3% conversion while TS-1 benchmark provided 4.5% conversion; modified method I, 5 h reaction time) [85]. The seek for further improvement of layered TS-1 catalytic performance led to preparation of silica pillared TS-1-PISi, similar to Ti-MCM-36 catalyst but the TS-1-PISi provided conversion 6.5% after 4 h while the Ti-MCM-36 gave 18% at the same time (conditions II) [82]. The real step forward was the silica-titania pillaring which was first demonstrated on TS-1-PITi [82]. Later on, the silica-titania pillaring was successfully used also for Si/Ti MCM-36E catalysts [43] and to prepare UTL-based purely mesoporous catalyst Ti-IPC-1-PITi [19]. The TS-1-PITi provided cyclooctene conversion up to 21% after 4 h (conditions II).

A parallel development route is the titanium grafting (also referred to as impregnation) with titanium(IV) alkoxides or titanium(IV) chloride. Titanium impregnation with previous acidic deboronation was used to transform several large-pore borosilicates into their titanosilicate analogues; however, the only promising catalysts is Ti-CON (Ti-SSZ-33 in the original reference) [62] (providing 26% resp. 37% after 4 h, depending on way of titanium incorporation). The Ti-CON has 3-dimensional pore system while other impregnated large pore titanosilicates (Ti-AFI, Ti-IFR and extra-large pore Ti-CFI) have only 1-dimensional channels which are not convenient for catalysis. The titanium grafted silica MFI nanosheets (lam MFI-G) provided cyclooctene conversion similar to

directly synthesized lam-TS-1 [96]. It was discussed above (Section 2.3.1) that the process of titanium sites formation is basically the same for silica-titania pillaring and titanium(IV) alkoxide grafting. In conclusion, catalysts prepared in one of these two ways are providing the highest cyclooctene conversions of all titanosilicate catalysts reported so far with hydrogen peroxide as oxidant and their comparison with Ti-IEZ-MWW catalysts would be worth. Note these catalysts contain also considerable amount of extra-framework titanium species (cf. Section 3.3.1 and UV/Vis spectra in references), which appear to contribute to the catalytic activity. This is an important observation, which together with other indicia [17,159], challenges the paradigm of tetrahedrally coordinated titanium species being the only desirable active site. Guo et al. [159] identified (using Raman spectroscopy), even 6-coordinated $\text{Ti}(\text{OSi})_2(\text{OH})_4$ species in the TS-1 and claim that also this 6-coordinated species contributes to the catalytic activity. There is a consensus that one of the initial steps in the titanosilicate catalyzed oxidation is weakening or hydrolysis of one of the Si-O-Ti bridges. Therefore, the species which is able to coordinate hydrogen peroxide is not $\text{Ti}(\text{OSi})_4$ but a defective $\text{Ti}(\text{OSi})_3\text{OH}$ [160]. This species then expands its coordination upon reaction with hydrogen peroxide and subsequently the substrate can be oxidized. The additional titanium sites created by silica-titania pillaring or Ti grafting are expected to be $\text{Ti}(\text{OSi})_3(\text{OH})$ or $\text{Ti}(\text{OSi})_3(\text{OH})_2$ (based on the UV/Vis spectra) and therefore we expect they possess the same ability to expand their coordination and form the peroxo-species as the formerly 4-coordinated framework Ti sites. Knowledge on reactivity of different Ti species in TS-1 has been reviewed, e.g., by Bordiga et al. [160].

The titanium-grafted catalysts does not provide only high conversion but also higher selectivity in comparison with conventional TS-1 (e.g., 55% at 10% conversion [19] vs. TS-1-PITi-(10)b 80% at 20% conversion, Ti-CON (TiCl_4) 90% at 20% conversion [62]) and they are active also in epoxidation with TBHP [48].

Table 13 lists data available for cyclodecene epoxidation with hydrogen peroxide. Cyclodecene oxide proved to be resistant toward epoxide ring opening under the testing reaction conditions and thus high selectivity (up to 97% at 10% conversion) and high epoxide yields (TS-1-PITi 10.9%, Ti-IPC-1PITi 18.6% after 2 h) were achieved when using catalysts with open structure (therefore the lowest diffusion limitations) and sufficient amount of the titanium centres on the external surface.

3.3 Epoxidation of terpenes

Terpenes are more structurally variable substrates in comparison with linear and cyclic alkenes. They also stand closer to real catalytic application of the titanosilicate catalysts because some of their oxides (i.e., α -pinene oxide, linalool oxide) have their applications in pharmacy or perfumery practice [161]. Therefore, testing of novel catalysts in selective oxidation of terpenes is

desirable and brings more detailed information on new material abilities and drawbacks.

Norbornene is structurally close to cyclohexene but the carbon bridge brings more rigidity to the molecule and it has more sphere-like shape than cyclohexene. In addition, its epoxide ring opening leads to a number of different diols, which are difficult to distinguish [162]. Note that more complicated rearrangements and side oxidation routes are characteristic also for other terpenes (e.g., α -pinene [163]). As a result, norbornene behaves similarly to cyclohexene during epoxidation reaction in term of selectivity (Table 14). At low conversion (up to about 5%), high selectivity (65–83%) is obtained using all the catalysts but at conversion over 10%, the selectivity drops considerably and the only catalysts providing at least 50% selectivity are silica and silica-titania pillared TS-1 [82] catalysts and TiCl_4 grafted Ti-CFI and Ti-CON [62].

On the other hand, observing the trends in conversion and yield, norbornene is closer to cyclooctene and cyclodecene: the more open is catalyst structure, the higher is the conversion. In addition, layered zeolite-based catalysts outperform mesoporous Ti-MCM-41. The titanium-grafted and silica-titania pillared catalysts provided the highest norbornene conversion (up to 57% after 4 h, Ti-IPC-1-PITi [19]) and epoxide yield (up to 15.4% after 4 h, Ti-CON (TiCl_4) [62]).

Linalool molecule possesses two different double bonds, which can be oxidized. C1 = C2 terminal double bond and C6 = C7 internal double bond bearing three alkyl substituents. Linalool oxidation was studied on titanium grafted large-pore zeolites [62] and Ti-UTL based Ti-IPC-1-PISi and Ti-IPC-1-PITi catalysts [19]. In all cases, only epoxidation of the internal double bond (which is more electron rich) was observed together with acid catalyzed intramolecular rearrangement of the resulting epoxide [164]. As a major product 2-(5-methyl-5-vinyltetrahydro-1-furyl)-2-propanol (known as linalool oxide) was formed and 2,2-dimethyl-3-hydroxy-6-methyl-6-vinyltetrahydropyran was the minor product. The intramolecular reactions proceeded immediately and thus epoxide itself was not observed. This is a known behavior also for other unsaturated alcohols having the general formula $\text{R}_1\text{R}_2\text{C} = \text{CH}(\text{CH}_2)_n\text{CR}_1\text{R}_2\text{OH}$ where R_1, R_2 are -H or $-\text{CH}_3$ and $n = 1-3$ under conditions of epoxidation over titanosilicate catalysts [165]. As for norbornene, Ti-CON (TBOTi) and silica-titania Ti-IPC-1-PITi were the catalysts providing the highest conversion (up to 47% [19]) and yield of the linalool oxide while the TS-1 and large-pore zeolites with 1-dimensional channels gave conversions an order of magnitude lower (2–4%).

Selective oxidation of α -pinene is a considerable challenge, because the α -pinene undergoes easily C = C double bond oxidation, allylic -C-H bonds oxidation and also rearrangements resulting from highly stressed C_4 ring present in the molecule [163,166]. When α -pinene is oxidized over titanosilicate

catalysts with H₂O₂, verbenone and campholeic aldehyde are usually the main products and epoxide (α -pinene oxide) is only a minor product [64,82,163,166]. The highest reported epoxide selectivity is 20% at 10% conversion obtained with Ti-MCM-36 catalyst [82] resp. 21% at 15% conversion provided by a mesoporous titanosilicate prepared from TS-1 protozeolitic units [166]. However, the epoxide ring opening reaction and rearrangements do not have to be a drawback in all cases. Fraille et al. demonstrated a four step tandem oxidative transformation of stilbene to benzophenone, effectively catalyzed by Ti-MCM-41 and Ti-HMS with TBHP as oxidant [127]. Although gaining a high selectivity required a use of fluorinated solvent (α,α,α -trifluorotoluene), the reaction was feasible also in acetonitrile and this work shows a different way of considering titanosilicate catalyst usage.

3.4 Epoxidation of industrially relevant substrates

Of the industrially relevant substrates to be epoxidized, the most important are molecules such as allylchloride, methallyl chloride(3-chloro-2-methyl-1-propene) and allyl alcohol which are used in epoxy-resin production. All these are small molecules for which medium-pore titanosilicates (namely TS-1) are well suitable catalysts. Therefore, being subject of research, main attention is given to optimization of reaction conditions in order to maximize epoxide yield and selectivity. In this sense, Wróblewska et al. investigated various reaction parameters in epoxidation of allyl alcohol to glycidol using TS-1 with H₂O₂ in a batch reactor [167], Similarly, Jiao et al. investigated epoxidation of methallyl chloride to 2-methyl epichlorhydrine [89]. In his study, Jiao et al. revealed several important findings on solvent influence on methallyl chloride epoxidation and demonstrated TS-1 to be to most suitable catalyst of TS-1, Ti-MWW, Ti-beta, and Ti-YNU-1 group regardless the solvent used. In short, *tert*-butanol was found to be the solvent providing the highest methallyl chloride conversion, epoxide selectivity and H₂O₂ efficiency, although when changing solvent from methanol to ethanol, propanol and butanol, the methallyl chloride conversion decreased considerably (e.g., MeOH 38.6% > ethanol 8.6% > 1-butanol 5.4% vs. *tert*-butanol 85.4% at otherwise same conditions using TS-1 catalyst). Although it is not directly concluded in the article, the explanation of the solvent effect is following: methanol, ethanol, 2-propanol, and 1-butanol are molecules small enough to enter the micropore system of TS-1 together with reactant molecules. There, the solvent molecules cause decrease of the reactant concentration in the vicinity of the titanium sites thus slowing down the reaction. On the other hand, *tert*-butanol (similarly to TBHP) is too bulky to diffuse easily though the TS-1 channels. As a result, it fulfills its solvent role outside the TS-1 crystals but inside, the reaction occurs as under solvent free conditions. Deng et al. followed these finding in a study investigating methallyl chloride epoxidation in continuous slurry reactor using TS-1 prepared in the form of microspheres [168]. In this

article, tuning of the process parameters such as temperature, residence time, ratios of reactants, and additives such as ammonia (to suppress acid catalyzed side reactions) is demonstrated. Finally, a 257 h long continuous test run has been presented maintaining H_2O_2 conversion above 97%, H_2O_2 efficiency above 90% and 2-methyl epichlorhydrine selectivity over 95%. These characteristics might be a good starting for considering a real production unit but before reaching the production scale also issues such as long time catalyst stability, catalyst regeneration, heat management, and others need to be addressed as well as overall economy of the process.

Except these small molecules, epoxidation of unsaturated fatty acids methylesters is another reaction gaining attention [169] and currently methyl oleate epoxidation has been examined also using titanosilicate catalysts with hydrogen peroxide as oxidant [25,170]. Interestingly, when using excess of H_2O_2 even conventional TS-1 is able to catalyze the methyl oleate epoxidation and use of layered TS-1 as well as in other cases, brings the advantage of enhanced accessibility of its active sites.

3.5 Oxidation of organic sulphides

Organic sulphoxides and sulphones are intermediates [171] and building blocks of pharmaceuticals [172] and agrochemicals [173]. In addition, oxidative desulphurization processes are nowadays considered in academia as an alternative route to hydrodesulphurization (HDS) [174]. Corma et al. [175], Hulea et al. [176], and Moreau et al. [177] were the pioneers investigating oxidation of organic sulphides to corresponding sulphoxides and sulphones over titanosilicate catalysts (Ti-beta, Ti-MCM-41, and TS-1). Summarizing their findings, the oxidation of organic sulphides occur smoothly at ambient or slightly elevated temperature (25–40°C) with both H_2O_2 and TBHP as oxidants. Both sulphoxide and sulphone are usually formed at the same time while sulphoxide (first oxidation product) is the major product in early stages of the reaction (before sulphide is depleted). In addition, shape selectivity can be observed clearly. For instance, Corma et al. examined oxidation of methylphenyl sulphide (MPS) and phenyl-*iso*-pentyl sulphide over titanosilicate catalysts (Ti-beta, Ti-MCM-41) with both hydrogen peroxide and *tert*-butylhydroperoxide [175]. The Ti-beta provided higher MPS conversion (95% vs. 80% after 30 min at 40°C) confirming higher intrinsic activity of crystalline titanosilicates, but in oxidation of phenyl-*iso*-pentyl sulphide the diffusion limitations manifested themselves and the Ti-MCM-41 provided higher conversion (20% vs. 60% after 6 h at 40°C). These characteristics make the sulphoxidation also a very convenient test reaction with well-defined and well-detectable and stable products.

Recently, several reports on sulphide oxidation over some of the novel titanosilicate catalysts have been published [65,79,117]. Data for diphenyl

Table 15. Oxidation of Ph₂S with hydrogen peroxide over different titanasilicate catalysts; data are sorted by reaction temperature and conversion.

Catalyst	Catalyst classification	Si/Ti	Temp. (°C)	Time (h)	X ^a (%)	S ^a (%)	Experimental conditions ^b	Ref
Blank	–	–	40	18	11	45	VII	[117]
TS-1	medium pore	72	40	18	16	50	VII	[117]
Ti- MWW	medium pore	57	40	18	36	81	VII	[117]
Ti-IEZ- MWW	IEZ	86	40	18	64	79	VII , 1.2 mmol H ₂ O ₂	[117]
TS-1	medium pore	39	40	4	22	91	VIII	[65]
Ti- UTL	extra-large pore	139	40	4	23	83	VIII	[65]
lam TS-1	layered	36	40	4	34	88	VIII	[65]
Ti-IPC-1-PISi	pillared	480	40	4	39	79	VIII	[65]
TS-1-PITi	Si-Ti-pillared	31	40	4	59	78	VIII	[65]
MTS-1	hierarchical	38.5	30	10	99	98	IX	[79]

^a X – sulphide conversion, S – sulphoxide selectivity

^b **VII** - 1 mmol S, 1 mmol H₂O₂, 10 mg cat., no solv., **VIII** - 4 mmol S, 4 mmol H₂O₂, 10 ml ACN, 50 mg cat., **IX** - 7 mmol S, 5.8 mmol H₂O₂, 5 ml MeOH, 40 mg cat.

sulphide (Ph₂S) are compared in Table 15. Comparing conversion over various catalysts, the accessibility of the active sites can be followed. The better is the accessibility; the higher is conversion (under the same reaction conditions). The Ti-IPC-1-PISi represents an exception due to its extremely low titanium content but on the other hand it shows the potential of pillared catalysts. It is a purely mesoporous material but the titanium sites are present in crystalline layers thus preserving structure characteristic for crystalline titanasilicate and not a mesoporous molecular sieves. As a result, it provides conversion comparable with other layered titanosilicates exhibiting and an order of magnitude higher activity.

In addition to the above data, Kang et al. [79] realized that water slow down the consecutive oxidation of sulphoxide to sulphone thus increasing the reaction selectivity. Our group later clarified that one of the selectivity driving parameters is the actual concentration of the oxidant in the reaction mixture. Dosing of H₂O₂ in 5 steps during the course of reaction resulted in an increase of the sulphoxide selectivity from 87% (when all the oxidant was added at once) to 91% at 40% conversion using the lam-TS-1 catalyst. Thus the dosing provided an effect similar to H₂O₂ dilution with water.

Kon et al. investigated competitive oxidation of methylphenyl sulphide (MPS) and *para*-substituted methylphenyl sulphides which was evaluated using the Hammett free energy plot [178]. It was found that the substrates with electron donating groups (methyl, methoxy groups) were oxidized faster in comparison with MPS (e.g., methyl-*p*-methoxyphenyl sulphide conversion 5.5% vs. MPS conversion 2.7% after 5 min in a competitive experiment) and *para*-halogen substituted MPS were oxidized slower than the MPS (e.g., methyl-*p*-chlorophenyl sulphide conversion 7.3% vs. MPS conversion 8.6% after 5 min). This further confirms the electrophilic character of the titanium active species.

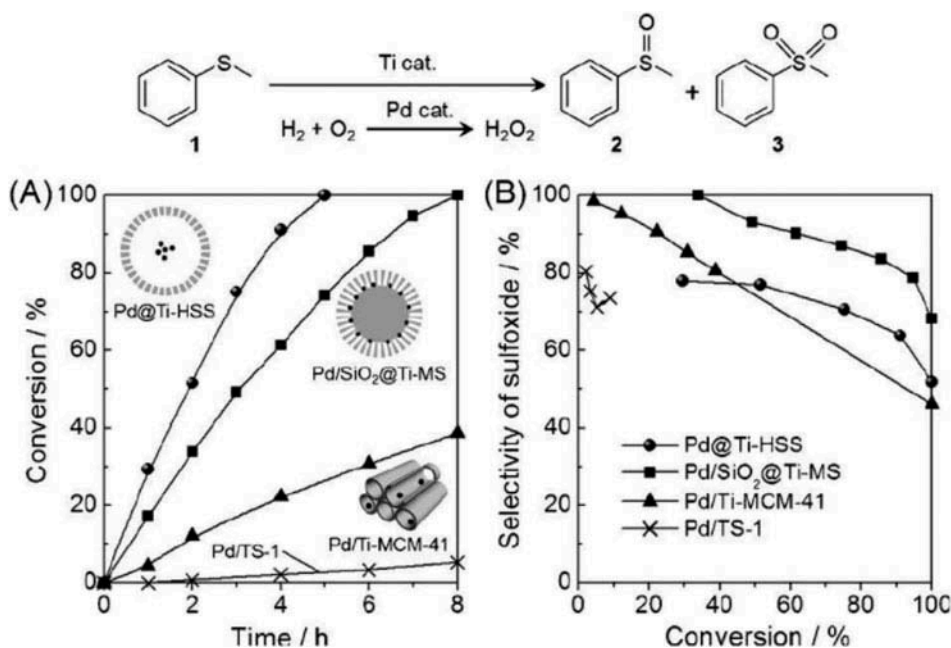


Figure 9. Conversion curve (A) and dependence of selectivity on conversion (B) during MPS oxidation with in-situ generated H₂O₂ over different Pd/titanosilicate composites at 30°C. Reprinted with permission from Kuwahara et al. [148]. Copyright John Wiley and Sons (2017) .

Oxidation of MPS was used also as a test reaction for Pd/titanosilicate composites with the ability to produce hydrogen peroxide *in-situ* from H₂ and O₂ [145,146,148] (Figure 9). The advantages of nanoreactors with Pd as active phase for H₂O₂ generation placed in the core of titanosilicate particle responsible for subsequent selective oxidation of and organic molecule are clearly visible. The oxidation rate over Pd/TS-1 was only 1.64 μmol/h, over Pd/Ti-MCM-41 15.9 μmol/h, over Pd/SiO₂@Ti-MS (a catalyst with solid silica core) 44.6 μmol/h and using Pd@Ti-HHS nanoreactor the oxidation rate was 60 μmol/h under given conditions.

3.6 Hydroxylation of phenol

Titanosilicate catalysts, acting as electrophilic oxidants, are able to oxidize both aliphatic and aromatic hydrocarbons towards corresponding alcohols and ketones and phenols, respectively [20,30]. Presence of electron donating substituent on aromatic ring (such as methyl or hydroxyl) makes further hydroxylation even easier. In this respect, titanosilicates are advantageous catalysts for phenol hydroxylation to hydroquinone and catechol and this process has been already commercialized by Eni [7,9]. Therefore, other catalysts are also being evaluated in this reaction with particular attention

to the *para*-selectivity of the reaction (selectivity towards formation of hydroquinone and *para*-benzoquinone).

Table 16 shows that TS-1 and other medium-pore titanosilicates (e.g., Ti-MEL) exhibited no selectivity between hydroquinone and catechol or slightly more catechol was produced. On the other hand, large pore MSE-type titanosilicates exhibited high selectivity towards formation of hydroquinone (and *para*-benzoquinone as product of subsequent oxidation) [17]. The authors speculated that high *para*-selectivity (up to 92% in sum of hydroquinone and *para*-benzoquinone) results from presence of a defect site close to the titanium site in the 12-ring channel. The defect site helped to stabilize the phenol molecule via hydrogen bond in the right position favoring the oxidation in *para*-position. Thus the observed phenomenon is believed to be more complex than classical shape selectivity; but to verify it a comparison with other large-pore titanosilicates (e.g., Ti-beta or Ti-OKO) would be necessary.

4. Concluding remarks

Novel titanosilicate oxidation catalysts developed in past seven years has been reviewed from structural and catalytic point of view. Recently, several large pore and extra-large pore titanosilicate zeolites have been prepared by direct synthesis (Ti-ITQ-39, Ti-CFI, Ti-UTL) and by post-synthesis modification (Ti-MSE, Ti-CON, Ti-IPC-2, Ti-IPC-4).

In addition, Ti-IEZ-MWW-based materials were investigated intensively with particular aim to increase their titanium content while preserving their high intrinsic activity. Novel approaches to synthesis of lamellar zeolites (restricted crystal growth synthesis and top-down and ADOR method) were demonstrated also for titanosilicate zeolites. The novel approaches enabled to prepare materials taking the advantages of both crystalline titanosilicate zeolites and mesoporous molecular sieves.

It was found that well accessible and active titanium sites can be created by post-synthesis grafting with titanium(IV) alkoxides. The resulting catalysts proved ability to activate both H₂O₂ and TBHP. Last but not least, metal/titanosilicate bifunctional catalysts are being investigated for processes involving *in-situ* formation of H₂O₂ from hydrogen and oxygen gases.

Summarizing the catalytic data, it appears that the best catalytic performance is achieved when the pore size of a catalyst and molecular size of substrate suits. In this sense, TS-1 was optimal for small substrates such as methallylchloride, Ti-MWW, and Ti-MSE were found to be the most active catalysts for linear olefins such as 1-hexene and 1-octene, Ti-IEZ-MWW catalysts and hierarchical TS-1 catalysts were the most efficient for cyclohexene epoxidation and pillared and silica-titania pillared catalysts were found best suitable for bulky cyclooctene, cyclodecene, and norbornene. However, the activity of, e.g., layered TS-1 in epoxidation of linear olefins is much

Table 16. Phenol hydroxylation with hydrogen peroxide over different titanasilicate catalysts; data are sorted by reaction temperature and phenol conversion.

Catalyst	Catalyst ^a classification	Si/Ti	Temp. (°C)	Solvent	Time (h)	X ^b (%)	Main product	y ^b (%)	S ^b (%)	Exp. conditions ^c	Ref
Ti-COE-3	IEZ	149	80	H ₂ O	4	9.7	catechol	5.9	61	I	[33]
Ti-COE-4	IEZ	150	80	H ₂ O	4	15	catechol	9.2	63	I	[33]
HPB-TS-1	hierarchical	41	80	H ₂ O	4	18	catechol	9.0	51	X	[81]
TS-1	medium pore	35	80	H ₂ O	4	21	catechol	12	57	X	[81]
MTS-2	layered	36	80	Acetone	6	24	catechol	12	51	XI	[18]
TS-1	medium pore	47	80	Acetone	6	26	catechol	14	52	XI	[18]
TS-1	medium pore	31	80	H ₂ O	4	28	catechol	14	50	I	[33]
TS-1	medium pore	46	100	None	0.17	1.7	hydroquinone	0.9	53	XII	[17]
Ti-MCM-68-cal	large pore	67	100	None	0.17	6.5	hydroquinone	4.4	69	XII	[17]
Ti-YNU-2 (250, 10)	large pore	90	100	none	0.17	15	hydroquinone	12	79	XII	[17]

^a IEZ – interlayer expanded zeolite^b X – phenol conversion, y – main product yield, S – selectivity to the main product^c **X** – 5 mmol S, 1.66 mmol H₂O₂, 15ml solv., 50 mg cat., **XI** – 21 mmol S, 7 mmol H₂O₂, 1.6 ml solv., 100 mg cat., **XII** – 21.4 mmol S, 4.3 mmol H₂O₂, 20 mg cat.

lower in comparison with TS-1 and Ti-MWW. Finding and explanation for this behavior might be a key to tailor a catalyst for a particular substrate. In addition to the above issue, evaluating and driving the catalyst hydrophilicity appears to deserve a systematic attention. Regardless the above findings, the basic rules remains valid within a narrower groups of similar catalysts and for reactions with TBHP in general: (i) wider pores brings lower diffusion limitations and therefore higher reaction rate and (ii) the more active sites, the higher reaction rate while the size and dimensionality of the pore system is similar.

Regarding the metal/titanosilicate composites development, these materials should be tuned and tested not only for oxidation of sulphides but also for epoxidation and phenol hydroxylation. This would require more test reaction as well as apparatus optimization but based on the above data it should not be and an unfeasible goal.

Funding

The author thanks the Czech Science Foundation for the financial support from project P106/12/G015.

References

- [1] De Jong, K. P. General Aspects. In *Synthesis of Solid Catalysts*; De Jong, K. P., Ed.; Wiley-VCH: Weinheim; **2009**; pp. 3–12.
- [2] Al-Khattaf, S.; Ali, S. A.; Aitani, A. M.; Žilková, N.; Kubička, D.; Čejka, J. Recent Advances in Reactions of Alkylbenzenes over Novel Zeolites: The Effects of Zeolite Structure and Morphology. *Catal. Rev.* **2014**, *56* (4), 333–402. DOI: [10.1080/01614940.2014.946846](https://doi.org/10.1080/01614940.2014.946846).
- [3] Weckhuysen, B. M.; Yu, J. Recent Advances in Zeolite Chemistry and Catalysis. *Chem. Soc. Rev.* **2015**, *44* (20), 7022–7024. DOI: [10.1039/C5CS90100F](https://doi.org/10.1039/C5CS90100F).
- [4] Čejka, J.; Morris, R. E.; Serrano, D. P. Catalysis on Zeolites - Catalysis Science & Technology. *Catal. Sci. Technol.* **2016**, *6* (8), 2465–2466. DOI: [10.1039/C6CY90042A](https://doi.org/10.1039/C6CY90042A).
- [5] Mintova, S.; Barrer, M., Eds. *Verified Syntheses of Zeolitic Materials*, 3rd ed.; Synthesis Commission of the International Zeolite Association, **2016**.
- [6] Baerlocher, C.; McCusker, L. B., Database of Zeolite Structures: <http://www.iza-structure.org/databases/>.
- [7] Eni, Titanium Silicalite (TS-1) Zeolite Based Proprietary Catalyst., <https://www.scribd.com/document/208913719/TS1-Flyer-Lug09> (13.5.2017).
- [8] Eni, Cyclohexanone Oxime Ammoximation of Cyclohexanone with Titanium Silicalite (TS-1) Proprietary Catalyst, https://www.versalis.eni.com/irj/go/km/docs/versalis/Contenuti%20Versalis/EN/Documenti/La%20nostra%20offerta/Licensing/Catalizzatori/ESE_Tecnica_Cyclohexanone_180214.pdf (13.5.2017).
- [9] Perego, C.; Carati, A.; Ingallina, P.; Mantegazza, M. A.; Bellussi, G. Production of Titanium Containing Molecular Sieves and Their Application in Catalysis. *Appl. Catal. A-Gen.* **2001**, *221* (1–2), 63–72. DOI: [10.1016/S0926-860X\(01\)00797-9](https://doi.org/10.1016/S0926-860X(01)00797-9).
- [10] Taramasso, M.; Perego, G.; Notari, B. *US Pat.* 4410501, 1983

- [11] Tatsumi, T. Metal-Substituted Zeolites as Heterogenous Oxidation Catalysts. In *Modern Heterogenous Oxidation Catalysis*; Mizuno, N., Ed.; Wiley-VCH: Weinheim, **2009**; pp. 125–153.
- [12] Wu, P.; Tatsumi, T.; Komatsu, T.; Yashima, T. A Novel Titanosilicate with MWW Structure: II. Catalytic Properties in the Selective Oxidation of Alkenes. *J. Catal.* **2001**, *202* (2), 245–255. DOI: [10.1006/jcat.2001.3278](https://doi.org/10.1006/jcat.2001.3278).
- [13] Tang, B.; Dai, W.; Sun, X.; Guan, N.; Li, L.; Hunger, M. A Procedure for the Preparation of Ti-Beta Zeolites for Catalytic Epoxidation with Hydrogen Peroxide. *Green Chem.* **2014**, *16* (4), 2281–2291. DOI: [10.1039/C3GC42534G](https://doi.org/10.1039/C3GC42534G).
- [14] Roth, W. J.; Nachtigall, P.; Morris, R. E.; Čejka, J. Two-Dimensional Zeolites: Current Status and Perspectives. *Chem. Rev.* **2014**, *114* (9), 4807–4837. DOI: [10.1021/cr400600f](https://doi.org/10.1021/cr400600f).
- [15] Na, K.; Jo, C.; Kun, J.; Ahn, W. S.; Ryoo, R. MFI Titanosilicate Nanosheets with Single-Unit-Cell Thickness as an Oxidation Catalyst Using Peroxides. *ACS Catal.* **2011**, *1* (8), 901–907. DOI: [10.1021/cs2002143](https://doi.org/10.1021/cs2002143).
- [16] Kumar, A.; Srinivas, D. Selective Oxidation of Cyclic Olefins over Framework Ti-Substituted, Three-Dimensional, Mesoporous Ti-SBA-12 and Ti-SBA-16 Molecular Sieves. *Catal. Today.* **2012**, *198* (1), 59–68. DOI: [10.1016/j.cattod.2012.01.035](https://doi.org/10.1016/j.cattod.2012.01.035).
- [17] Sasaki, M.; Sato, Y.; Tsuboi, Y.; Inagaki, S.; Kubota, Y. Ti-YNU-2: A Microporous Titanosilicate with Enhanced Catalytic Performance for Phenol Oxidation. *ACS Catal.* **2014**, *4* (8), 2653–2657. DOI: [10.1021/cs5007926](https://doi.org/10.1021/cs5007926).
- [18] Chen, H. L.; Li, S. W.; Wang, Y. M. Synthesis and Catalytic Properties of Multilayered MEL-type Titanosilicate Nanosheets. *J. Mater. Chem. A.* **2015**, *3* (11), 5889–5900. DOI: [10.1039/C4TA06473A](https://doi.org/10.1039/C4TA06473A).
- [19] Přečh, J.; Čejka, J. UTL Titanosilicate: An Extra-Large Pore Epoxidation Catalyst with Tunable Textural Properties. *Catal. Today.* **2016**, *277*, 2–8. DOI: [10.1016/j.cattod.2015.09.036](https://doi.org/10.1016/j.cattod.2015.09.036).
- [20] Ratnasamy, P.; Srinivas, D.; Knözinger, H. Active Sites and Reactive Intermediates in Titanium Silicate Molecular Sieves. *Adv. Catalysis; Acad.* **2004**, *48*, 1–169.
- [21] Wu, P.; Kubota, Y.; Yokoi, T. A Career in Catalysis: Takashi Tatsumi. *ACS Catal.* **2014**, *4* (1), 23–30. DOI: [10.1021/cs4006056](https://doi.org/10.1021/cs4006056).
- [22] Wu, P.; Xu, H.; Xu, L.; Liu, Y.; He, M. *MWW-Type Titanosilicate*; Springer-Verlag: Berlin Heidelberg, **2013**.
- [23] Moliner, M.; Corma, A. Advances in the Synthesis of Titanosilicates: From the Medium Pore TS-1 Zeolite to Highly-Accessible Ordered Materials. *Microporous Mesoporous Mater.* **2014**, *189*, 31–40. DOI: [10.1016/j.micromeso.2013.08.003](https://doi.org/10.1016/j.micromeso.2013.08.003).
- [24] Xu, H.; Wu, P. Recent Progresses in Titanosilicates. *Chin. J. Chem.* **2017**, *35*, 836–844.
- [25] Wilde, N.; Přečh, J.; Pelz, M.; Kubů, M.; Čejka, J.; Gläser, R. Accessibility Enhancement of TS-1-based Catalysts for Improving the Epoxidation of Plant Oil-Derived Substrates. *Catal. Sci. Technol.* **2016**, *6*, 7280–7288. DOI: [10.1039/C6CY01232A](https://doi.org/10.1039/C6CY01232A).
- [26] Jana, S. K.; Nishida, R.; Shindo, K.; Kugita, T.; Namba, S. Pore Size Control of Mesoporous Molecular Sieves Using Different Organic Auxiliary Chemicals. *Microporous Mesoporous Mater.* **2004**, *68* (1–3), 133–142. DOI: [10.1016/j.micromeso.2003.12.010](https://doi.org/10.1016/j.micromeso.2003.12.010).
- [27] Opanasenko, M. V.; Roth, W. J.; Čejka, J. Two-Dimensional Zeolites in Catalysis: Current Status and Perspectives. *Catal. Sci. Technol.* **2016**, *6* (8), 2467–2484. DOI: [10.1039/C5CY02079D](https://doi.org/10.1039/C5CY02079D).
- [28] Millini, R.; Previde Massara, E.; Perego, G.; Bellussi, G. Framework Composition of Titanium Silicalite-1. *J. Catal.* **1992**, *137* (2), 497–503. DOI: [10.1016/0021-9517\(92\)90176-I](https://doi.org/10.1016/0021-9517(92)90176-I).

- [29] Notari, B.; Titanium Silicalites. *Catal. Today*. **1993**, *18* (2), 163–172. DOI: [10.1016/0920-5861\(93\)85029-Y](https://doi.org/10.1016/0920-5861(93)85029-Y).
- [30] Notari, B.; Microporous Crystalline Titanium Silicates. *Adv. Catalysis* **1996**, *41*, 253–334.
- [31] Lamberti, C.; Bordiga, S.; Zecchina, A.; Carati, A.; Fitch, A. N.; Artioli, G.; Petrini, G.; Salvalaggio, M.; Marra, G. L. Structural Characterization of Ti-Silicalite-1: A Synchrotron Radiation X-Ray Powder Diffraction Study. *J. Catal.* **1999**, *183* (2), 222–231. DOI: [10.1006/jcat.1999.2403](https://doi.org/10.1006/jcat.1999.2403).
- [32] Vayssilov, G. N.; Structural and Physicochemical Features of Titanium Silicalites. *Catal. Rev.* **1997**, *39* (3), 209–251. DOI: [10.1080/01614949709353777](https://doi.org/10.1080/01614949709353777).
- [33] Xiao, F. S.; Xie, B.; Zhang, H. Y.; Wang, L.; Meng, X. J.; Zhang, W. P.; Bao, X. H.; Yilmaz, B.; Muller, U.; Gies, H.; Imai, H.; Tatsumi, T.; De Vos, D. Interlayer-Expanded Microporous Titanosilicate Catalysts with Functionalized Hydroxyl Groups. *Chem. Cat. Chem.* **2011**, *3* (9), 1442–1446. DOI: [10.1002/cctc.201100144](https://doi.org/10.1002/cctc.201100144).
- [34] Lakiss, L.; Rivallan, M.; Goupil, J.-M.; El Fallah, J.; Mintova, S. Self-Assembled Titanosilicate TS-1 Nanocrystals in Hierarchical Structures. *Catal. Today*. **2011**, *168* (1), 112–117. DOI: [10.1016/j.cattod.2010.12.045](https://doi.org/10.1016/j.cattod.2010.12.045).
- [35] Müller, U.; Steck, W. Ammonium-Based Alkaline-Free Synthesis of MFI-Type Boron- and Titanium Zeolites. In *Stud. Surf. Sci. Catal.*; Weitkamp, J., Karge, H. G., Pfeifer, H., Hölderich, W., Eds.; Elsevier: Amsterdam, **1994**; pp 203–210.
- [36] Gang, L.; Xinwen, G.; Xiangsheng, W.; Qi, Z.; Xinhe, B.; Xiuwen, H.; Liwu, L. Synthesis of Titanium Silicalites in Different Template Systems and Their Catalytic Performance. *Appl. Catal. A-Gen.* **1999**, *185* (1), 11–18. DOI: [10.1016/S0926-860X\(99\)00115-5](https://doi.org/10.1016/S0926-860X(99)00115-5).
- [37] Zuo, Y.; Liu, M.; Zhang, T.; Meng, C.; Guo, X.; Song, C. Enhanced Catalytic Performance of Titanium Silicalite-1 in Tuning the Crystal Size in the Range 1200–200 Nm in a Tetrapropylammonium Bromide System. *Chem. Cat. Chem.* **2015**, *7* (17), 2660–2668. DOI: [10.1002/cctc.201500440](https://doi.org/10.1002/cctc.201500440).
- [38] Wu, P.; Tatsumi, T.; Komatsu, T.; Yashima, T. Hydrothermal Synthesis of a Novel Titanosilicate with MWW Topology. *Chem. Lett.* **2000**, *29* (7), 774–775. DOI: [10.1246/cl.2000.774](https://doi.org/10.1246/cl.2000.774).
- [39] Wu, P.; Tatsumi, T.; Komatsu, T.; Yashima, T. A Novel Titanosilicate with MWW Structure. I. Hydrothermal Synthesis, Elimination of Extraframework Titanium, and Characterizations. *J. Phys. Chem. B* **2001**, *105* (15), 2897–2905. DOI: [10.1021/jp002816s](https://doi.org/10.1021/jp002816s).
- [40] Xu, H.; Fu, L.; Jiang, J.-G.; He, M.; Wu, P. Preparation of Hierarchical MWW-type Titanosilicate by Interlayer Silylation with Dimeric Silane. *Microporous Mesoporous Mater.* **2014**, *189*, 41–48. DOI: [10.1016/j.micromeso.2013.09.041](https://doi.org/10.1016/j.micromeso.2013.09.041).
- [41] Ouyang, X.; Wanglee, Y.-J.; Hwang, S.-J.; Xie, D.; Rea, T.; Zones, S. I.; Katz, A. Novel Surfactant-Free Route to Delaminated All-Silica and Titanosilicate Zeolites Derived from a Layered Borosilicate MWW Precursor. *Dalton Trans.* **2014**, *43* (27), 10417–10429. DOI: [10.1039/C4DT00383G](https://doi.org/10.1039/C4DT00383G).
- [42] Yoshioka, M.; Yokoi, T.; Tatsumi, T. Effectiveness of the Reversible Structural Conversion of MWW Zeolite for Preparation of Interlayer-Expanded Ti-MWW with High Catalytic Performance in Olefin Epoxidation. *Micropor. Mesopor. Mater.* **2014**, *200*, 11–18. DOI: [10.1016/j.micromeso.2014.08.007](https://doi.org/10.1016/j.micromeso.2014.08.007).
- [43] Jin, F.; Chang, C.-C.; Yang, C.-W.; Lee, J.-F.; Jang, L.-Y.; Cheng, S. New Mesoporous Titanosilicate MCM-36 Material Synthesized by Pillaring Layered ERB-1 Precursor. *J. Mater. Chem. A*. **2015**, *3* (16), 8715–8724. DOI: [10.1039/C5TA00364D](https://doi.org/10.1039/C5TA00364D).

- [44] Kubota, Y.; Koyama, Y.; Yamada, T.; Inagaki, S.; Tatsumi, T. Synthesis and Catalytic Performance of Ti-MCM-68 for Effective Oxidation Reactions. *Chem. Commun.* **2008**, (46), 6224–6226.
- [45] Kubota, Y.; Inagaki, S. High-Performance Catalysts with MSE-Type Zeolite Framework. *Top. Catal.* **2015**, 58 (7), 480–493. DOI: [10.1007/s11244-015-0389-6](https://doi.org/10.1007/s11244-015-0389-6).
- [46] Inagaki, S.; Tsuboi, Y.; Sasaki, M.; Mamiya, K.; Park, S.; Kubota, Y. Enhancement of Para-Selectivity in the Phenol Oxidation with H₂O₂ over Ti-MCM-68 Zeolite Catalyst. *Green Chem.* **2016**, 18 (3), 735–741. DOI: [10.1039/C5GC01237F](https://doi.org/10.1039/C5GC01237F).
- [47] Koyama, Y.; Ikeda, T.; Tatsumi, T.; Kubota, Y. A Multi-Dimensional Microporous Silicate that Is Isomorphous to Zeolite MCM-68. *Angew. Chem. Int. Ed.* **2008**, 47 (6), 1042–1046. DOI: [10.1002/\(ISSN\)1521-3773](https://doi.org/10.1002/(ISSN)1521-3773).
- [48] Chang, -C.-C.; Jin, F.; Jang, L.-Y.; Lee, J.-F.; Cheng, S. Effect of the Grafting Agent on the Structure and Catalytic Performance of Ti-MCM-22. *Catal. Sci. Technol.* **2016**, 6 (20), 7631–7642. DOI: [10.1039/C6CY01591C](https://doi.org/10.1039/C6CY01591C).
- [49] Corma, A.; Diaz-Cabanas, M. J.; Domine, M. E.; Rey, F. Ultra Fast and Efficient Synthesis of Ti-ITQ-7 and Positive Catalytic Implications. *Chem. Commun.* **2000**, (18), 1725–1726. DOI: [10.1039/b004203j](https://doi.org/10.1039/b004203j).
- [50] Moliner, M.; Serna, P.; Cantín, Á.; Sastre, G.; Díaz-Cabañas, M. J.; Corma, A. Synthesis of the Ti–Silicate Form of BEC Polymorph of B-Zeolite Assisted by Molecular Modeling. *J. Phys. Chem. C.* **2008**, 112 (49), 19547–19554. DOI: [10.1021/jp805400u](https://doi.org/10.1021/jp805400u).
- [51] Cambor, M. A.; Corma, A.; Martínez, A.; Pérez-Pariente, J. Synthesis of a Titaniumsilicoaluminate Isomorphous to Zeolite Beta and Its Application as a Catalyst for the Selective Oxidation of Large Organic Molecules. *J. Chem. Soc. Chem. Commun.* **1992**, 8, 589–590. DOI: [10.1039/C39920000589](https://doi.org/10.1039/C39920000589).
- [52] Cambor, M. A.; Corma, A.; Pérez-Pariente, J. Synthesis of Titanoaluminosilicates Isomorphous to Zeolite Beta, Active as Oxidation Catalysts. *Zeolites.* **1993**, 13 (2), 82–87. DOI: [10.1016/0144-2449\(93\)90064-A](https://doi.org/10.1016/0144-2449(93)90064-A).
- [53] Cambor, M. A.; Costantini, M.; Corma, A.; Gilbert, L.; Esteve, P.; Martínez, A.; Valencia, S. Synthesis and Catalytic Activity of Aluminium-Free Zeolite Ti-[Small Beta] Oxidation Catalysts. *Chem. Commun.* **1996**, (11), 1339–1340.
- [54] Van Der Waal, J. C.; Lin, P.; Rigutto, M. S.; Van Bekkum, H. Synthesis of Aluminium Free Titanium Silicate with the BEA Structure Using a New and Selective Template and Its Use as a Catalyst in Epoxidations. In *Stud. Surf. Sci. Catal.*; Hakze Chon, S.-K. I., Young Sun, U., Eds.; Elsevier: Amsterdam, **1997**; pp 1093–1100.
- [55] Sasidharan, M.; Bhaumik, A. Designing the Synthesis of Catalytically Active Ti-[Small Beta] by Using Various New Templates in the Presence of Fluoride Anion. *Phys. Chem. Chem. Phys.* **2011**, 13 (36), 16282–16294. DOI: [10.1039/c1cp21013k](https://doi.org/10.1039/c1cp21013k).
- [56] Blasco, T.; Cambor, M. A.; Corma, A.; Esteve, P.; Guil, J. M.; Martínez, A.; Perdigón-Melón, J. A.; Valencia, S. Direct Synthesis and Characterization of Hydrophobic Aluminum-Free Ti–Beta Zeolite. *J. Phys. Chem. B.* **1998**, 102 (1), 75–88. DOI: [10.1021/jp973288w](https://doi.org/10.1021/jp973288w).
- [57] Tatsumi, T.; Jappar, N. Properties of Ti-Beta Zeolites Synthesized by Dry-Gel Conversion and Hydrothermal Methods. *J. Phys. Chem. B.* **1998**, 102 (37), 7126–7131. DOI: [10.1021/jp9816216](https://doi.org/10.1021/jp9816216).
- [58] Cambor, M. A.; Constantini, M.; Corma, A.; Esteve, P.; Gilbert, L.; Martínez, A.; Valencia, S. A New Highly Efficient Method for the Synthesis of Ti-Beta Zeolite Oxidation Catalyst. *Appl. Catal. A-Gen.* **1995**, 133 (2), L185–L189. DOI: [10.1016/0926-860X\(95\)00252-9](https://doi.org/10.1016/0926-860X(95)00252-9).

- [59] Van Der Waal, J. C.; Rigutto, M. S.; Van Bekkum, H. Zeolite Titanium Beta as a Selective Catalyst in the Epoxidation of Bulky Alkenes. *Appl. Catal. A-Gen.* **1998**, *167* (2), 331–342. DOI: [10.1016/S0926-860X\(97\)00323-2](https://doi.org/10.1016/S0926-860X(97)00323-2).
- [60] Corma, A.; Esteve, P.; Martinez, A.; Valencia, S. Oxidation of Olefins with Hydrogen Peroxide and tert-Butyl Hydroperoxide on Ti-Beta Catalyst. *J. Catal.* **1995**, *152* (1), 18–24. DOI: [10.1006/jcat.1995.1055](https://doi.org/10.1006/jcat.1995.1055).
- [61] Moliner, M.; Corma, A. Direct Synthesis of a Titanosilicate Molecular Sieve Containing Large and Medium Pores in Its Structure. *Microporous Mesoporous Mater.* **2012**, *164*, 44–48. DOI: [10.1016/j.micromeso.2012.06.035](https://doi.org/10.1016/j.micromeso.2012.06.035).
- [62] Přech, J.; Vitvarová, D.; Lupínková, L.; Kubů, M.; Čejka, J. Titanium Impregnated Borosilicate Zeolites for Epoxidation Catalysis. *Microporous Mesoporous Mater.* **2015**, *212*, 28–34. DOI: [10.1016/j.micromeso.2015.03.015](https://doi.org/10.1016/j.micromeso.2015.03.015).
- [63] Balkus, K. J., Jr; Gabrielov, A. G.; Zones, S. I. The Synthesis of UTD-1, Ti-UTD-1 and Ti-UTD-8 Using CP*2CoOH as a Structure Directing Agent. In *Stud. Surf. Sci. Catal.*; Laurent, B., Serge, K., Eds.; Elsevier: Amsterdam, **1995**; pp. 519–525.
- [64] Přech, J.; Kubů, M.; Čejka, J. Synthesis and Catalytic Properties of Titanium Containing Extra-Large Pore Zeolite CIT-5. *Catal. Today.* **2014**, *227*, 80–86. DOI: [10.1016/j.cattod.2014.01.003](https://doi.org/10.1016/j.cattod.2014.01.003).
- [65] Přech, J.; Morris, R. E.; Čejka, J. Selective Oxidation of Bulky Organic Sulphides over Layered Titanosilicate Catalysts. *Catal. Sci. Technol.* **2016**, *6* (8), 2775–2786. DOI: [10.1039/C5CY02083B](https://doi.org/10.1039/C5CY02083B).
- [66] Wu, P.; Komatsu, T.; Yashima, T. Characterization of Titanium Species Incorporated into Dealuminated Mordenites by Means of IR Spectroscopy and 18o-Exchange Technique. *J. Phys. Chem.* **1996**, *100* (24), 10316–10322. DOI: [10.1021/jp960307d](https://doi.org/10.1021/jp960307d).
- [67] Wu, P.; Komatsu, T.; Yashima, T. Ammoximation of Ketones over Titanium Mordenite. *J. Catal.* **1997**, *168* (2), 400–411. DOI: [10.1006/jcat.1997.1679](https://doi.org/10.1006/jcat.1997.1679).
- [68] Wu, P.; Komatsu, T.; Yashima, T. Hydroxylation of Aromatics with Hydrogen Peroxide over Titanosilicates with MOR and MFI Structures: Effect of Ti Peroxo Species on the Diffusion and Hydroxylation Activity. *J. Phys. Chem. B.* **1998**, *102* (46), 9297–9303. DOI: [10.1021/jp982951t](https://doi.org/10.1021/jp982951t).
- [69] Roth, W. J.; Nachtigall, P.; Morris, R. E.; Wheatley, P. S.; Seymour, V. R.; Ashbrook, S. E.; Chlubná, P.; Grajciar, L.; Položij, M.; Zukal, A.; Shvets, O.; Čejka, J. A Family of Zeolites with Controlled Pore Size Prepared Using A Top-Down Method. *Nat. Chem.* **2013**, *5* (7), 628–633. DOI: [10.1038/nchem.1662](https://doi.org/10.1038/nchem.1662).
- [70] Eliášová, P.; Opanasenko, M.; Wheatley, P. S.; Shamzhy, M.; Mazur, M.; Nachtigall, P.; Roth, W. J.; Morris, R. E.; Čejka, J. The ADOR Mechanism for the Synthesis of New Zeolites. *Chem. Soc. Rev.* **2015**, *44* (20), 7177–7206. DOI: [10.1039/C5CS00045A](https://doi.org/10.1039/C5CS00045A).
- [71] Mazur, M.; Wheatley, P. S.; Navarro, M.; Roth, W. J.; Položij, M.; Mayoral, A.; Eliášová, P.; Nachtigall, P.; Čejka, J.; Morris, R. E. Synthesis of ‘Unfeasible’ Zeolites. *Nat. Chem.* **2016**, *8* (1), 58–62. DOI: [10.1038/nchem.2374](https://doi.org/10.1038/nchem.2374).
- [72] Morris, S. A.; Bignami, G. P. M.; Tian, Y.; Navarro, M.; Firth, D. S.; Čejka, J.; Wheatley, P. S.; Dawson, D. M.; Slawinski, W. A.; Wragg, D. S.; Morris, R. E.; Ashbrook, S. E. In Situ Solid-State NMR and XRD Studies of the ADOR Process and the Unusual Structure of Zeolite IPC-6. *Nat. Chem.* **2017**. DOI: [10.1038/nchem.2761](https://doi.org/10.1038/nchem.2761).
- [73] Kasneryk, V.; Shamzhy, M.; Opanasenko, M.; Wheatley, P. S.; Morris, S. A.; Russell, S. E.; Mayoral, A.; Trachta, M.; Čejka, J.; Morris, R. E. Expansion of the ADOR Strategy for the Synthesis of Zeolites: The Synthesis of IPC-12 from Zeolite UOV. *Angew. Chem. Int. Ed.* **2017**, *56* (15), 4324–4327. DOI: [10.1002/anie.201700590](https://doi.org/10.1002/anie.201700590).

- [74] Verboekend, D.; Perez-Ramirez, J. Design of Hierarchical Zeolite Catalysts by Desilication. *Catal. Sci. Technol.* **2011**, *1* (6), 879–890. DOI: [10.1039/c1cy00150g](https://doi.org/10.1039/c1cy00150g).
- [75] Groen, J. C.; Moulijn, J. A.; Perez-Ramirez, J. Desilication: On the Controlled Generation of Mesoporosity in MFI Zeolites. *J. Mater. Chem.* **2006**, *16* (22), 2121–2131. DOI: [10.1039/B517510K](https://doi.org/10.1039/B517510K).
- [76] Perez-Ramirez, J.; Christensen, C. H.; Egeblad, K.; Christensen, C. H.; Groen, J. C. Hierarchical Zeolites: Enhanced Utilisation of Microporous Crystals in Catalysis by Advances in Materials Design. *Chem. Soc. Rev.* **2008**, *37* (11), 2530–2542. DOI: [10.1039/b809030k](https://doi.org/10.1039/b809030k).
- [77] Schmidt, I.; Krogh, A.; Wienberg, K.; Carlsson, A.; Brorson, M.; Jacobsen, C. J. H. Catalytic Epoxidation of Alkenes with Hydrogen Peroxide over First Mesoporous Titanium-Containing Zeolite. *Chem. Commun.* **2000**, (21), 2157–2158.
- [78] Xin, H.; Zhao, J.; Xu, S.; Li, J.; Zhang, W.; Guo, X.; Hensen, E. J. M.; Yang, Q.; Li, C. Enhanced Catalytic Oxidation by Hierarchically Structured TS-1 Zeolite. *J. Phys. Chem. C* **2010**, *114* (14), 6553–6559. DOI: [10.1021/jp912112h](https://doi.org/10.1021/jp912112h).
- [79] Kang, Z.; Fang, G.; Ke, Q.; Hu, J.; Tang, T. Superior Catalytic Performance of Mesoporous Zeolite TS-1 for the Oxidation of Bulky Organic Sulfides. *Chem. Cat. Chem.* **2013**, *5* (8), 2191–2194. DOI: [10.1002/cctc.201300084](https://doi.org/10.1002/cctc.201300084).
- [80] Singh, B.; Rana, B. S.; Sivakumar, L. N.; Bahuguna, G. M.; Sinha, A. K. Efficient Catalytic Epoxidation of Olefins with Hierarchical Mesoporous TS-1 Using TBHP as an Oxidant. *J. Porous Mater.* **2013**, *20* (2), 397–405. DOI: [10.1007/s10934-012-9609-7](https://doi.org/10.1007/s10934-012-9609-7).
- [81] Cheng, W.; Jiang, Y.; Xu, X.; Wang, Y.; Lin, K.; Pescarmona, P. P. Easily Recoverable Titanosilicate Zeolite Beads with Hierarchical Porosity: Preparation and Application as Oxidation Catalysts. *J. Catal.* **2016**, *333*, 139–148. DOI: [10.1016/j.jcat.2015.09.017](https://doi.org/10.1016/j.jcat.2015.09.017).
- [82] Přečh, J.; Eliášová, P.; Aldhayan, D.; Kubů, M. Epoxidation of Bulky Organic Molecules over Pillared Titanosilicates. *Catal. Today*. **2015**, *243*, 134–140. DOI: [10.1016/j.cattod.2014.07.002](https://doi.org/10.1016/j.cattod.2014.07.002).
- [83] Wang, B.; Lin, M.; Peng, X.; Zhu, B.; Shu, X. Hierarchical TS-1 Synthesized Effectively by Post-Modification with TPAOH and Ammonium Hydroxide. *RSC Adv.* **2016**, *6* (51), 44963–44971. DOI: [10.1039/C6RA06657G](https://doi.org/10.1039/C6RA06657G).
- [84] Tekla, J.; Tarach, K. A.; Olejniczak, Z.; Girman, V.; Góra-Marek, K. Effective Hierarchization of TS-1 and Its Catalytic Performance in Cyclohexene Epoxidation. *Micropor. Mesopor. Mater.* **2016**, *233*, 16–25. DOI: [10.1016/j.micromeso.2016.06.031](https://doi.org/10.1016/j.micromeso.2016.06.031).
- [85] Ok, D.-Y.; Jiang, N.; Prasetyanto, E. A.; Jin, H.; Park, S.-E. Epoxidation of Cyclic-Olefins over Carbon Template Mesoporous TS-1. *Micropor. Mesopor. Mater.* **2011**, *141* (1–3), 2–7. DOI: [10.1016/j.micromeso.2010.12.031](https://doi.org/10.1016/j.micromeso.2010.12.031).
- [86] Jiang, Y.; Li, X.; Zhang, S.; He, Y.; Li, G.; Li, D.; Xu, X.; Lin, K. Titanosilicate Composite with Zeolite-Large-Crystal Core and Mesoporous Shell Structures: One-Step Synthesis and Application in Catalytic Oxidations. *Mater. Lett.* **2014**, *132*, 270–272.
- [87] Silvestre-Albero, A.; Grau-Atienza, A.; Serrano, E.; García-Martínez, J.; Silvestre-Albero, J. Desilication of TS-1 Zeolite for the Oxidation of Bulky Molecules. *Catal. Commun.* **2014**, *44*, 35–39. DOI: [10.1016/j.catcom.2013.08.004](https://doi.org/10.1016/j.catcom.2013.08.004).
- [88] Wu, P.; Xu, H.; Xu, L.; Liu, Y.; He, M. *Synthesis of Ti-MWW Zeolite, MWW-Type Titanosilicate: Synthesis, Structural Modification and Catalytic Applications to Green Oxidations*; Springer Berlin Heidelberg: Berlin, Heidelberg, **2013**; pp. 9–34.
- [89] Jiao, W.; He, Y.; Li, J.; Wang, J.; Tatsumi, T.; Fan, W. Ti-Rich TS-1: A Highly Active Catalyst for Epoxidation of Methallyl Chloride to 2-Methyl Epichlorohydrin. *Appl. Catal. A-Gen.* **2015**, *491*, 78–85. DOI: [10.1016/j.apcata.2014.11.030](https://doi.org/10.1016/j.apcata.2014.11.030).

- [90] Koo, J. B.; Jiang, N.; Saravanamurugan, S.; Bejblova, M.; Musilova, Z.; Čejka, J.; Park, S. E. Direct Synthesis of Carbon-Templating Mesoporous ZSM-5 Using Microwave Heating. *J. Catal.* **2010**, *276* (2), 327–334. DOI: [10.1016/j.jcat.2010.09.024](https://doi.org/10.1016/j.jcat.2010.09.024).
- [91] Burton, A. W.; Zones, S. I. Chapter 5 - Organic Molecules in Zeolite Synthesis: Their Preparation and Structure-Directing Effects. In *Stud. Surf. Sci. Catal.*; Čejka, J., Van Bakkum, H., Corma, A., Schüth, F., Eds.; Elsevier: Amsterdam, **2007**; pp. 137–179.
- [92] Roth, W. J.; Gil, B.; Marszalek, B. Comprehensive System Integrating 3D and 2D Zeolite Structures with Recent New Types of Layered Geometries. *Catal. Today*. **2014**, *227* (0), 9–14. DOI: [10.1016/j.cattod.2013.09.032](https://doi.org/10.1016/j.cattod.2013.09.032).
- [93] Roth, W. J.; Čejka, J. Two-Dimensional Zeolites: Dream or Reality? *Catal. Sci. Technol.* **2011**, *1* (1), 43–53. DOI: [10.1039/c0cy00027b](https://doi.org/10.1039/c0cy00027b).
- [94] Wang, J. G.; Xu, L.; Zhang, K.; Peng, H. G.; Wu, H. H.; Jiang, J. G.; Liu, Y. M.; Wu, P. Multilayer Structured MFI-type Titanosilicate: Synthesis and Catalytic Properties in Selective Epoxidation of Bulky Molecules. *J. Catal.* **2012**, *288*, 16–23. DOI: [10.1016/j.jcat.2011.12.023](https://doi.org/10.1016/j.jcat.2011.12.023).
- [95] Jin, F.; Chen, S.-Y.; Jang, L.-Y.; Lee, J.-F.; Cheng, S. New Ti-Incorporated MCM-36 as an Efficient Epoxidation Catalyst Prepared by Pillaring MCM-22 Layers with Titanosilicate. *J. Catal.* **2014**, *319*, 247–257. DOI: [10.1016/j.jcat.2014.09.009](https://doi.org/10.1016/j.jcat.2014.09.009).
- [96] Kim, J.; Chun, J.; Ryoo, R. MFI Zeolite Nanosheets with Post-Synthetic Ti Grafting for Catalytic Epoxidation of Bulky Olefins Using H₂O₂. *Chem. Commun.* **2015**, *51* (66), 13102–13105. DOI: [10.1039/C5CC04510J](https://doi.org/10.1039/C5CC04510J).
- [97] Li, C.-G.; Lu, Y.; Wu, H.; Wu, P.; He, M. A Hierarchically Core/Shell-Structured Titanosilicate with Multiple Mesopore Systems for Highly Efficient Epoxidation of Alkenes. *Chem. Commun.* **2015**, *51* (80), 14905–14908. DOI: [10.1039/C5CC05278E](https://doi.org/10.1039/C5CC05278E).
- [98] Choi, M.; Na, K.; Kim, J.; Sakamoto, Y.; Terasaki, O.; Ryoo, R. Stable Single-Unit-Cell Nanosheets of Zeolite MFI as Active and Long-Lived Catalysts. *Nature* **2009**, *461* (7265), 828–828. DOI: [10.1038/nature08493](https://doi.org/10.1038/nature08493).
- [99] Park, W.; Yu, D.; Na, K.; Jelfs, K. E.; Slater, B.; Sakamoto, Y.; Ryoo, R. Hierarchically Structure-Directing Effect of Multi-Ammonium Surfactants for the Generation of MFI Zeolite Nanosheets. *Chem. Mater.* **2011**, *23* (23), 5131–5137. DOI: [10.1021/cm201709q](https://doi.org/10.1021/cm201709q).
- [100] Kim, S.-Y.; Ban, H.-J.; Ahn, W.-S. Ti-MCM-36: A New Mesoporous Epoxidation Catalyst. *Catal. Lett.* **2007**, *113* (3), 160–164. DOI: [10.1007/s10562-007-9022-z](https://doi.org/10.1007/s10562-007-9022-z).
- [101] Zhang, X.; Liu, D.; Xu, D.; Asahina, S.; Cychosz, K. A.; Agrawal, K. V.; Al Wahedi, Y.; Bhan, A.; Al Hashimi, S.; Terasaki, O.; Thommes, M.; Tsapatsis, M. Synthesis of Self-Pillared Zeolite Nanosheets by Repetitive Branching. *Science* **2012**, *336* (6089), 1684–1687. DOI: [10.1126/science.1221111](https://doi.org/10.1126/science.1221111).
- [102] Corma, A.; Diaz, U.; Domine, M. E.; Fornés, V. AlITQ-6 and TiITQ-6: Synthesis, Characterization, and Catalytic Activity. *Angew. Chem. Int. Ed.* **2000**, *39* (8), 1499–1501. DOI: [10.1002/\(SICI\)1521-3773\(20000417\)39:8<1499::AID-ANIE1499>3.0.CO;2-0](https://doi.org/10.1002/(SICI)1521-3773(20000417)39:8<1499::AID-ANIE1499>3.0.CO;2-0).
- [103] Corma, A.; Fornes, V.; Pergher, S. B.; Maesen, T. L. M.; Buglass, J. G. Delaminated Zeolite Precursors as Selective Acidic Catalysts. *Nature* **1998**, *396* (6709), 353–356. DOI: [10.1038/24592](https://doi.org/10.1038/24592).
- [104] Corma, A.; Diaz, U.; Fornes, V.; Jorda, J. L.; Domine, M.; Rey, F. Ti/ITQ-2, a New Material Highly Active and Selective for the Epoxidation of Olefins with Organic Hydroperoxides. *Chem. Commun.* **1999**, (9), 779–780.
- [105] Wu, P.; Nuntasri, D.; Ruan, J. F.; Liu, Y. M.; He, M. Y.; Fan, W. B.; Terasaki, O.; Tatsumi, T. Delamination of Ti-MWW and High Efficiency in Epoxidation of Alkenes with Various Molecular Sizes. *J. Phys. Chem. B.* **2004**, *108* (50), 19126–19131. DOI: [10.1021/jp037459a](https://doi.org/10.1021/jp037459a).

- [106] Wang, L. L.; Wang, Y.; Liu, Y. M.; Chen, L.; Cheng, S. F.; Gao, G. H.; He, M. Y.; Wu, P. Post-Transformation of MWW-type Lamellar Precursors into MCM-56 Analogues. *Micropor. Mesopor. Mater.* **2008**, *113* (1–3), 435–444. DOI: [10.1016/j.micromeso.2007.11.044](https://doi.org/10.1016/j.micromeso.2007.11.044).
- [107] Corma, A.; Diaz, U.; Domine, M. E.; Fornés, V.; Aluminosilicate, N. Titanosilicate Delaminated Materials Active for Acid Catalysis, and Oxidation Reactions Using H₂O₂. *J. Am. Chem. Soc.* **2000**, *122* (12), 2804–2809. DOI: [10.1021/ja9938130](https://doi.org/10.1021/ja9938130).
- [108] Yang, B.-T.; Wu, P. Post-Synthesis and Catalytic Performance of FER Type Sub-Zeolite Ti-ECNU-8. *Chin. Chem. Lett.* **2014**, *25* (12), 1511–1514. DOI: [10.1016/j.ccllet.2014.09.003](https://doi.org/10.1016/j.ccllet.2014.09.003).
- [109] Wu, P.; Ruan, J. F.; Wang, L. L.; Wu, L. L.; Wang, Y.; Liu, Y. M.; Fan, W. B.; He, M. Y.; Terasaki, O.; Tatsumi, T. Methodology for Synthesizing Crystalline Metallosilicates with Expanded Pore Windows through Molecular Alkoxysilylation of Zeolitic Lamellar Precursors. *J. Am. Chem. Soc.* **2008**, *130* (26), 8178–8187. DOI: [10.1021/ja0758739](https://doi.org/10.1021/ja0758739).
- [110] Fan, W. B.; Wu, P.; Namba, S.; Tatsumi, T. A Titanosilicate that Is Structurally Analogous to an MWW-type Lamellar Precursor. *Angew. Chem. Int. Ed.* **2004**, *43* (2), 236–240. DOI: [10.1002/\(ISSN\)1521-3773](https://doi.org/10.1002/(ISSN)1521-3773).
- [111] Ruan, J.; Wu, P.; Slater, B.; Terasaki, O. Structure Elucidation of the Highly Active Titanosilicate Catalyst Ti-YNU-1. *Angew. Chem. Int. Ed.* **2005**, *44* (41), 6719–6723. DOI: [10.1002/\(ISSN\)1521-3773](https://doi.org/10.1002/(ISSN)1521-3773).
- [112] Shen, X. H.; Fan, W. B.; He, Y.; Wu, P.; Wang, J. G.; Tatsumi, T. Epoxidation of Alkenes and Their Derivatives over Ti-YNU-1. *Appl. Catal. A-Gen.* **2011**, *401* (1–2), 37–45. DOI: [10.1016/j.apcata.2011.04.044](https://doi.org/10.1016/j.apcata.2011.04.044).
- [113] Fan, W. B.; Wu, P.; Namba, S.; Tatsumi, T. Synthesis and Catalytic Properties of a New Titanosilicate Molecular Sieve with the Structure Analogous to MWW-type Lamellar Precursor. *J. Catal.* **2006**, *243* (1), 183–191. DOI: [10.1016/j.jcat.2006.07.003](https://doi.org/10.1016/j.jcat.2006.07.003).
- [114] Song, S. S.; Wang, P. F.; He, Y.; Li, J. F.; Dong, M.; Wang, J. G.; Tatsumi, T.; Fan, W. B. Preparation, Characterization and Catalytic Properties of Ti-Rich Ti-YNU-1. *Micropor. Mesopor. Mater.* **2012**, *159*, 74–80. DOI: [10.1016/j.micromeso.2012.04.009](https://doi.org/10.1016/j.micromeso.2012.04.009).
- [115] Moliner, M.; Corma, A. Synthesis of Expanded Titanosilicate MWW-Related Materials from a Pure Silica Precursor. *Chem. Mater.* **2012**, *24* (22), 4371–4375. DOI: [10.1021/cm302509m](https://doi.org/10.1021/cm302509m).
- [116] Wang, L. L.; Wang, Y.; Liu, Y. M.; Wu, H. H.; Li, X. H.; He, M. Y.; Wu, P. Alkoxysilylation of Ti-MWW Lamellar Precursors into Interlayer Pore-Expanded Titanosilicates. *J. Mater. Chem.* **2009**, *19* (45), 8594–8602. DOI: [10.1039/b910886f](https://doi.org/10.1039/b910886f).
- [117] Kon, Y.; Yokoi, T.; Yoshioka, M.; Tanaka, S.; Uesaka, Y.; Mochizuki, T.; Sato, K.; Tatsumi, T. Selective Hydrogen Peroxide Oxidation of Sulfides to Sulfoxides or Sulfones with MWW-type Titanosilicate Zeolite Catalyst under Organic Solvent-Free Conditions. *Tetrahedron* **2014**, *70* (41), 7584–7592. DOI: [10.1016/j.tet.2014.07.091](https://doi.org/10.1016/j.tet.2014.07.091).
- [118] Inagaki, S.; Yokoi, T.; Kubota, Y.; Tatsumi, T. Unique Adsorption Properties of Organic-Inorganic Hybrid Zeolite IEZ-1 with Dimethylsilylene Moieties. *Chem. Commun.* **2007**, (48), 5188–5190.
- [119] Kresge, C. T.; Leonowicz, M. E.; Roth, W. J.; Vartuli, J. C.; Beck, J. S. Ordered Mesoporous Molecular Sieves Synthesized by a Liquid-Crystal Template Mechanism. *Nature* **1992**, *359* (6397), 710–712. DOI: [10.1038/359710a0](https://doi.org/10.1038/359710a0).
- [120] Corma, A.; Navarro, M. T.; Pariente, J. P. Synthesis of an Ultralarge Pore Titanium Silicate Isomorphous to MCM-41 and Its Application as a Catalyst for Selective Oxidation of Hydrocarbons. *J. Chem. Soc. Chem. Commun.* **1994**, (2), 147–148.

- [121] Tanev, P. T.; Chibwe, M.; Pinnavaia, T. J. Titanium-Containing Mesoporous Molecular Sieves for Catalytic Oxidation of Aromatic Compounds. *Nature* **1994**, 368 (6469), 321–323. DOI: [10.1038/368321a0](https://doi.org/10.1038/368321a0).
- [122] Koyano, K. A.; Tatsumi, T. Synthesis of Titanium-Containing Mesoporous Molecular Sieves with a Cubic Structure. *Chem. Commun.* **1996**, (2), 145–146. DOI: [10.1039/cc9960000145](https://doi.org/10.1039/cc9960000145).
- [123] Wu, P.; Tatsumi, T.; Komatsu, T.; Yashima, T. Postsynthesis, Characterization, and Catalytic Properties in Alkene Epoxidation of Hydrothermally Stable Mesoporous Ti-SBA-15. *Chem. Mater.* **2002**, 14 (4), 1657–1664. DOI: [10.1021/cm010910v](https://doi.org/10.1021/cm010910v).
- [124] Anand, C.; Srinivasu, P.; Mane, G. P.; Talapaneni, S. N.; Dhawale, D. S.; Wahab, M. A.; Priya, S. V.; Varghese, S.; Sugi, Y.; Vinu, A. Preparation of Mesoporous Titanosilicate Molecular Sieves with a Cage Type 3D Porous Structure for Cyclohexene Epoxidation. *Micropor. Mesopor. Mater.* **2012**, 160, 159–166. DOI: [10.1016/j.micromeso.2012.05.014](https://doi.org/10.1016/j.micromeso.2012.05.014).
- [125] Maschmeyer, T.; Rey, F.; Sankar, G.; Thomas, J. M. Heterogeneous Catalysts Obtained by Grafting Metallocene Complexes onto Mesoporous Silica. *Nature* **1995**, 378 (6553), 159–162. DOI: [10.1038/378159a0](https://doi.org/10.1038/378159a0).
- [126] Guidotti, M.; Psaro, R.; Batonneau-Gener, I.; Gavrilova, E. Heterogeneous Catalytic Epoxidation: High Limonene Oxide Yields by Surface Silylation of Ti-MCM-41. *Chem. Eng. Technol.* **2011**, 34 (11), 1924–1927. DOI: [10.1002/ceat.v34.11](https://doi.org/10.1002/ceat.v34.11).
- [127] Fraile, J. M.; García, N.; Mayoral, J. A.; Santomauro, F. G.; Guidotti, M. Multifunctional Catalysis Promoted by Solvent Effects: Ti-MCM41 for a One-Pot, Four-Step, Epoxidation–Rearrangement–Oxidation–Decarboxylation Reaction Sequence on Stilbenes and Styrenes. *ACS Catal.* **2015**, 5 (6), 3552–3561. DOI: [10.1021/cs501671a](https://doi.org/10.1021/cs501671a).
- [128] Blasco, T.; Corma, A.; Navarro, M. T.; Pariente, J. P. Synthesis, Characterization, and Catalytic Activity of Ti-MCM-41 Structures. *J. Catal.* **1995**, 156 (1), 65–74. DOI: [10.1006/jcat.1995.1232](https://doi.org/10.1006/jcat.1995.1232).
- [129] Morey, M. S.; O'Brien, S.; Schwarz, S.; Stucky, G. D. Hydrothermal and Postsynthesis Surface Modification of Cubic, MCM-48, and Ultralarge Pore SBA-15 Mesoporous Silica with Titanium. *Chem. Mater.* **2000**, 12 (4), 898–911. DOI: [10.1021/cm9901663](https://doi.org/10.1021/cm9901663).
- [130] Kamegawa, T.; Suzuki, N.; Tsuji, K.; Sonoda, J.; Kuwahara, Y.; Mori, K.; Yamashita, H. Preparation of Hydrophobically Modified Single-Site Ti-Containing Mesoporous Silica (Tisba-15) and Their Enhanced Catalytic Performances. *Catal. Today* **2011**, 175 (1), 393–397. DOI: [10.1016/j.cattod.2011.04.012](https://doi.org/10.1016/j.cattod.2011.04.012).
- [131] Kamegawa, T.; Suzuki, N.; Che, M.; Yamashita, H. Synthesis and Unique Catalytic Performance of Single-Site Ti-Containing Hierarchical Macroporous Silica with Mesoporous Frameworks. *Langmuir*. **2011**, 27 (6), 2873–2879. DOI: [10.1021/la1048634](https://doi.org/10.1021/la1048634).
- [132] Lin, K.; Li, L.; Sels, B. F.; Jacobs, P. A.; Pescarmona, P. P. Titanosilicate Beads as Versatile Catalysts for the Conversion of Trioses to Lactates and for the Epoxidation of Alkenes. *Catal. Today* **2011**, 173 (1), 89–94. DOI: [10.1016/j.cattod.2011.03.055](https://doi.org/10.1016/j.cattod.2011.03.055).
- [133] Zhang, S.; Jiang, Y.; Li, S.; Xu, X.; Lin, K. Synthesis of Bimodal Mesoporous Titanosilicate Beads and Their Application as Green Epoxidation Catalyst, *Appl. Catal. A-Gen.* **2015**, 490, 57–64. DOI: [10.1016/j.apcata.2014.11.004](https://doi.org/10.1016/j.apcata.2014.11.004).
- [134] Tatsumi, T.; Koyano, K.; Igarashi, N. Remarkable Activity Enhancement by Trimethylsilylation in Oxidation of Alkenes and Alkanes with H₂O₂ Catalyzed by Titanium-Containing Mesoporous Molecular Sieves. *Chem. Commun.* **1998**, 3, 325–326. DOI: [10.1039/a706175g](https://doi.org/10.1039/a706175g).
- [135] Nakatsuka, K.; Mori, K.; Okada, S.; Ikurumi, S.; Kamegawa, T.; Yamashita, H. Hydrophobic Modification of Pd/SiO₂@Single-Site Mesoporous Silicas by Triethoxyfluorosilane: Enhanced Catalytic Activity and Selectivity for One-Pot Oxidation. *Chem. Eur. J.* **2014**, 20 (27), 8348–8354. DOI: [10.1002/chem.201402586](https://doi.org/10.1002/chem.201402586).

- [136] Campos-Martin, J. M.; Blanco-Brieva, G.; Fierro, J. L. G. Hydrogen Peroxide Synthesis: An Outlook beyond the Anthraquinone Process. *Angew. Chem. Int. Ed.* **2006**, *45* (42), 6962–6984. DOI: [10.1002/anie.200503779](https://doi.org/10.1002/anie.200503779).
- [137] Samanta, C.; Direct Synthesis of Hydrogen Peroxide from Hydrogen and Oxygen: An Overview of Recent Developments in the Process. *Appl. Catal. A-Gen.* **2008**, *350* (2), 133–149. DOI: [10.1016/j.apcata.2008.07.043](https://doi.org/10.1016/j.apcata.2008.07.043).
- [138] Hayashi, T.; Tanaka, K.; Haruta, M. Selective Vapor-Phase Epoxidation of Propylene over Au/TiO₂ Catalysts in the Presence of Oxygen and Hydrogen. *J. Catal.* **1998**, *178* (2), 566–575. DOI: [10.1006/jcat.1998.2157](https://doi.org/10.1006/jcat.1998.2157).
- [139] Sinha, A. K.; Seelan, S.; Tsubota, S.; Haruta, M. A Three-Dimensional Mesoporous Titanosilicate Support for Gold Nanoparticles: Vapor-Phase Epoxidation of Propene with High Conversion. *Angew. Chem. Int. Ed.* **2004**, *43* (12), 1546–1548. DOI: [10.1002/\(ISSN\)1521-3773](https://doi.org/10.1002/(ISSN)1521-3773).
- [140] Mul, G.; Zwijnenburg, A.; Van Der Linden, B.; Makkee, M.; Moulijn, J. A. Stability and Selectivity of Au/TiO₂ and Au/TiO₂/SiO₂ Catalysts in Propene Epoxidation: An in Situ FT-IR Study. *J. Catal.* **2001**, *201* (1), 128–137. DOI: [10.1006/jcat.2001.3239](https://doi.org/10.1006/jcat.2001.3239).
- [141] Cumaratunge, L.; Delgass, W. N. Enhancement of Au Capture Efficiency and Activity of Au/TS-1 Catalysts for Propylene Epoxidation. *J. Catal.* **2005**, *232* (1), 38–42. DOI: [10.1016/j.jcat.2005.02.006](https://doi.org/10.1016/j.jcat.2005.02.006).
- [142] Taylor, B.; Lauterbach, J.; Delgass, W. N. Gas-Phase Epoxidation of Propylene over Small Gold Ensembles on TS-1. *Appl. Catal. A-Gen.* **2005**, *291* (1–2), 188–198. DOI: [10.1016/j.apcata.2005.02.039](https://doi.org/10.1016/j.apcata.2005.02.039).
- [143] Feng, X.; Duan, X.; Qian, G.; Zhou, X.; Chen, D.; Yuan, W. Au Nanoparticles Deposited on the External Surfaces of TS-1: Enhanced Stability and Activity for Direct Propylene Epoxidation with H₂ and O₂. *Appl. Catal. B-Env.* **2014**, *150–151*, 396–401. DOI: [10.1016/j.apcatb.2013.12.041](https://doi.org/10.1016/j.apcatb.2013.12.041).
- [144] Mori, K.; Miura, Y.; Shironita, S.; Yamashita, H. New Route for the Preparation of Pd and PdAu Nanoparticles Using Photoexcited Ti-Containing Zeolite as an Efficient Support Material and Investigation of Their Catalytic Properties. *Langmuir* **2009**, *25* (18), 11180–11187. DOI: [10.1021/la9015367](https://doi.org/10.1021/la9015367).
- [145] Okada, S.; Mori, K.; Kamegawa, T.; Che, M.; Yamashita, H. Active Site Design in a Core-Shell Nanostructured Catalyst for a One-Pot Oxidation Reaction. *Chem. Eur. J.* **2011**, *17* (33), 9047–9051. DOI: [10.1002/chem.v17.33](https://doi.org/10.1002/chem.v17.33).
- [146] Okada, S.; Ikurumi, S.; Kamegawa, T.; Mori, K.; Yamashita, H. Structural Design of Pd/SiO₂@Ti-Containing Mesoporous Silica Core-Shell Catalyst for Efficient One-Pot Oxidation Using in Situ Produced H₂O₂. *J. Phys. Chem. C.* **2012**, *116* (27), 14360–14367. DOI: [10.1021/jp3025073](https://doi.org/10.1021/jp3025073).
- [147] Kuwahara, Y.; Sumida, Y.; Fujiwara, K.; Yamashita, H. Facile Synthesis of Yolk-Shell Nanostructured Photocatalyst with Improved Adsorption Properties and Molecular-Sieving Properties. *Chem. Cat. Chem.* **2016**, *8* (17), 2781–2788. DOI: [10.1002/cctc.v8.17](https://doi.org/10.1002/cctc.v8.17).
- [148] Kuwahara, Y.; Ando, T.; Kango, H.; Yamashita, H. Palladium Nanoparticles Encapsulated in Hollow Titanosilicate Spheres as an Ideal Nanoreactor for One-Pot Oxidation. *Chem. Eur. J.* **2017**, *23* (2), 380–389. DOI: [10.1002/chem.v23.2](https://doi.org/10.1002/chem.v23.2).
- [149] Wulff, H. P.; *GB Pat.* 1249079, **1971**.
- [150] Sheldon, R. A.; Van Doorn, J. A.; Schram, C. W. A.; De Jong, A. J. Metal-Catalyzed Epoxidation of Olefins with Organic Hydroperoxides. *J. Catal.* **1973**, *31* (3), 438–443. DOI: [10.1016/0021-9517\(73\)90315-1](https://doi.org/10.1016/0021-9517(73)90315-1).

- [151] Sheldon, R. A.; Wallau, M.; Arends, I. W. C. E.; Schuchardt, U. Heterogeneous Catalysts for Liquid-Phase Oxidations: Philosophers' Stones or Trojan Horses? *Acc. Chem. Res.* **1998**, *31* (8), 485–493. DOI: [10.1021/ar9700163](https://doi.org/10.1021/ar9700163).
- [152] Fang, X.; Wang, Q.; Zheng, A.; Liu, Y.; Wang, Y.; Deng, X.; Wu, H.; Deng, F.; He, M.; Wu, P. Fluorine-Planted Titanosilicate with Enhanced Catalytic Activity in Alkene Epoxidation with Hydrogen Peroxide. *Catal. Sci. Technol.* **2012**, *2* (12), 2433–2435. DOI: [10.1039/c2cy20446k](https://doi.org/10.1039/c2cy20446k).
- [153] Tatsumi, T.; Nakamura, M.; Yuasa, K.; Tominaga, H.-O. Shape Selective Epoxidation of Alkenes Catalyzed by Titanosilicate. *Chem. Lett.* **1990**, *19* (2), 297–298. DOI: [10.1246/cl.1990.297](https://doi.org/10.1246/cl.1990.297).
- [154] Clerici, M. G.; Ingallina, P. Epoxidation of Lower Olefins with Hydrogen Peroxide and Titanium Silicalite. *J. Catal.* **1993**, *140* (1), 71–83. DOI: [10.1006/jcat.1993.1069](https://doi.org/10.1006/jcat.1993.1069).
- [155] Van Der Waal, J. C.; Van Bekkum, H. Zeolite Titanium Beta: A Versatile Epoxidation Catalyst. Solvent Effects. *J. Mol. Catal. A-Chem.* **1997**, *124* (2–3), 137–146. DOI: [10.1016/S1381-1169\(97\)00074-5](https://doi.org/10.1016/S1381-1169(97)00074-5).
- [156] Fan, W.; Wu, P.; Tatsumi, T. Unique Solvent Effect of Microporous Crystalline Titanosilicates in the Oxidation of 1-Hexene and Cyclohexene. *J. Catal.* **2008**, *256* (1), 62–73. DOI: [10.1016/j.jcat.2008.03.001](https://doi.org/10.1016/j.jcat.2008.03.001).
- [157] Wu, P.; Tatsumi, T. Unique Trans-Selectivity of Ti-MWW in Epoxidation of Cis/Trans-Alkenes with Hydrogen Peroxide. *J. Phys. Chem. B.* **2002**, *106* (4), 748–753. DOI: [10.1021/jp0120965](https://doi.org/10.1021/jp0120965).
- [158] Přech, J. unpublished results, **2015**.
- [159] Guo, Q.; Sun, K.; Feng, Z.; Li, G.; Guo, M.; Fan, F.; Li, C. A Thorough Investigation of the Active Titanium Species in TS-1 Zeolite by in Situ UV Resonance Raman Spectroscopy. *Chem. Eur. J.* **2012**, *18* (43), 13854–13860. DOI: [10.1002/chem.201201319](https://doi.org/10.1002/chem.201201319).
- [160] Bordiga, S.; Bonino, F.; Damin, A.; Lamberti, C. Reactivity of Ti(IV) Species Hosted in TS-1 Towards H₂O₂-H₂O Solutions Investigated by Ab Initio Cluster and Periodic Approaches Combined with Experimental XANES and EXAFS Data: A Review and New Highlights. *Phys. Chem. Chem. Phys.* **2007**, *9* (35), 4854–4878. DOI: [10.1039/b706637f](https://doi.org/10.1039/b706637f).
- [161] Bombarda, I.; Cezanne, L.; Gaydou, E. M. Epoxidation–Cyclization of Rosewood Oxides. *Flavour Frag. J.* **2004**, *19* (4), 275–280. DOI: [10.1002/ffj.1311](https://doi.org/10.1002/ffj.1311).
- [162] Crandall, J. K.; Rearrangements of Norbornene Oxide. *J. Org. Chem.* **1964**, *29* (10), 2830–2833. DOI: [10.1021/jo01033a005](https://doi.org/10.1021/jo01033a005).
- [163] Cánepa, A. L.; Herrero, E. R.; Crivello, M. E.; Eimer, G. A.; Casuscelli, S. G. H₂O₂ Based A-Pinene Oxidation over Ti-MCM-41. A Kinetic Study. *J. Mol. Catal. A-Chem.* **2011**, *347* (1–2), 1–7. DOI: [10.1016/j.molcata.2011.06.006](https://doi.org/10.1016/j.molcata.2011.06.006).
- [164] Corma, A.; Iglesias, M.; Sanchez, F. Large Pore Bifunctional Titanium-Aluminosilicates: The Inorganic Non-Enzymatic Version of the Epoxidase Conversion of Linalool to Cyclic Ethers, *J. Chem. Soc. Chem. Commun.* **1995**, (16), 1635–1636. DOI: [10.1039/C39950001635](https://doi.org/10.1039/C39950001635).
- [165] Bhaumik, A.; Tatsumi, T. Intramolecular Rearrangement of Epoxides Generated in Situ over Titanium Silicate Molecular Sieves. *J. Catal.* **1999**, *182* (2), 349–356. DOI: [10.1006/jcat.1998.2355](https://doi.org/10.1006/jcat.1998.2355).
- [166] Eimer, G. A.; Díaz, I.; Sastre, E.; Casuscelli, S. G.; Crivello, M. E.; Herrero, E. R.; Perez-Pariente, J. Mesoporous Titanosilicates Synthesized from TS-1 Precursors with Enhanced Catalytic Activity in the A-Pinene Selective Oxidation. *Appl. Catal. A-Gen.* **2008**, *343* (1–2), 77–86. DOI: [10.1016/j.apcata.2008.03.028](https://doi.org/10.1016/j.apcata.2008.03.028).

- [167] Wróblewska, A.; Fajdek, A. Epoxidation of Allyl Alcohol to Glycidol over the Microporous TS-1 Catalyst. *J. Haz. Mater.* **2010**, *179* (1–3), 258–265. DOI: [10.1016/j.jhazmat.2010.02.088](https://doi.org/10.1016/j.jhazmat.2010.02.088).
- [168] Deng, Z.; Yang, Y.; Lu, X.; Ding, J.; He, M.; Wu, P. Studies on the Epoxidation of Methylallyl Chloride over TS-1 Microsphere Catalysts in a Continuous Slurry Reactor. *Catal. Sci. Technol.* **2016**, *6* (8), 2605–2615. DOI: [10.1039/C5CY02002F](https://doi.org/10.1039/C5CY02002F).
- [169] Gunstone, F. D.; Padley, F. B. In *Lipid Technologies and Applications*; Gunstone, F.D., Ed.; Marcel Dekker: New York, **1997**; p 759.
- [170] Wilde, N.; Worch, C.; Suprun, W.; Gläser, R. Epoxidation of Biodiesel with Hydrogen Peroxide over Ti-Containing Silicate Catalysts. *Micropor. Mesopor. Mater.* **2012**, *164*, 182–189. DOI: [10.1016/j.micromeso.2012.06.047](https://doi.org/10.1016/j.micromeso.2012.06.047).
- [171] Trost, B. M.; Chemical Chameleons. Organosulfones as Synthetic Building Blocks. *B. Chem. Soc. Jpn.* **1988**, *61* (1), 107–124. DOI: [10.1246/bcsj.61.107](https://doi.org/10.1246/bcsj.61.107).
- [172] Satoh, H.; Chiba, T.; Malferttheiner, P.; Satoh, H., Eds. *Proton Pump Inhibitors: A Balanced View*; Karger: Basel, **2013**; p. 1.
- [173] Roberts, T.; Hutson, D., Eds. *Metabolic Pathways of Agrochemicals: Insecticides and Fungicides*; The Royal Society of Chemistry: Cambridge, **1999**.
- [174] Fraile, J. M.; Gil, C.; Mayoral, J. A.; Muel, B.; Roldán, L.; Vispe, E.; Calderón, S.; Puente, F. Heterogeneous Titanium Catalysts for Oxidation of Dibenzothiophene in Hydrocarbon Solutions with Hydrogen Peroxide: On the Road to Oxidative Desulfurization, *Appl. Catal. B-Env.* **2016**, *180*, 680–686. DOI: [10.1016/j.apcatb.2015.07.018](https://doi.org/10.1016/j.apcatb.2015.07.018).
- [175] Corma, A.; Iglesias, M.; Sánchez, F. Large Pore Ti-Zeolites and Mesoporous Ti-Silicalites as Catalysts for Selective Oxidation of Organic Sulfides. *Catal. Lett.* **1996**, *39* (3), 153–156. DOI: [10.1007/BF00805575](https://doi.org/10.1007/BF00805575).
- [176] Hulea, V.; Moreau, P.; Di Renzo, F. Thioether Oxidation by Hydrogen Peroxide Using Titanium-Containing Zeolites as Catalysts. *J. Mol. Catal. A-Chem.* **1996**, *111* (3), 325–332. DOI: [10.1016/1381-1169\(96\)00203-8](https://doi.org/10.1016/1381-1169(96)00203-8).
- [177] Moreau, P.; Hulea, V.; Gomez, S.; Brunel, D.; Di Renzo, F. Oxidation of Sulfoxides to Sulfones by Hydrogen Peroxide over Ti-Containing Zeolites. *Appl. Catal. A-Gen.* **1997**, *155* (2), 253–263. DOI: [10.1016/S0926-860X\(96\)00400-0](https://doi.org/10.1016/S0926-860X(96)00400-0).
- [178] Hammett, L. P.; The Effect of Structure upon the Reactions of Organic Compounds. Benzene Derivatives. *J. Am. Chem. Soc.* **1937**, *59* (1), 96–103. DOI: [10.1021/ja01280a022](https://doi.org/10.1021/ja01280a022).